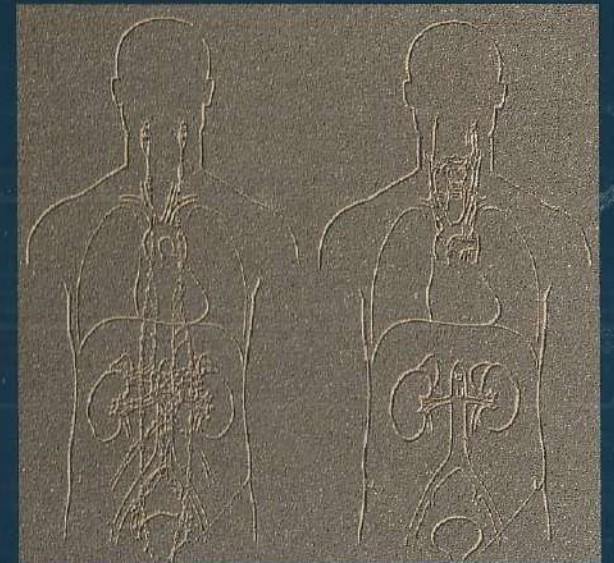


# PARAGANGLIOMAS

MR IMAGING  
AND  
MIBG SCINTIGRAPHY



PARAGANGLIOMAS MR IMAGING AND MIBG SCINTIGRAPHY

A.P.G. van Gils

A.P.G. van Gils

# PARAGANGLIOMAS

MR IMAGING AND MIBG SCINTIGRAPHY

# PARAGANGLIOMAS

MR IMAGING AND MIBG SCINTIGRAPHY

PROEFSCHRIFT

TER VERKRIJGING VAN DE GRAAD VAN DOCTOR  
AAN DE RIJKSUNIVERSITEIT TE LEIDEN,  
OP GEZAG VAN DE RECTOR MAGNIFICUS DR. L. LEERTOUWER,  
HOGLERAAR IN DE FACULTEIT DER GODGELEERDHEID,  
VOLGENS BESLUIT VAN HET COLLEGE VAN DEKANEN  
TE VERDEDIGEN OP DONDERDAG 27 JANUARI 1994  
TE KLOKKE 16.15 UUR

DOOR

Adrianus Petrus Gerardus van Gils  
geboren te Diessen in 1955

**Promotiecommissie:**

Promotoren: Prof. Dr. E.K.J. Pauwels  
Prof. Dr. T.H.M. Falke (Vrije Universiteit van  
Amsterdam)

Referent: Dr. C.J.M. Lips (Rijksuniversiteit Utrecht)

Overige leden: Prof. Dr. P.H. Schmidt  
Prof. Dr. J.L. Bloem

# C ONTENTS

© 1994 A.P.G. van Gils, Leiden, The Netherlands.

All rights are reserved. No part of this publication may be reproduced or transmitted in any form or by any means, electronic or mechanical, including photocopy, recording, or any information storage and retrieval system, without permission in writing from the copyright owner.

Cover design and lay-out by J.J. Beentjes. Preparation of the photographic material by J.J. Beentjes, G. Kracht & R.A.M. van Dijk.  
Karstens Drukkers bv, Leiden, The Netherlands.

CIP - GEGEVENS KONINKLIJKE BIBLIOTHEEK, DEN HAAG.

Gils, Adrianus Petrus Gerardus van

PARAGANGLIOMAS: MR imaging and MIBG scintigraphy /  
Adrianus Petrus Gerardus van Gils; [ill. J.J. Beentjes, et al.]. - [S.l. : s.n.]  
Proefschrift Leiden. - Met lit. opg. - Met samenvatting in het Nederlands.  
ISBN 90-9006728-0  
Trefw.: Paraganglioma / Magnetic Resonance Imaging / nucleaire geneeskunde.

1.	INTRODUCTION	11
	1.1. General	
	1.2. Goal of the study	
	1.3. Outline of the thesis	
	1.4. References	
2.	THE PARAGANGLIONIC SYSTEM	15
	2.1. Anatomy and pathology	
	2.2. Clinical aspects	
	2.3. Imaging procedures	
	Metaiodobenzylguanidine scintigraphy	
	Magnetic resonance imaging	
	2.4. References	
3.	I-123 METAIODOBENZYLGUANIDINE SCINTIGRAPHY IN PATIENTS WITH PARAGANGLIOMAS OF THE HEAD AND NECK REGION	33
	3.1. Introduction	
	3.2. Material and methods	
	Scintigraphy	
	Computer tomography	
	Magnetic resonance imaging	
	Catecholamine measurements	
	3.3. Results	
	3.4. Discussion	
	3.5. References	
4.	MR IMAGING AND MIBG IMAGING OF PHAEOCHROMOCYTOMAS AND EXTRA-ADRENAL FUNCTIONING PARAGANGLIOMAS	47
	4.1. Introduction	
	4.2. Clinical and radiological characteristics	
	Clinical characteristics	
	Radiological characteristics	

4.3.	Material and methods		
4.4.	Results		
	Lesion detection		
	Tumour characterization		
4.5.	Discussion		
4.6.	Proposed protocol for MR imaging examination		
4.7.	Conclusions		
4.8.	References		
5.	MR IMAGING SCREENING OF KINDRED AT RISK OF DEVELOPING PARAGANGLIOMAS	69	
5.1.	Introduction		
5.2.	Patients and methods		
	Patients		
	Magnetic resonance imaging		
	Catecholamine measurements		
	Scintigraphy		
	Statistical analysis		
5.3.	Results		
	Glomus tumours		
	Functioning paragangliomas		
	Hereditary aspects		
5.4.	Discussion		
5.5.	References		
6.	QUANTITATIVE EVALUATION OF GADOPENTETATE DIMEGLUMINE PERFORMANCE IN MR IMAGING OF HEAD AND NECK PARAGANGLIOMAS INCLUDING AFROC ANALYSIS	81	
6.1.	Introduction		
6.2.	Material and methods		
	Patient selection		
	MR imaging technique		
	Image interpretation		
	Statistical analysis		
6.3.	Results		
	Image findings		
	Comparison of MR imaging pulse sequences		
6.4.	Discussion		
6.5.	References		
7.	GENERAL DISCUSSION		95
	7.1. Introduction		
	7.2. Merits and demerits in perspective		
	7.3. Future directions and developments		
	7.4. References		
8.	SUMMARY		103
9.	SAMENVATTING		107
	LIST OF OWN PUBLICATIONS USED IN THIS THESIS		111
	ACKNOWLEDGEMENTS		113
	CURRICULUM VITAE		115

### 1.1. GENERAL

Paragangliomas are tumours originating from the autonomic nervous system and are potentially capable of catecholamine production. Although rare in the general population (estimated incidence 0.001% - 0.002%) they carry a considerable risk to those affected [1]. In these patients there is a marked tendency towards multiple tumours, occurring simultaneously or consecutively over an extended period [2-4]. At least 10% of the patients has a family history of paraganglioma occurrence. Familial cases demonstrate a higher incidence of multiple lesions compared to non-familial cases. Patients with sporadic or familial paragangliomas may also have associated disorders such as neurofibromatosis, von Hippel-Lindau disease, multiple endocrine neoplasia syndromes (MEN II and MEN III), and other endocrine tumours including islet cell tumours, pituitary tumours, carcinoid tumours and aldosteronomas [5].

Initially, paragangliomas are often small and extremely slow-growing and hardly cause symptoms. However, early diagnosis and treatment of new cases as well as new lesions and associated diseases in known patients is important since tumour growth may eventually lead to destruction of adjacent structures and to harmful hormonal activity [6]. Given early and adequate localization, surgical cure is certainly possible in 90% of cases [6-8].

From a clinical point of view, paragangliomas are divided into those originating in the head and neck area and those that arise in the trunk. The former, also known as chemodectomas, are often first encountered by the otolaryngologist, the general surgeon or the neurosurgeon, when the patient presents with a mass lesion in the neck, hearing loss, pulsatile tinnitus or paralysis of cranial nerves. Hormonal activity is only rarely at the forefront, but should always be evaluated, because of the catastrophic results of surgery in unidentified cases [9]. Choice of treatment depends primarily on site and size of the tumour. Paragangliomas in the neck are best resected when small, whereas paragangliomas of the skull base require a 'wait and see' policy [6].

Paragangliomas of the trunk, commonly referred to as pheochromocytomas are usually first seen by the endocrinologist due to the symptoms of

hormonal over-activity. Surgical therapy is mandatory, irrespective of site and size.

Even though the majority of these tumours originates in the adrenal medulla, they may be situated anywhere from the base of the skull to the bladder. In patients with adrenal paragangliomas it is therefore common practice to perform extensive surgical exploration of multiple predilection sites in the retroperitoneum and pelvis [10]. Confident preoperative localization of sympathomedullary disease justifies posterior adrenalectomy without extensive surgical exploration in most patients, reducing the average hospitalization from 16 to 6 days [11]. It has been shown that morbidity and mortality rates associated with surgery decrease if extensive surgical exploration is replaced by reliable preoperative localization of all functioning paragangliomas present [11, 12]. Uncontrollable hypertension or even sudden death may not only occur during surgery, including minor unrelated surgery, but also during diagnostic procedures such as angiography or venous catheterization [13-15].

For both tumour types, a non-invasive, highly sensitive and specific imaging modality could thus play a major role in the detection and localization of paragangliomas, in the periodic examination of persons at risk of developing these tumours and in the monitoring of paragangliomas of the skull base.

Of the anatomic radiographic techniques, computed tomography (CT) has until recently been the most widely used initial screening procedure for visualization of paragangliomas [16]. However, CT is limited in its ability to localize extra-adrenal sources of catecholamine excess, due to cumbersome 'salami technique' (limited area of examination), low contrast resolution in the neck and skull base and inherent ionizing radiation. In addition, CT is also restricted in its ability to provide a specific diagnosis independent of clinical and biochemical findings.

## 1.2. GOAL OF THE STUDY

In recent years, the non-invasive imaging techniques magnetic resonance (MR) imaging and metaiodobenzylguanidine (MIBG) scintigraphy have become available for the diagnosis of paraganglionic tumours. The relative roles of these techniques are presently under debate. MIBG has been found accurate in the localization of functioning paragangliomas [17]. MR imaging has shown great potential both with regard to adrenal lesions and paraganglionic tumours situated at extra-adrenal sites [18, 19].

The purpose of this thesis is to explore and evaluate MR imaging and MIBG scintigraphy as procedures for detecting functioning as well as non-functioning paragangliomas and screening of at-risk persons. It also attempts to determine the relative roles of these techniques and the extent to which they can replace more invasive diagnostic procedures.

## 1.3. OUTLINE OF THE THESIS

The study is presented in eight chapters.

CHAPTER 1 includes the introduction, aim and outline of the study involved.

CHAPTER 2 discusses relevant anatomical, clinical and pathological aspects of paraganglionic tumours, with an introduction to MR imaging and MIBG scintigraphy of paragangliomas.

CHAPTER 3 reports on an MIBG scintigraphy study of 15 patients with head and neck paragangliomas. The serendipitous detection of functioning paragangliomas and pheochromocytomas is discussed.

CHAPTER 4 provides the results of a comparative study of MR imaging and MIBG scintigraphy in the detection of paragangliomas. The merits and demerits of both procedures are compared and illustrated by exemplary cases.

CHAPTER 5 deals with the application of MR imaging to the screening of a large kindred group at risk of developing paragangliomas.

CHAPTER 6 presents a comparison of gadopentetate dimeglumine-enhanced and unenhanced MR imaging of paragangliomas of the head and neck.

CHAPTER 7 comprises a general discussion on the use of MR imaging and MIBG scintigraphy for imaging paragangliomas. The complementary role of both modalities is discussed.

CHAPTER 8 contains an English summary of this thesis.

CHAPTER 9 contains a Dutch summary of this thesis.

## 1.4. REFERENCES

1. Beard CM, Sheps SG, Kurland LT, Carney JA, Lie JT. Occurrence of pheochromocytoma in Rochester, Minnesota, 1950 through 1979. *Mayo Clin Proc* 1983;58:802-804
2. Bogdasarian RS, Lotz PR. Multiple simultaneous paragangliomas of the head and neck in association with multiple retroperitoneal pheochromocytomas. *Otolaryngol Head Neck Surg* 1979;87:648-652
3. Karasov RS, Sheps SG, Carney JA, Heerden JA van, Quatro V de. Paragangliomatosis with numerous catecholamine producing tumors. *Mayo Clin Proc* 1982;57:590-595
4. Revak CS, Morris SE, Alexander GH. Pheochromocytoma and recurrent chemodectomas over a twenty-five year period. *Radiology* 1971;100:53-54
5. Grimley PM. Multicentric paragangliomas and associated neuroendocrine tumors. In: Local invasion and spread of cancer. Brunson KW, ed. Dordrecht. Kluwer academic publishers 1989;49-61
6. Mey AGL van der, Frijns JHM, Cornelisse CJ, et al. Does intervention improve the natural course of glomus tumors? *Ann Otol Rhinol Laryngol* 1992;101:635-642
7. Plouin PF, Chatellier G, Delahousse M, et al. Recherche, diagnostic et localisation du pheochromocytome. *Presse Med* 1987;16:2211-2215

8. Radin DR, Ralls PW, Boswell WD Jr, Colletti PM, Lapin SA, Halls JA. Pheochromocytoma: detection by unenhanced CT. *AJR* 1986;146:741-744
9. Schwaber MK, Glasscock ME, Nissen AJ, Jackson CG, Smith PG. Diagnosis and management of catecholamine secreting glomus tumors. *Laryngoscope* 1984;94:1008-1015
10. Hunt TK, Biglieri EG, Tyrrell JB. Adrenals. In: *Current surgical diagnosis and treatment*. Way LW, ed. East Norwalk. Appleton and Lange 1988;661-673
11. Grant CS, Carpenter P, Heerden JA van, Hamberger B. Primary aldosteronism; clinical management. *Arch Surg* 1984;119:585-590
12. Nolsøe CP, Jensen LT, Torp-Pedersen S, Rasmussen M, Juel Christensen N, Holm HH. Nine pheochromocytomas in the same patient: final mapping with ultrasound and angiography. *Acta Radiologica* 1988;29:515-518
13. Manger WM, Gifford RW. Hypertension secondary to pheochromocytoma. *Bull NY Acad Med* 1982;58:139-158
14. Rossi P, Young IS, Panke WF. Techniques, usefulness and hazards of arteriography of pheochromocytomas: review of 99 cases. *JAMA* 1968;205:547-553
15. St John Sutton MG, Sheps SG, Lie JT. Prevalence of clinically unsuspected pheochromocytoma. Review of a 50-year autopsy series. *Mayo Clin Proc* 1981;56:354-360
16. Moss AA. Computed tomography of the adrenal glands. In: *Computed tomography of the body*. Moss AA, Gamsu G, Genant HK, eds. Philadelphia. Saunders 1983;837-876
17. Shapiro B, Copp JE, Sisson JC, Eyre PL, Wallis J, Beierwaltes WH. Iodine-131 metaiodobenzylguanidine for the locating of suspected pheochromocytoma: experience in 400 cases. *J Nucl Med* 1985;26:576-585
18. Falke THM, Gils APG van, Seters AP van, Sandler MP. Magnetic resonance imaging of functioning paragangliomas. *Magn Reson Q* 1990;6:1-35
19. Schmedtje JF, Sax S, Pool JL, Goldfarb RA, Nelson EB. Localization of ectopic pheochromocytomas by magnetic resonance imaging. *Am J Med* 1987;83:770-772

## 2

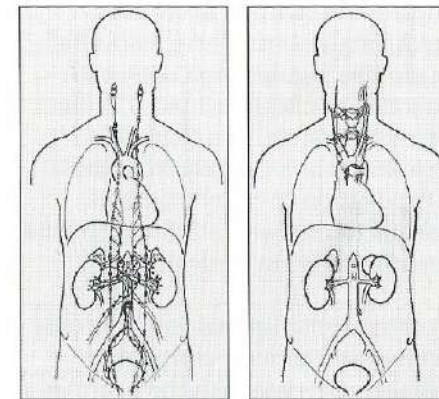
## THE PARAGANGLIONIC SYSTEM: CLINICAL ASPECTS AND NON-INVASIVE IMAGING PROCEDURES\*

### 2.1. ANATOMY AND PATHOLOGY

Paragangliomas are tumours emanating from paraganglion cells which lie adjacent to the ganglia and plexuses of the autonomic nervous system. The autonomic nervous system consists of two complementary divisions with contrasting functions - the sympathetic and the parasympathetic systems. The pre-ganglionic, efferent fibres of the sympathetic system emerge from

thoracic and lumbar spinal nerves (thoraco-lumbar outflow) and terminate in ganglia in the paraspinal sympathetic trunks, nearby plexus sites or in the adrenal medulla (figure 2.1). In contrast, the pre-ganglionic, efferent fibres of the parasympathetic system emerge from cranial nerves and sacral spinal nerves (cranio-sacral outflow) and terminate in ganglia very close to or within the walls of the innervated structures (figure 2.2).

The autonomic nervous system comprises central regions of neural integrations and peripheral nerves, ganglia and plexuses providing innervation to viscera, glands, blood vessels and smooth muscle.



2.1

Figure 2.1. Distribution of orthosympathetic system.

2.2

Figure 2.2. Distribution of parasympathetic chemoreceptor system. The sacral outflow is not shown.

Generally speaking, this system maintains internal homeostasis by regulating vegetative or automatic functions. Body metabolism, temperature, respiration, circulation and certain endocrine glands are largely under autonomic nervous control.

\* Based on: Non-invasive imaging of functioning paragangliomas (including pheochromocytomas). APG van Gils, THM Falke, AR van Erkel, CJH van de Velde, EKJ Pauwels. In *Front Eur Radiol* 1990;7:1-38, and on: Magnetic resonance imaging of functioning paragangliomas. THM Falke, APG van Gils, AP van Seters, MP Sandler. *Magn Reson Q* 1990;6:35-64.

Autonomic neural impulses of both parasympathetic and sympathetic preganglionic fibres are transmitted by release of acetylcholine at the nerve end, which is located in the ganglia. Acetylcholine is also the principal transmitter of the peripheral parasympathetic nerves. Norepinephrine is the principal neurotransmitter of the peripheral sympathetic nervous system. Epinephrine is the predominant catecholamine synthesized in and released from the adrenal medulla (basically a ganglion without axonal extensions).

Much confusion has resulted from the indiscriminate and often inconsistent use by various authors of the terms 'paraganglioma', 'phaeochromocytoma', 'chromaffinoma', 'chemodectoma' and 'glomus tumours'. It is therefore necessary to give a brief account of the classification of these tumours.

Former classifications relied heavily on the affinity of paraganglion tissue for dichromate salts [1]. Tumours arising from chromaffin cells in the adrenal medulla or in pre-vertebral and peripheral sympathetic ganglia were designated as phaeochromocytomas or chromaffinomas. Extra-adrenal tumours were often collectively termed 'ectopic phaeochromocytomas'. Adrenal and extra-adrenal phaeochromocytomas were particularly associated with the production of clinically significant catecholamines.

The non-chromaffin tissue chiefly comprised the carotid body, the aorticopulmonary paraganglia and the paraganglion structures associated with the lower cranial nerves such as the glomus jugulare and the vagal body. These were and still are taken to function as chemoreceptors in the reflexogenic regulation of the cardiopulmonary system. The chemodectomas, also called glomus tumours, were taken to arise largely from these structures and seldom to give rise to the production of catecholamines.

The paragangliomas in these classifications formed an ill-defined residual group of tumours arising from non-chromaffin cells but clinically resembling phaeochromocytomas.

It has, however, long been known that the chromaffin reaction is unsatisfactory as staining is frequently unpredictable and because chromaffin positivity of a paraganglioma does not reliably correlate with the pharmacological effects produced by the tumour [2]. Furthermore, it has been found that while a number of chromaffinomas are physiologically silent, occasional tumours arising from the carotid body systems are pharmacologically active [3]. Several studies have indicated that a rigid separation between chromaffin and non-chromaffin tumours can no longer be maintained [2, 4, 5].

In 1974 Glenner and Grimley devised a new classification of the paraganglion system [2]. This included tumours of both adrenal and extra-adrenal tissue, the chemodectomas and morphologically similar tumours arising in widely dispersed locations. In their approach, the adrenal medulla is part of the paraganglion system and its tumours, i.e. the phaeochromocytomas, may be either functioning or non-functioning.

The tumours of the extra-adrenal paraganglion system, including those deriving from chemoreceptors, are anatomically subdivided by Glenner and Grimley as originating from four families of paraganglia:

1. Branchiomic, including in particular the paraganglionic chemoreceptors of the carotid body and the glomus jugulare
2. Intravagal
3. Aorticosympathetic, including the para-aortic bodies of Zuckerkandl and the extramedullary chromaffin tissue related to the sympathetic chain and ganglia
4. Visceral-autonomic, situated in thoracic and abdominal organs.

The WHO classification [6], to which we broadly conform, comprises the following categories:

1. Phaeochromocytomas, i.e. tumours arising from the adrenal medulla
2. Sympathetic paragangliomas arising from neuroendocrine cells associated with the sympathetic chain
3. Parasympathetic paragangliomas which are generally non-chromaffin and include the branchiomic, vagal and visceral autonomic paragangliomas
4. Paragangliomas not further specified.

All paraganglia store catecholamines sequestered in the dense core vesicles of their tumour cells. The tumours to which they give rise may either be catecholamine-secreting or non-functioning. Phaeochromocytomas are hormonally active in more than 90% of cases. In contrast, about 50% of sympathetic paragangliomas are active and, although personal experience indicates a higher percentage, parasympathetic paragangliomas are supposed to be active in about 1% of cases [7].

About 80% of the functioning paragangliomas is located in the adrenal medulla (phaeochromocytomas proper). Another 16% is located in the abdomen. The remaining 4% can be found in the thorax and head and neck area [8]. Bilateral phaeochromocytomas occur in from 5% to 10% of cases.

About 10% of patients has a family history of paraganglioma occurrence. These familial tumours demonstrate a tendency towards multiplicity and bilaterality of up to 35%. This tendency is markedly lower with non-familial tumours. Among children, the incidence of bilateral tumours (30%) and multiple lesions (50%) is higher [9, 10].

Malignancy, as determined by distant spread, is said to occur in 10% of patients [1, 11]. It can however be argued that this percentage is too high, because in the region of the distribution of the autonomic nervous system differentiation between metastases in retroperitoneal lymph nodes and multiple primary tumours is almost impossible. Only when a tumour clearly arises outside of the autonomic nervous system distribution, can it be considered a metastasis beyond doubt. A somewhat lower percentage of malignancy therefore seems more realistic [12]. Malignancy probably occurs

more in extra-adrenal paragangliomas and in dopamine-producing paragangliomas [13, 14].

Patients with sporadic or familial paragangliomas may also have associated disorders including other endocrine tumours such as islet cell tumours, pituitary tumours, carcinoid tumours and aldosteronomas [15]. Further association has been demonstrated with neuro-ectodermal disorders such as neurofibromatosis and von Hippel-Lindau disease [16-18]. Functioning paragangliomas are part of the MEN II and MEN III syndromes [19]. The phaeochromocytomas in MEN patients are thought to arise from hyperplastic adrenal medullae, whereas sporadic phaeochromocytomas develop in a normal adrenal medulla [20]. Gastric epithelioid leiomyosarcomas and pulmonary chondromas have been observed in combination with paragangliomas [21].

Furthermore, the production and secretion of parathyroid hormone, calcitonin, gastrin, serotonin and ACTH by paragangliomas has been described in a small number of cases [22, 23].

## 2.2. CLINICAL ASPECTS

As regards clinical presentation there is a clear, although not complete distinction between paragangliomas of the head and neck, and functioning paragangliomas located predominantly in the thorax and abdomen, as already mentioned often called phaeochromocytomas.

Paragangliomas in the head and neck, also known as chemodectomas or glomus tumours are highly vascular, slow-growing tumours. The four most common types are 1) the carotid body tumour located at the carotid bifurcation, 2) the vagal body tumour arising from nests of paraganglionic tissue within the perineurium of the vagal nerve near its ganglion nodosum, 3) the glomus jugulare tumour originating from the glomus bodies of the jugular bulb and 4) the glomus tympanicum tumour deriving from the glomus bodies of the tympanicum plexus of Jacobson's nerve in the mucosa of the cochlear promontory. Carotid and vagal body tumours mostly present as a slow-growing mass in the upper neck with relatively few other symptoms. Symptoms of glomus jugulare and tympanicum tumours include pulsatile tinnitus, hearing loss and cranial nerve palsy as the lesion expands. A phaeochromocytoma-like syndrome occurs only rarely [24, 25].

Surgical removal of carotid and solitary vagal body tumours is quite possible without major complications: the smaller the tumour, the more easy the resection. Usually the resection prevents future morbidity as it is almost always radical [26]. For jugular and tympanic glomus tumours a monitored 'wait and see policy' is considered more appropriate and surgical therapy should only be performed when the tumour causes progressively invalidat-

ing cranial nerve palsy or becomes life-threatening due to intracranial extension [26].

The clinical presentation of truncal paragangliomas is of a somewhat different nature and almost exclusively determined by hormonal over-activity. A characteristic feature of phaeochromocytomas is the production by the neoplastic cells themselves of pharmacologically active substances. This feature, however, is known to be shared on occasion both by the other types of paragangliomas discussed here, and by neuroblastomas and their differentiating derivatives. The presence of norepinephrine in phaeochromocytomas was first demonstrated by Holton in 1949 and while most tumours are known to secrete a combination of epinephrine and norepinephrine, the latter is usually released in larger concentrations than the former [27]. Occasionally dopamine, dopa and serotonin are synthesized by paragangliomas [3, 14, 28].

Several diagnostic methods exist for the detection of these substances in plasma and urine. The sensitivity and specificity of plasma catecholamine measurements are limited because of the often intermittent secretion by paragangliomas and because intravenous sampling causes stress, which raises plasma catecholamines in a nonspecific way [29]. At present 24-hours urinary determination of free norepinephrine by gas chromatography or high-performance liquid chromatography (HPLC) are considered the most sensitive methods [17, 30].

The secretion of pressure amines, norepinephrine being the most important, by the tumour, produces the well-recognized syndrome of paroxysmal or permanent hypertension associated with vasomotor crises. The symptoms include headache, pallor, perspiration, palpitations, unusual lability of blood-pressure and severe hypertension. Sometimes a palpable mass is present [31].

The symptoms, entirely or in part, are episodic in the vast majority of cases. During each episode or paroxysm, two or more symptoms are generally experienced simultaneously [17, 32]. The paroxysms may be spontaneous or provoked by exercise, bending over, urination, defecation, pressure on the abdomen, palpation of the tumour, induction of anaesthesia, and intravenous administration of a number of drugs. In 99% of cases the manifestations include at least one symptom in the triad of excessive diaphoresis, headache and palpitation or tachycardia [11].

In contrast to sporadic functioning paragangliomas, the functioning paragangliomas in MEN syndromes are asymptomatic in about 50% of cases, especially in the early course of development, and are only diagnosed as a result of increased suspicion [19, 33, 34].

Despite fairly widespread acquaintance with the characteristics of catecholamine-secreting paragangliomas, there has been a considerable discrepancy between the frequency of clinical detection of these tumours and their discovery at autopsy (1:4) [31, 35]. It is probable that the availability of the

latest imaging techniques, which will be discussed in the following sections, has reduced the extent of this discrepancy but this has not as yet been established.

Conversely, even when strict criteria are applied for the diagnosis of functioning paragangliomas (hypertension and/or spells characterized by headache, sweating, palpitations, anxiety or tremor and the presence of one or more abnormal measurements of the plasma or urinary catecholamine concentrations), a substantial number of patients not suffering from the disease will inevitably be imaged. In one series of 312 patients suspected of having a sporadic benign pheochromocytoma on the basis of symptoms or abnormal biochemical tests, it was eventually shown that 83% did not suffer from pheochromocytoma and in another series of 31 patients with clinical and biochemical findings suggesting a functioning paraganglioma, 40% were found not to have such a tumour on follow-up [36, 37].

The paroxysmal effects of excess catecholamine production on the cardiovascular system remain life-threatening until all functioning tumours are excised. An anterior transperitoneal approach is usual as it permits wide exposure and visualization of the retroperitoneal space [38]. Adequate pre-operative localization and delineation of a single adrenal paraganglioma, however, permits a postero-lateral approach thus avoiding the complications of the transabdominal approach [12].

Intra-operative or postoperative hypotension and arrhythmia are grave risks for which the surgeon and anaesthetist must always be prepared, even when there are no overt functional signs or symptoms [38]. These risks can be reduced by tailored preoperative alpha and beta receptor blockade.

### 2.3. IMAGING PROCEDURES

When the presence of a functioning paraganglioma is suggested by biochemical measurements, accurate location of the tumour and the exclusion or demonstration of multiple tumours is of utmost importance to successful surgical therapy.

Some of the imaging techniques used for the localization of functioning paragangliomas are invasive and may be hazardous, e.g. arteriography, venography and selective venous sampling of blood [39, 40]. Angiographic procedures in these patients carry a potential risk of inducing a hypertensive crisis or even sudden death [41]. Furthermore, angiographic examinations are also less suited to demonstrating in the span of one examination the presence of multiple tumours dispersed in the body. Because of the newer, non-invasive imaging techniques now available, angiography and venography are no longer first line imaging methods but rather used for pre-operative evaluation.

Real time sonography (US) can potentially demonstrate adrenal, retroperitoneal and cervical paragangliomas but is unable to visualize mediastinal paragangliomas and paragangliomas located near the skull base [42]. In addition US is operator-dependent and the technique is impaired by obesity, gas-filled bowel loops and bone.

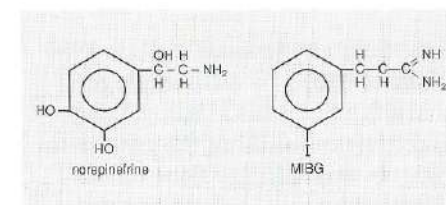
For localizing paragangliomas of the adrenal gland computed tomography (CT) is better than US and angiography with an accuracy of 96% [43]. However, CT is restricted in the detection of small adrenal tumours and of recurrent or residual tumours after previous surgical therapy [8]. CT is also limited in locating extra-adrenal paragangliomas because it is impractical to perform whole-body CT and because of the ionizing radiation. The latter certainly applies when searching for paragangliomas in genetically predisposed persons, in children and pregnant women [44, 45].

Two new techniques, metaiodobenzylguanidine (MIBG) scintigraphy and Magnetic Resonance (MR) imaging now open the option of imaging the entire region of interest in a non-invasive and feasible manner.

### Metaiodobenzylguanidine scintigraphy

#### Introduction

Metaiodobenzylguanidine is an analogue of the adrenergic neuron blocker, guanethidine, which was first synthesized in 1979 by Wieland at the University of Michigan [46]. Since the finding that its concentration in the adrenal medullae of dogs was sufficient to permit scintigraphic portrayal of such adrenergic structures, the potential of MIBG to image adrenergic tumours, and in particular pheochromocytomas, has been clearly demonstrated [36, 47]. The molecular structure of MIBG has a number of features in

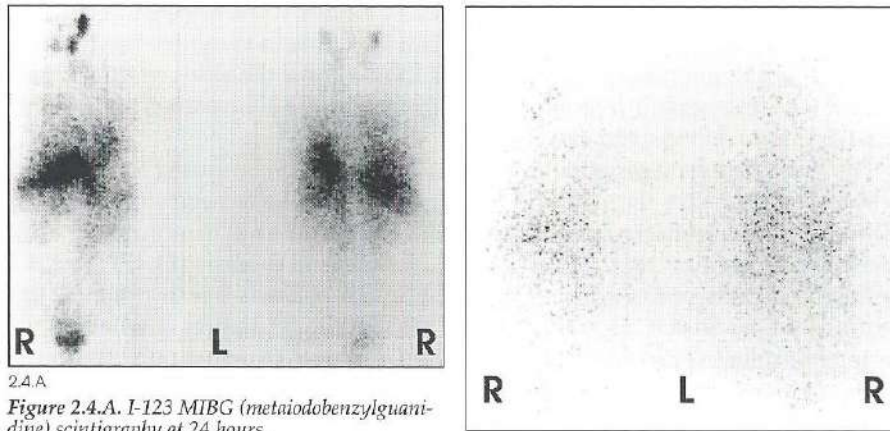


2.3  
Figure 2.3. Molecular structures of norepinephrine (left) and metaiodobenzylguanidine (right).

common with the adrenergic neuron blocker guanethidine and the neurotransmitter norepinephrine (figure 2.3). Furthermore MIBG is known to be concentrated in the same adrenergic granules of the adrenal medulla cells as those in which part of the norepinephrine secreted by exocytosis is stored [48].

Metaiodobenzylguanidine causes no pharmacological response [49].

Metaiodobenzylguanidine, bearing a guanidine side chain, thus follows the pathways of norepinephrine without being metabolized to any appreciable extent [50]. Within one day 40 to 55%, and after four days up to 90% of MIBG can be found unaltered in the urine.



2.4.A

Figure 2.4.A. I-123 MIBG (metaiodobenzylguanidine) scintigraphy at 24 hours.

Figure 2.4.B. I-131 MIBG scintigraphy at 48 hours performed in the same patient at a different time. The superior image quality of I-123 MIBG is

2.4.B

clearly shown in this patient who proved to have no paraganglioma.

Metaiodobenzylguanidine labelled with a radioactive isotope can be applied for imaging purposes. In man, only I-123 and I-131 are suitable as radioactive labels. The former has several advantages including superior physical and dosimetric properties. The photon energy of 159 KeV is more appropriate for modern gamma cameras and single photon emission computed tomography (SPECT) [51]. Furthermore I-123 lacks beta energy. This results in a far better image quality (figure 2.4) together with a lower radiation dose (total body dose of approximately 1 mGy/37 MBq for I-131 MIBG versus 0.2 mGy/370 MBq for I-123 MIBG) [52, 53]. However its shorter half-life and higher costs have limited the use of I-123 MIBG.

#### MIBG uptake and distribution

Using bovine adrenal cells in culture, it was shown by Jacques et al. in 1984 that two pathways are involved in the uptake of MIBG by adrenergic cells. One mechanism, dominating at low concentrations of MIBG (1  $\mu\text{mol}$ ) and norepinephrine, exhibits a number of characteristics fulfilling the criteria for the uptake-one system of adrenergic tissues, i.e. high affinity ( $K_m$  1.2-1.4  $\mu\text{mol}$ ), low capacity and saturability and dependence on sodium concentration, an energy source and temperature [54].

The second mechanism, dominating at higher concentrations (MIBG > 2  $\mu\text{mol}$  and norepinephrine > 20  $\mu\text{mol}$ ) appears to be characterized by passive diffusion of the agents. This mechanism is dependent upon temperature but independent of sodium concentration and an energy source, and apparently unsaturable [54]. MIBG and norepinephrine are competitive for the uptake-one system [55]. With the doses of MIBG used in diagnostic imaging,

concentrations will be low, so the uptake-one mechanism will be the predominant in-vivo mechanism [56].

Metaiodobenzylguanidine drawn from the cytoplasm by means of a ATPase-dependent proton pump is stored in the catecholamine containing granules [57].

Normal uptake by different organs of I-123 MIBG is illustrated in fig 2.4. In normal persons both I-123 and I-131 MIBG show high uptake in the heart, liver, spleen, bladder and salivary glands [58]. Most of the MIBG in the heart and salivary glands is concentrated in the adrenergic nerve endings, whereas the high concentration of MIBG in liver and bladder is due to the excretion in the biliary and urinary systems [49]. The thyroid is only visualized by free radiolabelled iodine if there is inadequate blockade with Lugol's solution. With I-131 MIBG the normal adrenals are seldom imaged, whereas I-123 MIBG permits identification of the left adrenal in most cases [59]. The right adrenal is more often concealed due to high background activity from the liver.

Uptake of MIBG in functioning paragangliomas and neuroblastomas is variable not only between patients, but even in multiple lesions within one patient [60, 61].

Bomanji et al. have shown a directly proportional correlation between the uptake of I-123 MIBG by paragangliomas and related tumours, and the number of neurosecretory granules in the tumour cell [62]. Probably as important as the uptake rate is the excretion of MIBG by the tumour. Von Moll suggested that in addition to low storage capability or the tumour's inability to take up MIBG, high rates of MIBG secretion may be another explanation for non-visualization of pheochromocytomas and other neural crest derived tumours. There is no obvious relationship between the secretion of catecholamines and MIBG uptake, as several non-functioning paragangliomas (including chemodectomas) also show MIBG uptake [3, 63].

Several drugs, such as reserpine, cocaine, tricyclic antidepressants, phenylpropanolamine and labetalol are known to interfere with MIBG uptake [64]. This specially applies to the latter as this drug is often used in patients with catecholamine excess. Direct experimental evidence in animals and indirect evidence in humans suggests that the effect of labetalol on MIBG uptake is mediated via blockade of the uptake-one mechanism. Therapy with labetalol should be discontinued for several days before performing MIBG scintigraphy in order to preclude false-negative results [65].

#### Scintigraphic technique used in this study

A dose of 370 MBq I-123 MIBG was injected intravenously with the patient in the supine position. I-123 MIBG was obtained from 'Cygne' B.V. (Eindhoven, The Netherlands). The synthesis of I-123 MIBG was performed by the method of Wieland et al. [66]. I-123 was produced by the Xe-124 (p,2n) reaction with specification of a maximum I-125 impurity of 0.01% at the time of

calibration. I-123 MIBG (specific activity at least 925 MBq per milligram) was diluted in bacteriostatic phosphate buffer (pH 6.0-6.5) to a specific concentration of at least 74 MBq/ml. The free iodine concentration was less than 0.2%. Thyroidal uptake was blocked by the administration of Lugol's solution, ten drops three times daily (50 mg of iodine) for five days, starting the day before the injection.

A large field-of-view gamma camera (Toshiba GCA 90B®, Toshiba, Tokyo, Japan) equipped with a low energy general purpose collimator and interfaced to a dedicated computer (Toshiba GMS-55®, Toshiba) was used. A 20% window was centred at 159 KeV. In all cases, anterior and posterior digitized images of the total body, and four images of the head and neck were obtained 24 hours and, in most cases, 48 hours after the injection. In selected cases additional single photon emission computer tomography (SPECT) of the head and neck area or the upper abdomen was performed 24 hours after the injection. From the SPECT study transaxial, sagittal and coronal slices, 5.3 mm thick, were reconstructed

## Magnetic Resonance imaging

### *Introduction*

In the course of its short history, Magnetic Resonance (MR) imaging has proved to be of considerable value in the portrayal of paragangliomas [8, 44]. Gradual technical advances have largely overcome the problems of poor anatomical resolution resulting from physiological movement, previously encountered during MR imaging of adrenal gland pathology. Consequently, MR imaging can now detect adrenal masses at a rate comparable to that of CT and is superior to CT in the localization of extra-adrenal functioning paragangliomas [8, 67]. Major advantages of MR imaging include the absence of radiation hazard, outstanding image contrast and the ability to acquire multiplanar images and achieve accurate three-dimensional localization.

### *Technical principles*

MR imaging is based on the principle that atomic nuclei with an odd number of protons or neutrons ( $^1\text{H}$ ,  $^{31}\text{P}$ ,  $^{13}\text{C}$ ,  $^{23}\text{Na}$  and  $^{19}\text{F}$ ) exhibit a nuclear spin. For imaging purposes only the hydrogen nucleus (proton) is used. Because of its spin and because of its charge the proton has a magnetic dipole and behaves somewhat like a compass needle. In the absence of a magnetic field, the protons are oriented at random in the organism. When placed in a strong external magnetic field (called  $B_0$ ), the protons tend to align parallel or antiparallel with the magnetic field and reach a state of equilibrium. At equilibrium there is a small excess of protons in the parallel position resulting in a net magnetic vector ( $M$ ). Transmission of energy carried by a

radio-frequency (RF) pulse of a particular frequency (called the Larmor or resonance frequency), forces the protons to flip from their equilibrium position (excitation) and thus causes the vector  $M$  to precess farther away from the direction of the magnetic field. When excitation is interrupted, the protons subsequently release the absorbed energy and return to their equilibrium position (relaxation). During relaxation the vector  $M$  induces an electric current in a radio antenna surrounding the patient (body coil) or a part of the patient (surface or local coil). This radio signal is used to create images.

The relaxation rate is determined by two independent phenomena, longitudinal ( $T_1$ ) and transverse ( $T_2$ ) relaxation times.  $T_1$  characterizes the return of the  $M$  vector to equilibrium along the longitudinal axis defined by  $B_0$  which is an incremental process.  $T_2$  characterizes the disappearance of the  $M$  vector in the transverse plane, perpendicular to  $B_0$ , which is a decremental process. Both relaxation times depend in a complex way on the physical and chemical characteristics of the tissue.

Signal intensity as displayed on the MR images depends on proton density i.e. the number of protons precessing in a certain tissue volume, as well as on the longitudinal and transverse relaxation time. Soft-tissue contrast with MR imaging is largely due to differences in  $T_1$  and  $T_2$  between various tissues. Because variations in  $T_1$ - and  $T_2$ -values are so much greater than variations in tissue density, MR imaging provides better soft-tissue contrast than plain radiography or CT [68].

By using specific pulses at given variable time intervals (repetition time, TR) and with given variable sampling times (echo time, TE), specific types of contrast are obtained. In conventional MR imaging predominantly spin-echo (SE) sequences are used. A SE pulse sequence with a short TR and a short TE emphasizes  $T_1$  differences between tissues and is called a  $T_1$ -weighted sequence. A SE pulse sequence with a long TR (> 1500 ms) and a long TE (> 60 ms) emphasizes  $T_2$  differences between tissues and is referred to as a  $T_2$ -weighted sequence. Proton density-weighted images are obtained with a long TR and a short TE.

More recently, various fast imaging sequences have been and are still being developed and are becoming more and more important, as they make it possible to shorten scanning times considerably [69-71]. For now it suffices to mention their ability to obtain  $T_1$ -,  $T_2$ -, and proton density-weighted images. For more detailed reading on MR imaging techniques the reader is referred to specialized textbooks.

### *MR imaging features of paragangliomas*

Paragangliomas of the head and neck can be recognized on MR images as clearly outlined lesions of intermediate signal intensity on all imaging sequences with some focal sites of high intensity scattered within the lesions on  $T_2$ -weighted images [72]. Characteristic findings with MR imaging are

the serpentine areas of low signal caused by vascular flow void in these tumours [72, 73]. After intravenous injection of gadopentetate dimeglumine (Magnevist®, Schering, Berlin, Germany) intense enhancement is seen [74].

Phaeochromocytomas show signal intensity characteristics with MR imaging that are very distinct from most other adrenal tumours. On T2-weighted images all phaeochromocytomas show a high signal intensity relative to the liver [75, 76]. This feature is known to be shared by other truncal paragangliomas [67, 77, 78]. Several studies have shown that phaeochromocytomas and adenomas can be differentiated on the basis of the signal intensity ratio tumour/liver on T2-weighted images, phaeochromocytomas having a ratio above 2.5 and silent adenomas having a ratio below 2.0. Overlap of relative intensity on T2-weighted images can be seen with other sympathomedullary tumours, cysts, haemorrhage and a number of metastases. Cysts can be differentiated from phaeochromocytomas on T1-weighted sequences based on the very low signal intensity and their specific morphological characteristics, whilst haemorrhages show a non-homogeneous high intensity on T1-weighted images [79-82].

#### *MR imaging technique used in this study*

When designing an imaging strategy for MR imaging of paragangliomas, one is confronted with an overwhelming number of options to choose from. In a clinical setting, the imaging protocols selected are necessarily a compromise between predicted optima, personal preferences, instrumental limitations and above all, procedure time in order to maintain an acceptable flow of patients. Our own procedural method represents, it should be stressed, only one of many possibilities.

Patients are examined using a body coil for initial screening of the abdomen (more than 95% of functioning paragangliomas is located in the abdomen). The imaging plane is transverse. The imaging technique includes multisection acquisition with a slice thickness of 1 cm, an intersection gap of approximately 1-2 mm, an acquisition matrix of 179 x 256 or 128 x 256 and a display matrix of 256 x 256. The field of view varies between 300 and 500 mm, depending on the slice orientation. In general, the plane resolution is less than 3 mm. The number of measurements per data line varies between two (T2-weighted sequences) and four (T1-weighted sequences). For contrast-enhanced studies, the T1-weighted MR sequence is repeated after injection of 0.1 mmol/kg body weight gadopentetate dimeglumine.

Following the investigation of the abdomen the region of the diaphragm up to the base of the skull is imaged. Imaging planes are coronal and transverse. The technique is similar to the one used for the abdomen, adjusted with ECG gating, when necessary. Imaging time varies from 1.5 to 2 hours depending on selected parameters.

We use intravenous contrast agents such as gadopentetate dimeglumine only in selected cases. Because of the natural contrast between vascular

structures and surrounding tissues in MR imaging, opacification of vessels with intravenous contrast agents as in CT is not necessary for delineation. Moreover, a disadvantage of intravenous contrast enhancement in MR imaging of the adrenals is that it may result in the reduction of contrast between normal and abnormal adrenals and surrounding retroperitoneal fat.

## 2.4. REFERENCES

1. Russell DS, Rubinstein LJ. Paragangliomas. In: Pathology of tumours of the nervous system. Russell DS, Rubinstein LJ, eds. London. Edward Arnold 1989:945-974
2. Glenner GC, Grimley PM. Tumors of the extra-adrenal paraganglion system (including chemoreceptors). Atlas of tumor pathology: second series: fascicle 9. Washington DC. Armed Forces Institute of Pathology 1974
3. Gils APG van, Mey AGL van der, Hoogma RPLM, et al. I-123 metaiodobenzylguanidine scintigraphy in patients with chemodectomas of the head and neck region. J Nucl Med 1990;31:1147-1155
4. Pryse-Davies J, Dawson IMP, Westbury G. Some morphologic, histochemical and chemical observations on chemodectomas and the normal carotid body, including a study of the chromaffin reaction and possible ganglion cell elements. Cancer 1964;17:185-202
5. Lawson W. The neuroendocrine nature of the glomus cells; an experimental, ultrastructural, and histochemical tissue culture study. Laryngoscope 1980;90:120-144
6. Williams ED, Siebenmann RE, Sobin LH. Histological typing of endocrine tumors. In: WHO international histological classification of tumors. Geneva. World Health Organisation 1980:33-39
7. Dunn GD, Brown MJ, Sapsford RN et al. Functioning middle mediastinal paraganglioma (phaeochromocytoma) associated with intercarotid paraganglioma. Lancet 1986;:1061-1064
8. Falke THM, Gils APG van, Seters AP van, Sandler MP. Magnetic resonance imaging of functioning paragangliomas. Magn Reson Q 1990;6:35-64
9. Kaufman BH, Telander RL, Heerden JA van, et al. Pheochromocytoma in the pediatric age group: current status. J Pediatric Surg 1983;18:879-884
10. Sheps SG. Pheochromocytoma. In: Clinical Medicine. Spittell JA Jr, ed. Philadelphia. Harper and Row 1981;1-22
11. Bravo EL, Gifford RW Jr. Pheochromocytoma: diagnosis, localization and management. N Engl J Med 1984;311:1298-1303
12. Scott HW. Anatomy of the adrenal glands and bilateral adrenalectomy. In: Mastery of surgery. Nyhus LM, Baker RJ, eds. Boston. Little, Brown and Company 1992;1373-1378
13. Heerden JA van, Sheps SG, Hamberger B, Sheedy II PF, Poston JG, ReMine WH. Pheochromocytoma: current status and changing trends. Surgery 1982;91:367-373
14. Proye C, Fossati, Fontaine P, et al. Dopamine-secreting pheochromocytoma: an unrecognized entity? Classification of pheochromocytomas according to their type of secretion. Surgery 1986;100:1154-1162

15. Grimley PM. Multicentric paragangliomas and associated neuroendocrine tumors. In: Local invasion and spread of cancer. Brunson KW, ed. Dordrecht. Kluwer academic publishers 1989;49-61
16. DeAngelis LM, Kelleher MB, Post KD, Fetell MR. Multiple paragangliomas in neurofibromatosis: a new neuroendocrine neoplasia. *Neurology* 1987;37:129-133
17. Sheps SG, Jiang NS, Klee GG. Diagnostic evaluation of pheochromocytoma. *Endocrin Metab Clin N Am* 1988;17:397-414
18. Jansson S, Tisell L-E, Hansson G, Stenström G. Multiple neuroectodermal abnormalities in pheochromocytoma patients. *World J Surg* 1988;12:710-717
19. Raue F, Frank K, Meybier H, Ziegler R. Pheochromocytoma in multiple endocrine neoplasia. *Cardiology* 1985;72 (suppl.):147-149
20. Webb TA, Sheps SG, Carney JA. Difference between sporadic pheochromocytoma and pheochromocytoma in multiple endocrine neoplasia, type 2. *Am J Surg Pathol* 1980;4:121-126
21. Carney JA. The triad of gastric epithelioid leiomyosarcomas, pulmonary chondroma, and functioning extra-adrenal paragangliomas: a five year review. *Medicine* 1983;62:159-169
22. White MC, Hickson BR. Multiple paragangliomas secreting catecholamines and calcitonin with intermittent hypercalcaemia. *J R Soc Med* 1979;72:532-538
23. Doppmann JL, Nieman L, Miller DL, et al. Ectopic adrenocorticotrophic hormone syndrome: localization studies in 28 patients. *Radiology* 1989;172:115-124
24. Lawson W. Glomus bodies and tumors. *New York J Med* 1980;80:1567-1575
25. Zak FG, Lawson W. The paraganglionic chemoreceptor system. Physiology, pathology, and clinical medicine. New York Springer Verlag Inc 1982
26. Mey AGL van der, Frijns JHM, Cornelisse CJ, et al. Does intervention improve the natural course of glomus tumors? *Ann Otol Rhinol Laryngol* 1992;101:635-642
27. Holton P. Noradrenaline in tumors of the adrenal medulla. *J Physiol* 1949;108:525-529
28. Azzarelli B, Felten S, Miyamoto R, Muller J, Purvin V. Dopamine in paragangliomas of the glomus jugulare. *Laryngoscope* 1988;98:573-578
29. Plouin PF, Chatellier G, Rougeot MA, et al. Recent developments in pheochromocytoma diagnosis and imaging. *Adv Nephrol* 1988;17:275-286
30. Duncan MW, Compton PC, Lazarus L, Smythe GA. Measurement of norepinephrine and 3,4-dihydroxyphenylglycol in urine and plasma for the diagnosis of pheochromocytoma. *N Engl J Med* 1988;319:136-142
31. St John Sutton MG, Sheps SG, Lie JT. Prevalence of clinically unsuspected pheochromocytoma. Review of a 50-year autopsy series. *Mayo Clin Proc* 1981;56:354-360
32. Gifford RW Jr, Kvale WF, Maher FT, Roth GM, Priestly JT. Clinical features, diagnosis and treatment of pheochromocytoma: a review of 76 cases. *Mayo Clin Proc* 1964;39:281-302
33. Telenius-Berg M, Berg B, Hamberger B, Tibblin S. Screening for early asymptomatic pheochromocytoma in MEN II. *Henry Ford Hosp Med J* 1987;35:110-114
34. Gagel RF, Tashjian AH Jr, Cummings I, et al. The clinical outcome of prospective screening for multiple endocrine neoplasia type 2a. *N Engl J Med* 1988;318:478-484
35. Samaan NA, Hickey RC, Shutts PE. Diagnosis, localization and management of pheochromocytoma. *Cancer* 1988;62:2451-2460
36. Shapiro B, Copp JE, Sisson JC, Eyre PL, Wallis J, Beierwaltes WH. Iodine-131 metaiodobenzylguanidine for the locating of suspected pheochromocytoma: experience in 400 cases. *J Nucl Med* 1985;26:576-585
37. Allison DJ, Brown MJ, Jones DH, Timmis JB. Role of venous sampling in locating a pheochromocytoma. *Br Med J* 1983;286:1122-1124
38. Scott HW, Van Way CW, Gray GF, Sussman CR. Pheochromocytoma. In: *Surgery of the adrenal glands*. Scott HW, ed. Philadelphia. JB Lippincott Company 1990;187-223
39. Agee OF, Kaude J, Lepasoon J. Preoperative localization of pheochromocytoma. *Acta Radiologica Diagnostica* 1973;14:548-560
40. Sutton D. The radiological diagnosis of adrenal tumours. *Br J Radiol* 1975;48:237-258.
41. Costello P, Clouse ME, Kane RA, Paris A. Problems in the diagnosis of adrenal tumors. *Radiology* 1977;125:335-341
42. Derchi LE, Serafini C, Rabbia C, et al. Carotid body tumors: US evaluation. *Radiology* 1992;182:457-459
43. Moss AA. Computed tomography of the adrenal glands. In: *Computed tomography of the body*. Moss AA, Gamsu G, Genant HK, eds. Philadelphia. Saunders 1983:837-876
44. Greenberg M, Moawad AH, Wieties BM, et al. Extraadrenal pheochromocytoma: detection during pregnancy using MR imaging. *Radiology* 1986;161:475-476
45. Jackson CE, Tashjian AH. Limited progression of hereditary medullary thyroid cancer after conservative management (abstr). *Am J Hum Genet* 1992;51(P):235
46. Wieland DM, Swanson DP, Brown LE, Beierwaltes WH. Imaging of the adrenal medulla with an I-131-labeled antiadrenergic agent. *J Nucl Med* 1979;20:155-158
47. Sisson JC, Frager MS, Valk TW, et al. Scintigraphic localization of pheochromocytoma. *N Engl J Med* 1981;305:12-17
48. Wieland DM, Brown LE, Tobes MC, et al. Imaging the primate adrenal medulla with I-123 and I-131 Metaiodobenzylguanidine: concise communication. *J Nucl Med* 1981;22:358-364
49. Sisson JC, Wieland DM. Radiolabeled meta-iodobenzylguanidine: pharmacology and clinical studies. *Am J Physiol Imag* 1986;1:96-103
50. Mangner TJ, Tobes MC, Wieland DW, Sisson JC, Shapiro B. Metabolism of Iodine-131 Metaiodobenzylguanidine in patients with metastatic pheochromocytoma. *J Nucl Med* 1986;27:37-44
51. Sandler MP. The expanding role of MIBG in clinical medicine. *J Nucl Med* 1988;29:1457-1458
52. Gross MD, Shapiro B. Scintigraphic studies in adrenal hypertension. *Sem Nucl Med* 1989;19:122-143
53. Lindberg S, Fjalling M, Jacobsen L, Jansson S, Tisell L-E. Methodology and dosimetry in adrenal medullary imaging with Iodine-131 MIBG. *J Nucl Med* 1988;29:1638-1643
54. Jacques S Jr, Tobes MC, Sisson JC, Baker JA, Wieland DM. Comparison of the sodium dependency of uptake of meta-iodobenzylguanidine and norepinephrine into cultured bovine adrenomedullary cells. *Mol Pharmacol* 1984;26:539-546
55. Tobes MC, Jacques S Jr, Wieland DM, Sisson JC. Effect of uptake-one inhibitors on the uptake of norepinephrine and metaiodobenzylguanidine. *J Nucl Med* 1985;26:897-907

56. Bomanji J, Bouloux PMG, Levison DA, et al. Observations on the function of normal adrenomedullary tissue in patients with pheochromocytomas and other paragangliomas. *Eur J Nucl Med* 1987;13:86-89
57. Gasnier B, Roisen MP, Scherman D, Coornaert S, Desplanches G, Henry JP. Uptake of metaiodobenzylguanidine by bovine chromaffin granule membranes. *Mol Pharmacol* 1985;29:275-280
58. Nakajo M, Shapiro B, Copp J, et al. The normal and abnormal distribution of the adrenomedullary agent <sup>131</sup>I-metaiodobenzylguanidine (<sup>131</sup>I-MIBG) in man: evaluation by scintigraphy. *J Nucl Med* 1983;24:672-682
59. Lynn MD, Shapiro B, Sisson JC, et al. Portrayal of pheochromocytoma and normal human adrenal medulla by <sup>123</sup>I-meta-iodobenzylguanidine(<sup>123</sup>I-MIBG). *J Nucl Med* 1984;25:436-440
60. McEwan AJ, Shapiro B, Sisson JC, Beierwaltes WH, Ackery DM. Radioiodobenzylguanidine for the scintigraphic location and therapy of adrenergic tumors. *Sem Nucl Med* 1985;15:132-153
61. Moyes JSE, Babich JW, Carter R, Meller ST, Agrawal M, McElwain T. Quantitative study of radioiodinated metaiodobenzylguanidine uptake in children with neuroblastoma: correlation with tumor histopathology. *J Nucl Med* 1989;30:474-480
62. Bomanji J, Levison DA, Flatman WD, et al. Uptake of Iodine-123 MIBG by pheochromocytomas, paragangliomas, and neuroblastomas: a histopathological comparison. *J Nucl Med* 1987;28:973-978
63. Moll L von, McEwan AJ, Shapiro B, et al. Iodine-131 MIBG scintigraphy of neuroendocrine tumors other than pheochromocytoma and neuroblastoma. *J Nucl Med* 1987;28:979-988
64. Solanki KK, Bomanji J, Moyes J, Mather SJ, Trainer PJ, Britton KJ. A pharmacological guide to medicines which interfere with the biodistribution of radiolabelled meta-iodobenzylguanidine (MIBG). *Nucl Med Com* 1992;13:513-521
65. Khafagi FA, Shapiro B, Fig LM, Malette S, Sisson JC. Labetalol reduces Iodine-131 MIBG uptake by pheochromocytoma and normal tissues. *J Nucl Med* 1989;30:481-489
66. Wieland DM, Wu JL, Brown JL, et al. Radiolabeled adrenergic neuron-blocking agents: adrenomedullary imaging with <sup>131</sup>I-iodobenzylguanidine. *J Nucl Med* 1980;21:349-353
67. Schmedtje JE, Sax S, Pool JL, Goldfarb RA, Nelson EB. Localization of ectopic pheochromocytomas by magnetic resonance imaging. *Am J Med* 1987;83:770-772
68. Edelman RR, Warach S. Magnetic resonance imaging. *N Engl J Med* 1993;328:708-716
69. Winkler ML, Ortendahl DA, Mills TC, et al. Characteristics of partial flip angle and gradient reversal MR imaging. *Radiology* 1988;166:17-26
70. Matthaei D, Frahm J, Haase A, Hänicke W, Merboldt K-D. Three-dimensional flash MR imaging of thorax and abdomen without triggering or gating. *Magn Reson Imaging* 1986;4:381-386
71. Jones KM, Mulkern RV, Schwartz RB, Oshio K, Barnes PD, Jolesz FA. Fast spin-echo MR imaging of the brain and spine: current concepts. *AJR* 1992;158:1313-1320
72. Som PM, Sacher M, Stollman AL, Biller HF, Lawson W. Common tumors of the parapharyngeal space: refined imaging diagnosis. *Radiology* 1988;169:81-85

73. Rippe DJ, Grist TM, Uglietta JP, Fuller GN, Boyko OB. Carotid body tumor: flow sensitive pulse sequences and MR angiography. *J Comput Assist Tomogr* 1989;13:874-877
74. Vogl T, Brüning R, Schedel H, et al. Paragangliomas of the jugular bulb and carotid body: MR imaging with short sequences and Gd-DTPA enhancement. *AJNR* 1989;10:823-827
75. Glazer GM, Woolsey EJ, Borello J, et al. Adrenal tissue characterization using MR imaging. *Radiology* 1986;158:73-79
76. Fink IJ, Reinig JW, Dwyer AJ, Doppman JL, Linehan WM, Keiser HR. MR imaging of pheochromocytomas. *J Comput Assist Tomogr* 1985;9:454-458
77. Fisher MR, Higgins CB, Andereck W. MR imaging of an intrapericardial pheochromocytoma. *J Comput Assist Tomogr* 1985;9:1103-1105
78. Flickinger FW, Yuh WTC, Behrendt DM. Magnetic resonance imaging of mediastinal paraganglioma. *Chest* 1988;94:652-654
79. Reinig JW, Doppman JL, Dwyer AJ, Johnson AR, Knop RH. Adrenal masses differentiated by MR. *Radiology* 1986;158:81-84
80. Chezmar JL, Robbins SM, Nelson RC, Steinberg HV, Torres WE, Bernadino ME. Adrenal masses: characterization with T1-weighted MR imaging. *Radiology* 1988;166:357-359
81. Krestin GP, Steinbrich W, Friedman G. Adrenal masses: evaluation with fast gradient-echo MR imaging and Gd-DTPA-enhanced dynamic studies. *Radiology* 1989;171:675-680
82. Kier R, McCarthy S. MR characterization of adrenal masses: field strength and pulse sequence considerations. *Radiology* 1989;171:671-674

# 3

## I-123 METAIODOBENZYLGUANIDINE SCINTIGRAPHY IN PATIENTS WITH PARAGANGLIOMAS OF THE HEAD AND NECK REGION\*

### 3.1. INTRODUCTION

Chemodectomas, also known as glomus tumours, arise from paraganglionic tissue in the carotid body, the jugular fossa, the middle ear and superior mediastinum. Chemodectomas are extremely rare and of unknown incidence [1]. About 30% of the cases are familial in origin. The hereditary pattern of familial chemodectomas appears to be autosomal dominant [1]. Multiple chemodectomas occur in approximately 25% to 35% of the patients with familial chemodectoma but in less than 5% of those with the non-familial type [2]. Malignancy occurs in approximately 10% [3]. Together with the aorticosympathetic, visceral-autonomic and intravagal paragangliomas and pheochromocytomas they form a class of tumours known as paragangliomas [4-6]. Paraganglion cells are derived from the neural crest and migrate in close association with the autonomic ganglion cells. The common feature of these cells is the presence of numerous neurosecretory granules containing catecholamine in their cytoplasm. The highest concentration of these paraganglion cells is in the adrenal medulla, however they are also found in abundance along the aorta and great vessels [7, 8].

Functioning paragangliomas may arise wherever paraganglion tissue exists but are called pheochromocytomas when they develop in the adrenal gland [4]. The proportion of hormonally active paragangliomas is thought to be high for adrenal pheochromocytomas, intermediate for aorticosympathetic and visceral-autonomic paragangliomas and low for chemodectomas [9]. The percentage of hormonally active chemodectomas has been estimated to be about 1% [10]. The association of head and neck chemodectomas with other paragangliomas (usually pheochromocytomas) as well as several other tumours (carcinoid, pituitary adenoma, thyroid carcinoma) deriving from the neural crest has been reported [2, 9, 11-18], but these combinations are considered to be very rare [16].

The uptake of radioactive labelled metaiodobenzylguanidine (MIBG) has been demonstrated in pheochromocytomas [19] and neuroblastomas [20] as

\* Based on: I-123 metaiodobenzylguanidine scintigraphy in patients with chemodectomas of the head and neck region. APG van Gils, AGL van der Mey, RPLM Hoogma, THM Falke, AJ Moolenaar, EKJ Pauwels, MJP van Kroonenburgh. J Nucl Med 1990;31:1147-1155

well as in carcinoids [21], medullary carcinomas of the thyroid and chemodectomas [22-24]. The largest study on chemodectomas so far comprised five patients, imaged with I-131 MIBG [22]. We performed an I-123 MIBG study in 15 patients with a total of 24 chemodectomas. Urinary catecholamines and vanillylmandelic acid (VMA) levels were measured for correlation with the findings of I-123 MIBG imaging. Patients with elevated urinary catecholamine secretion and/or unexpected I-123 MIBG concentrations outside the head and neck region underwent further investigations to detect the source of catecholamine production.

### 3.2. MATERIAL AND METHODS

Between January and November 1988, 15 patients, ranging in age from 22 to 65 years (mean age 45 years) were referred for endocrinological analysis and I-123 MIBG scintigraphy by the Department of Otolaryngology. All patients gave informed consent. In the head and neck region of these patients 24 chemodectomas were present: 11 jugular glomus tumours, seven carotid body tumours and six vagal body tumours. In this series no tympanic glomus tumours were seen. Nine patients were followed because of incomplete tumour removal, attributable mainly to the technical limitations encountered in the safe excision of these tumours from the cranial base. Four patients were analyzed preoperatively and in two cases surgery was either not performed or not planned, for technical reasons. The patients exhibited the common presenting symptoms of the carotid and vagal body tumours, with a painless pulsating lateral cervical mass near the angle of the mandible. The glomus jugulare tumours gave rise to aural symptoms, such as conductive hearing loss, pulsatile tinnitus, a discoloured eardrum and sometimes cranial nerve palsy. In all 15 patients the diagnosis of chemodectoma was based on these clinical symptoms and characteristic findings on angiograms, as described elsewhere [3]. Except for patient No. 10 histological confirmation of the chemodectoma(s) was present in all patients. Twelve cases were familial, involving nine kindreds. Ten patients showed multiple chemodectomas on angiography. In two of these ten patients, one or more chemodectomas had already been removed prior to scintigraphy. A list of all drugs recently used was obtained to rule out interference with I-123 MIBG uptake; special attention was paid to drugs such as reserpine, tricyclic antidepressants, phenylpropanolamine, labetalol and sympatholytic agents [25].

#### Scintigraphy.

Each patient was injected intravenously with 370 MBq I-123 MIBG while in the supine position. I-123 MIBG was obtained from 'Cygne' B.V. (Eindhoven,

The Netherlands). The synthesis of I-123 MIBG was performed by the method of Wieland et al. [26]. I-123 was produced by the Xe-124 (p,2n) reaction with specification of a maximum I-125 impurity of 0.01% at the time of calibration. I-123 MIBG (specific activity at least 925 MBq per milligram) was diluted in bacteriostatic phosphate buffer (pH 6.0-6.5) to a specific concentration of at least 74 MBq/ml. The free iodine concentration was less than 0.2%. Thyroidal uptake was blocked by the administration of Lugol's solution, ten drops three times daily (50 mg of iodine) for five days, starting the day before the injection.

A large field-of-view gamma camera (Toshiba GCA 90B<sup>®</sup>, Toshiba, Tokyo, Japan) equipped with a low energy general purpose collimator and interfaced to a dedicated computer (Toshiba GMS-55<sup>®</sup>, Toshiba) was used. A 20% window was centred at 159 KeV. In all cases anterior and posterior digitized images of the total body and four images of the head and neck were obtained 24 hours and, in most cases, 48 hours after the injection. Additional single photon emission computer tomography (SPECT) of the head and neck of all patients was performed 24 hours after the injection. From the SPECT study transaxial, sagittal and coronal slices, 5.3 mm thick, were reconstructed.

#### Computer tomography.

Seven patients with elevated catecholamine levels (patients 1,3,6,7,10,12 and 14) of whom five had abnormal I-123 MIBG concentrations outside the head and neck region were subsequently examined with a Tomoscan 350<sup>®</sup> (Philips, Best, The Netherlands) scanner. Initial screening of the abdomen was performed using 10 mm thick adjacent slices. If this routine scan was equivocal or negative, a more meticulous examination of the region showing abnormal I-123 MIBG uptake was carried out. Such a procedure included narrow collimation in combination with geometric enlargement and back projection magnification. Care was taken that the entire region was visualized and that no major anatomical gaps were introduced by inconsistent expiration between individual slices. In three cases the CT examination was repeated after intravenous injection of 50 cc meglumine ioxitolate (Telebrix 350<sup>®</sup>, Guerbet, Aulnay-sous-Bois, France).

#### Magnetic Resonance imaging.

Patients 1,3,6,7,10,12 and 14 were examined at 0.5 T using a Gyroscan-S5<sup>®</sup> (Philips) scanner. In all cases a body coil was used. Imaging technique included multisectonal acquisition of the adrenal area with 1 cm-thick transverse slices, intersection gaps of approximately 1 mm, an acquisition

**Table 3.1. Demographic, scintigraphic and hormone data on patients with chemodectoma.**

Patient No.	Age	Sex	Kindred*	Multi centricity	MIBG uptake in chemodectoma	Abnormal MIBG uptake elsewhere	Urinary Excretion				Measurements		
							Vanillylmandelic acid $\mu\text{mol}/24\text{hr}$ range	mean	Norepinephrine $\mu\text{mol}/24\text{hr}$ range	mean		Dopamine $\mu\text{mol}/24\text{hr}$ range	mean
1	41	F	—	—	+	—	22 - 35	28.5	0.72 - 1.42	1.02	0.76 - 1.78	1.40	5
2	36	M	A	+	+	—	15 - 22	18.0	0.13 - 0.34	0.25	1.58 - 1.90	1.72	3
3	24	M	B	—	—	left adrenal	36 - 102	73.0	4.35 - 6.50	5.27	1.69 - 7.42	3.22	7
4	31	M	A	+	—	—	14 - 28	20.7	0.18 - 0.42	0.32	0.91 - 1.73	1.54	3
5	22	F	C	+	—	—							
6	49	F	D	+	—	left adrenal	21 - 27	25.0	1.04 - 1.82	1.53	1.70 - 2.50	1.98	3
7	39	F	E	—	—	—	19 - 27	23.0	0.24 - 0.34	0.30	2.52 - 5.88	4.66	3
8	65	F	F	+	+	—	20 - 26	23.0	0.20 - 0.21	0.21	0.69 - 0.76	0.72	3
9	50	F	F	—	+	—	25 - 37	29.0	0.20 - 0.26	0.23	0.21 - 0.90	0.59	3
10	62	F	—	+	+	right adrenal	10 - 24	18.3	0.31 - 0.82	0.56	1.08 - 1.44	1.30	3
11	48	F	G	+	—	—	17 - 18	17.3	0.26 - 0.32	0.28	1.89 - 2.09	2.01	3
12	41	F	H	+	—	left adrenal	10 - 17	13.3	0.41 - 0.75	0.53	2.31 - 3.34	2.68	3
13	58	F	—	+	+	—	15 - 18	16.7	0.11 - 0.20	0.16	0.21 - 0.90	0.59	3
14	64	M	I	+	+	left paramedian mid-abdominal	20 - 28	25.0	0.35 - 0.88	0.56	0.35 - 3.57	2.14	4
15	26	M	B	—	+	—	21 - 27	23.3	0.22 - 0.38	0.28	1.94 - 2.44	2.13	3
							<i>Normal values</i> < 30		<i>Normal values</i> 0.06 - 0.47		<i>Normal values</i> 0.46 - 3.40		

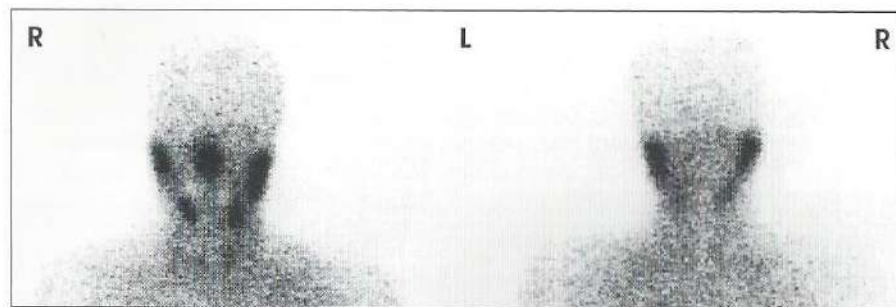
\*Letters A-I denote separate kindreds

matrix of 179 x 256 and a display matrix of 256 x 256. The field of view was 400 mm. Patients were examined with a spin-echo sequence TR 300/TE 20 and a spin-echo sequence TR 2000/TE 50-100. After imaging of the adrenal area, T2-weighted coronal images of the lower abdomen and mediastinum were taken in two series using a field of view of 500 mm. If this routine scan was equivocal, a more meticulous examination of the area of interest was carried out using transverse T1- and T2-weighted images. In all cases plane resolution was less than 3 mm. The number of measurements per data line was two (T2-weighted sequences) or six (T1-weighted sequences). Software

for motion compensation was not used. Total procedure time varied from 1.5 to 2 hours.

#### Catecholamine measurements.

The urinary excretion of free norepinephrine, epinephrine, dopamine and vanillylmandelic acid was assessed in 24-hour urine samples collected on three consecutive days. Free norepinephrine, epinephrine and dopamine



3.1.A

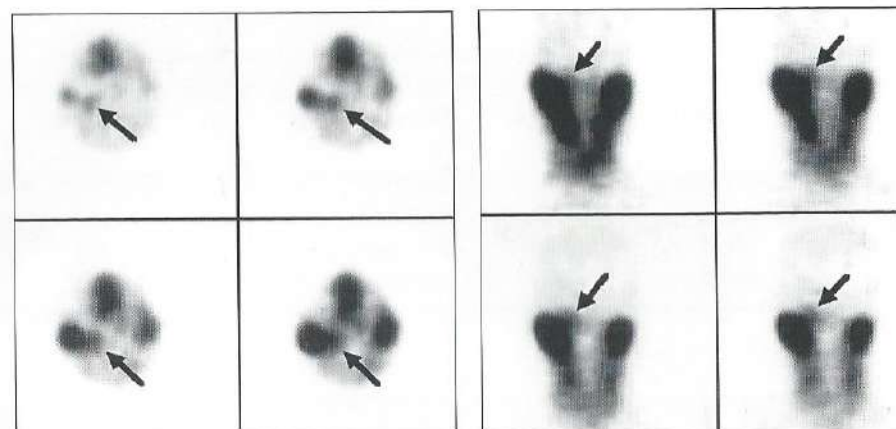
Figure 3.1. A) Anterior and posterior I-123 MIBG images of the head do not reveal any uptake in a chemodectoma. B and C) Transaxial and coronal SPECT images show distinct uptake of I-123 MIBG in right jugular chemodectoma (arrows). (L = left, R = right).

levels were assayed by high-performance liquid chromatography (HPLC) and electrochemical detection (Coulchem 5100 A ESAR). VMA levels were measured by colorimetry after paper chromatography. For four patients (3,6,7 and 14) the levels of norepinephrine, epinephrine and dopamine in the tumour tissue were determined by the HPLC method and expressed as mmol/g tumour tissue.

### 3.3. RESULTS

Fourteen of the fifteen patients completed the study. One patient (No. 5) underwent the clinical examination and scintigraphy but failed to supply the 24-hour urine samples (lack of co-operation). The clinical examinations in the fifteen patients rendered the following additional information: only one of the fifteen patients (No. 14) had a history, that was indicative of a functioning paraganglioma, i.e. hypertension, episodic headaches, palpitations and heavy perspiration. This had been disregarded for more than 20 years. On physical examination five patients (1,8,9,10 and 14) had hypertension, according to the definition of the W.H.O. [27]; only one patient (No. 14) received medication (verapamil chloride) for it. The other patients had no signs or symptoms suggesting a hormonally active tumour.

None of the patients experienced any side effects of the I-123 MIBG injection. Table 3.1 lists the patient data, the scintigraphic findings and the urinary levels of free norepinephrine, free epinephrine, dopamine and VMA. I-123 MIBG uptake in one or more chemodectomas in seven patients (1, 2, 8, 10, 13, 14 and 15) was visualized on planar views and SPECT images. In one patient (No. 9) I-123 MIBG uptake by a chemodectoma was detected only by SPECT (figure 3.1). In total 13 of the 24 chemodectomas were visualized. Neither the planar views nor the SPECT images revealed any uptake in the chemodectomas of the other seven patients. For each patient showing I-123



3.1.B

3.1.C

MIBG uptake all known chemodectomas were visualized. Most chemodectomas showed low to moderate uptake of I-123 MIBG. Only patient 1 showed a high uptake in a sporadic chemodectoma which proved to be a norepinephrine-secreting chemodectoma.

In five patients (3,6,10,12 and 14) abnormal locations of I-123 MIBG were noted in the abdomen. Only one of them (No. 14) showed simultaneous moderate I-123 MIBG uptake in a chemodectoma.

Seven patients (1,3,6,7,10,12 and 14) with elevated catecholamine levels of whom five had abnormal I-123 MIBG concentrations in the abdomen underwent further examination. The results of the CT and MR imaging investigations in these seven patients and the histopathological data are shown in table 3.2. Patients 3 and 6 had a pheochromocytoma of the left adrenal gland that was excised under labetalol prophylaxis without adverse effects. In patient 14 an aorticosympathetic paraganglioma was removed. Histologically these tumours resembled the paraganglionic tissue found in pheochromocytomas. The tumours contained only norepinephrine. In all three patients (3, 6 and 14) catecholamine secretion normalized postoperatively. Patient 14 became free of symptoms.

Patient 1 had a left-sided glomus jugulare tumour that was partially removed. During and after the operation periods of severe hypertension developed but could be managed with 400 mg labetalol three times a day. Postoperatively, norepinephrine excretion normalized, but VMA excretion was elevated on one follow-up visit. In two patients (10 and 12) no lesions were revealed by either CT or MR imaging, although distinct abdominal deposits of I-123 MIBG had been seen on two consecutive days. Patient 7 underwent partial resection of a vagal body tumour that was not revealed by I-123 MIBG imaging. The tumour contained only dopamine.

Table 3.2. Analysis of patients with elevated catecholamine excretion.

Patient No.	Vanillylmandelic Acid		Norepinephrine		Dopamine		CT /MRI Abdomen	Histological Diagnosis	Tumour content	
	Elevated no. of measurements	Total no. of measurements	Elevated no. of measurements	Total no. of measurements	Elevated no. of measurements	Total no. of measurements			Norepinephrine $\mu\text{mol/g}$	Dopamine (nmol/g)
1	2	5	5	5	0	5	normal	jugular chemodectoma	(measurement not performed)	
3	7	7	7	7	1	7	phaeochromocytoma in left adrenal	phaeochromocytoma	2.35	0
6	0	3	3	3	0	3	phaeochromocytoma in left adrenal	phaeochromocytoma	22.1	0
7	0	3	0	3	2	3	normal	vagal chemodectoma	0	15
10	0	3	2	3	0	3	normal	—	—	—
12	0	3	1	3	0	3	normal	—	—	—
14	0	4	2	4	1	4	para-aortic paraganglioma	paraganglioma	3.4	0

Postoperatively, the average dopamine excretion decreased but did not normalize, probably because a large part of the tumour remained in situ.

### 3.4. DISCUSSION

The standard for diagnosis of chemodectomas is angiography. However, this is an invasive procedure and is therefore only performed preoperatively to demonstrate the vascular supply of these lesions [3]. For screening purposes and postoperative control, contrast-enhanced CT is used [28]. A scintigraphic method offers several potential advantages such as better detection of recurrent lesions in a scarred field, the absence of artifacts from clips, and the possibility of detecting metastases in the entire body. A further advantage is the absence of the small but appreciable risk of contrast reactions. For

these reasons we evaluated the use of I-123 MIBG in patients with chemodectomas.

Because normal I-123 MIBG uptake in parotid glands and submandibular glands interferes with the visualization of chemodectomas, planar views were supplemented by SPECT of the head and neck area. SPECT made the delineation of chemodectomas easier and demonstrated a chemodectoma in one patient that was not visible on planar views. In total we noticed uptake ranging from low to high intensity in 13 of 24 chemodectomas accounting for 54%. Von Moll et al. using I-131 MIBG found uptake in 2 out of 5 chemodectomas (40%) [22]. The number of chemodectomas in the latter study is too small to make a valid comparison between the two isotopes. It is interesting to notice that the norepinephrine-secreting tumour in patient 1 showed the highest uptake. Shapiro et al. reported two catecholamine-secreting chemodectomas showing no I-131 MIBG uptake [19]. Whether this

discrepancy is caused by the lower dose of I-131 MIBG, or by differences in norepinephrine kinetics is not clear. As already stated by von Moll et al. the ability of a tumour to take up MIBG can be independent of its ability to secrete catecholamines [22]. The moderate sensitivity found in our study suggests a limited role for I-123 MIBG in patients with chemodectomas.

However, in performing I-123 MIBG scintigraphy and urinary screening for catecholamines, we unexpectedly found a high number of surgically proved catecholamine-secreting tumours of the paraganglia (functioning paragangliomas). I-123 MIBG uptake provided an important clue to the hormonal activity of four of the five functioning paragangliomas. This was particularly the case in patient 14 who initially showed only marginally elevated urinary catecholamine levels despite his obvious symptoms.

Hormonal activity in patients with chemodectomas can be caused by the chemodectoma itself or by an associated catecholamine-secreting tumour in the thorax or the abdomen. The percentage of hormonally active chemodectomas has been estimated to be about 1% [10]. Approximately 2000 patients with one or more chemodectomas have been described. There are 17 documented cases of associated functioning paragangliomas outside the head and neck region suggesting an overall incidence of less than 1% [9, 10, 29].

The high incidence of functioning paragangliomas (functioning chemodectomas included) in our study may be attributable to several factors.

First, we screened all patients for hormonal activity. In the past this was probably only performed in the event of clinical symptoms that suggested a hormonally active tumour. In our group, only patient 14 had symptoms suggesting a catecholamine-secreting tumour. These symptoms had, however, not been appreciated prior to this study. For the four other patients with a functioning paraganglioma, symptoms of a hormonally active tumour were equivocal or absent.

Secondly, not only the VMA levels in 24-hour urine samples were measured, as in the past [10], but also the free catecholamine levels. According to Duncan et al. this is the most sensitive method for detecting phaeochromocytomas [30]. The VMA levels were elevated in only one patient in our series and marginally elevated in a second. Even when elevated, the possibility of a functioning chemodectoma is sometimes disregarded. Smit et al. described a patient with a chemodectoma showing intense I-131 MIBG uptake and modestly elevated urinary VMA levels, which they attributed to cardiac failure rather than to excessive secretion of the chemodectoma [24].

Thirdly, we performed whole-body scintigraphy with I-123 MIBG, which is probably more sensitive in detecting phaeochromocytomas and provides better image quality than I-131 MIBG [31]. To our knowledge whole-body imaging has never been performed before in such a large group of patients with chemodectomas.

Of course some selection may have occurred. A high percentage of the patients studied were known to have a familial history of multiple chemo-

dectomas. Since the aim of our study was to evaluate I-123 MIBG scintigraphy of chemodectomas in the head and neck region, we could only investigate patients who had not been operated upon for technical reasons, i.e. those with multiple chemodectomas or those who had undergone only a partial resection. Patients with multiple chemodectomas may be more prone to develop an associated functioning paraganglioma. We reviewed the case reports collected by Dunn et al. and found that of the 16 patients with a functioning paraganglioma and one or more chemodectomas, at least 10 had multiple chemodectomas and 6 had a familial history [9]. In our patient population there was one patient with a solitary chemodectoma associated with a phaeochromocytoma, but chemodectomas occurred in his family history.

Retrospective analysis of the data on 20 patients with chemodectoma examined in our hospital in the past five years revealed another patient with a solitary, non-familial chemodectoma and a functioning mediastinal paraganglioma.

The familial occurrence of the association of chemodectoma with a paraganglioma has been described [2, 16]. As shown in table 3.1 the high incidence of functioning paragangliomas in this study was not due to the enrollment of several members of one family with both types of tumour.

Two patients (10 and 12) exhibited an increased uptake of I-123 MIBG in an adrenal gland with elevated levels of norepinephrine; however, these findings were not confirmed by CT or MR imaging. These two patients will be followed because phaeochromocytomas are known to develop gradually in the course of decades and an increase in the uptake of I-123 MIBG may be the earliest evidence of adrenal medullary disease [32, 33].

The patient with the dopamine-producing chemodectoma is the fourth patient to be reported in the literature [34]. The tumour was not visualized by I-123 MIBG. Proye et al. have described two cases of dopamine-producing phaeochromocytomas that were not revealed by I-131 MIBG either [35]. Interestingly, neither the chemodectoma nor the two phaeochromocytomas, described by Proye et al. contained any norepinephrine. The most likely explanation for the non-visualization of these dopamine-secreting paragangliomas is the absence of a specific norepinephrine uptake mechanism and/or a defective storage mechanism.

Although the number of chemodectomas taking up I-123 MIBG is limited, this does not imply that I-131 MIBG cannot play an important role in the treatment of irresectable chemodectomas, showing the capacity to store MIBG. Patient 1 is currently being considered for treatment with therapeutic doses of I-131 MIBG, because the chemodectoma showed its capacity for MIBG uptake and is not susceptible to further surgical treatment.

In conclusion, this study suggests that functioning paragangliomas in patients with chemodectomas are more common than is estimated in the literature. Because of the selection, the high percentage of functioning

paragangliomas cannot directly be extrapolated to solitary, non-familial chemodectomas. Nevertheless, with long-term follow-up and appropriate screening, functioning paragangliomas will be seen with increasing frequency in patients with chemodectomas. For this reason and because of the paucity of symptoms, we feel that patients with chemodectomas should be screened for elevated 24-hour urinary catecholamine levels.

### 3.5. REFERENCES

- Grufferman S, Gillman MW, Pasternak LR, Peterson CL, Young WG. Familial carotid body tumors: case report and epidemiologic review. *Cancer* 1980;46:2116-2122
- Parkin JL. Familial multiple glomus tumors and pheochromocytomas. *Ann Otol Rhinol Laryngol* 1981;90:60-63
- Zak FG, Lawson W. The paraganglionic chemoreceptor system. Physiology, pathology, and clinical medicine. New York. Springer Verlag Inc 1982;583
- Grimley PM, Glenner GC. Histology and ultrastructure of carotid body paragangliomas. Comparison with the normal gland. *Cancer* 1967;20:1473-1488
- Glenner GC, Grimley PM. Tumors of the extra-adrenal paraganglion system (including chemoreceptors). Atlas of tumor pathology: second series: fascicle 9. Washington DC: Armed Forces Institute of Pathology 1974
- Williams ED, Siebenmann RE, Sobin LH. Histological typing of endocrine tumors. In: WHO international histological classification of tumors. Geneva. World Health Organisation 1980;33-39
- Farr HW. Carotid body tumors: a 40-year study. *CA* 1980;30:260-265
- Karasov RS, Sheps SG, Carney JA, Heerden JA van, Quatro V de. Paragangliomatosis with numerous catecholamine producing tumors. *Mayo Clin Proc* 1982;57:590-595
- Dunn GD, Brown MJ, Sapsford RN, et al. Functioning middle mediastinal paraganglioma (phaeochromocytoma) associated with intercarotid paraganglioma. *Lancet* 1986;i:1061-1064
- Lawson W. Glomus bodies and tumors. *New York J Med* 1980;80:1567-1575
- Revak CS, Morris SE, Alexander GH. Pheochromocytoma and recurrent chemodectomas over a twentyfive year period. *Radiology* 1971;100:53-54
- Sato T, Saito H, Yoshinaga K, Shibota Y, Sasano N. Concurrence of carotid body tumor and pheochromocytoma. *Cancer* 1974;34:1787-1795
- Bogdasarian RS, Lotz PR. Multiple simultaneous paragangliomas of the head and neck in association with multiple retroperitoneal pheochromocytomas. *Otolaryngol Head Neck Surg* 1979;87:648-652
- White MC, Hickson BR. Multiple paragangliomas secreting catecholamines and calcitonin with intermittent hypercalcaemia. *J R Soc Med* 1979;72:532-538
- Kennedy DW, Nager GT. Glomus tumor and multiple endocrine neoplasia. *Otolaryngol Head Neck Surg* 1986;94:644-648
- Pritchett JW. Familial concurrence of carotid body tumor and pheochromocytoma. *Cancer* 1982;49:2578-2579
- Berg B, Biörklund A, Grimelius L, et al. A new pattern of multiple endocrine adenomatosis: chemodectoma, bronchial carcinoid, GH producing pituitary adenoma and hyperplasia of the parathyroid glands, and antral and duodenal gastrin cells. *Acta Med Scand* 1976;200:321-326
- Farrior JB, Hyams VJ, Benke RH, Farrior JB. Carcinoid apudoma arising in a glomus jugulare tumor: review of endocrine activity in glomus jugulare tumors. *Laryngoscope* 1980;90:110-119
- Shapiro B, Copp JE, Sisson JC, Eyre PL, Wallis J, Beierwaltes WH. Iodine-131 metaiodobenzylguanidine for the locating of suspected pheochromocytoma: experience in 400 cases. *J Nucl Med* 1985;26:576-585
- Hoefnagel CA, Voûte PA, Kraker J de, Marcuse HR. Radionuclide diagnosis and therapy of neural crest tumors using iodine-131 metaiodobenzylguanidine. *J Nucl Med* 1987;28:308-314
- Bomanji J, Leison DA, Zurarte J, Britton KE. Imaging of carcinoid tumors with Iodine-123 Metaiodobenzylguanidine. *J Nucl Med* 1987;28:1907-1910
- Moll L von, McEwan AJ, Shapiro B, et al. Iodine-131 MIBG scintigraphy of neuroendocrine tumors other than pheochromocytoma and neuroblastoma. *J Nucl Med* 1987;28:979-988
- Khafagi F, Egerton-Vernon J, Doorn T van, Foster W, McPhee JB, Allison RWG. Localization and treatment of familial nonfunctional paraganglioma with Iodine-131 MIBG: report of two cases. *J Nucl Med* 1987;28:528-531
- Smit AJ, Essen LH van, Hollema H, Muskiet FA, Piers DA. Meta-[I-131] Iodobenzylguanidine uptake in a nonsecreting paraganglioma. *J Nucl Med* 1984;25:984-986
- Khafagi FA, Shapiro B, Fig LM, Mallette S, Sisson JC. Labetalol reduces Iodine-131 MIBG uptake by pheochromocytoma and normal tissues. *J Nucl Med* 1989;30:481-489
- Wieland DM, Wu JL, Brown JL, et al. Radiolabeled adrenergic neuron-blocking agents: adrenomedullary imaging with 131-I- iodobenzylguanidine. *J Nucl Med* 1980;21:349-353
- World Health Organisation. First report of the expert committee on cardiovascular diseases in hypertension: Hypertension and coronary heart disease: classification and criteria for epidemiological studies. WHO Tech Rep Ser 1959;168:136-142
- Mafee MH. Dynamic CT and its application to otolaryngology - head and neck surgery. *J Otolaryngol* 1982;11(5):307-318
- DeAngelis LM, Kelleher MB, Post KD, Fetell MR. Multiple paragangliomas in neurofibromatosis: a new neuroendocrine neoplasia. *Neurology* 1987;37(1):129-133
- Duncan MW, Compton PC, Lazarus L, Smythe GA. Measurement of norepinephrine and 3,4 dihydroxyphenylglycol in urine and plasma for the diagnosis of pheochromocytoma. *N Engl J Med* 1988;319:136-142
- Lynn MD, Shapiro B, Sisson JC, et al. Portrayal of phaeochromocytoma and the normal adrenal medulla: improved visualization with I-123 MIBG scintigraphy. *Radiology* 1985;155:789-792
- Valk TW, Frager MS, Gross MD, et al. Spectrum of pheochromocytoma in multiple endocrine neoplasia. A scintigraphic portrayal using I-131 metaiodobenzylguanidine. *Ann Intern Med* 1981;94:762-767

33. Quint LE, Glazer GM, Francis JR, Shapiro B, Chevenert TL. Pheochromocytoma and paraganglioma: comparison of MR imaging with CT and I-131 MIBG scintigraphy. *Radiology* 1987;165:89-93
34. Azzarelli B, Felten S, Miyamoto R, Muller J, Purvin V. Dopamine in paragangliomas of the glomus jugulare. *Laryngoscope* 1988;98:573-578
35. Proye C, Fossati P, Fontaine P, et al. Dopamine-secreting pheochromocytoma: an unrecognized entity? Classification of pheochromocytomas according to their type of secretion. *Surgery* 1986;100:1154-1162

# 4

## MR IMAGING AND MIBG IMAGING OF PHAEOCHROMOCYTOMAS AND EXTRA-ADRENAL FUNCTIONING PARAGANGLIOMAS\*

### 4.1. INTRODUCTION

Functioning paragangliomas are catecholamine-secreting tumours which, although rare, may carry grave risks for the affected patient. Excessive catecholamine production by these tumours causes labile or sustained hypertension, combined with attacks of perspiration, palpitations and anxiety. When not diagnosed in time, a great number of cases eventually end fatally. However, given adequate preoperative localization, surgical cure is certainly possible in the majority of cases [1].

In the past decade metaiodobenzylguanidine (MIBG) scintigraphy, computed tomography (CT) and magnetic resonance (MR) imaging have emerged as the primary techniques for localization of functioning paragangliomas. These new techniques are now more generally available and have made invasive procedures such as angiography and venous sampling obsolete. The relative role of these three techniques is presently under debate. MIBG scintigraphy has been found to be accurate in the localization of functioning paragangliomas in the thorax and the abdomen [2]. CT has proved to be valuable in the demonstration of phaeochromocytomas and chemodectomas but its capabilities in the localization of other extra-adrenal sources of catecholamine excess are limited. In addition, CT does not provide enough information to make a specific diagnosis independent of clinical and biochemical findings [3]. MR imaging has shown great potential with respect to the detection and characterization of adrenal lesions as well as paraganglionic tumours situated at extra-adrenal sites [4, 5].

In this chapter the clinical characteristics and the MR imaging and MIBG appearance of functioning paragangliomas are described. The results of a comparative study between MR imaging and MIBG investigations performed in 33 patients with clinical symptoms of catecholamine excess are presented and the expanding role of MR imaging in the localization of

\* Based on: MRI and MIBG imaging of pheochromocytomas and extra-adrenal functioning paragangliomas. APG van Gils, THM Falke, AR van Erkel, J-W Arndt, MP Sandler, AGL van der Mey, RPLM Hoogma. *Radiographics* 1991;11:37-57

functioning paragangliomas is discussed. A protocol for MR imaging in patients suspected of having these neoplasms is set out.

## 4.2. CLINICAL AND RADIOLOGICAL CHARACTERISTICS

### Clinical characteristics

Paraganglionic cells belong to the amine-precursor-uptake decarboxylation (APUD) system and are characterized by cytoplasmic vesicles containing catecholamines. The tumours to which these cells give rise may either be catecholamine-secreting or non-functioning. The classification of these tumours is discussed at some length in chapter 2 [6]. The proportion of hormonally active paragangliomas is thought to be high for phaeochromocytomas, intermediate for aorticosympathetic and low for parasympathetic paragangliomas [7]. Phaeochromocytomas secrete a combination of epinephrine and norepinephrine, whereas extra-adrenal paragangliomas are known to secrete only norepinephrine. Occasionally, paragangliomas produce predominantly dopamine [8]. The secretion of these pressure amines by the tumour produces paroxysmal or permanent hypertension associated with headache, pallor, perspiration and palpitations. The cardiovascular effects, in particular, can be life-threatening.

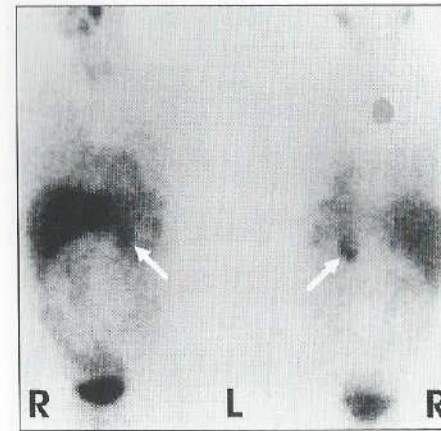
Several laboratory tests exist for the detection of catecholamines in plasma and urine. The sensitivity and specificity of plasma catecholamine measurements are limited because of the often intermittent secretion by paragangliomas and because intravenous sampling causes stress, which raises plasma catecholamines in a non-specific way. At present, determination of free norepinephrine by gas chromatography or high-performance liquid chromatography (HPLC) performed on 24-hour urine specimens, is considered the most sensitive method for diagnosing a functioning paraganglioma [1].

Invasive diagnostic procedures, including angiography and intravenous administration of contrast material, induction of anaesthesia, surgery and even palpation of the tumour require pharmacologic preparation and continuous monitoring of the patient because the manipulations may lead to collapse or death. However, given adequate localization, surgical removal of the tumour is the best therapy and is usually followed by disappearance of all symptoms, including hypertension.

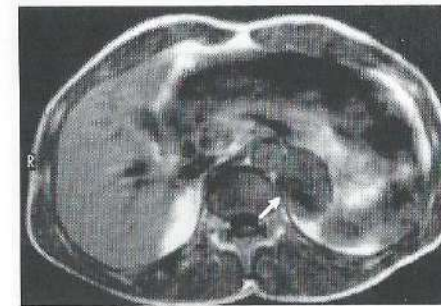
### Radiological characteristics

#### *Solitary phaeochromocytoma*

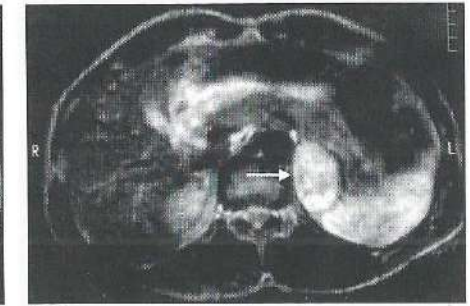
The adrenal medulla is the most frequent site of hormonally active tumours of the paraganglionic system. Intra-adrenal paragangliomas (phaeochromocytomas proper) account for more than 80% of all catecholamine-secreting neoplasms [1]. Norepinephrine constitutes a considerable percentage of these catecholamines. MIBG, either labelled with I-123 or I-131, is a norepinephrine analogue that follows the same pathways as norepinephrine but is not metabolized to any appreciable extent [9]. The capacity of most phaeochromocytomas to store radiolabelled MIBG permits scintigraphic portrayal (figure 4.1).



4.1.A



4.1.B



4.1.C

**Figure 4.1.** Solitary phaeochromocytoma in a 40-year-old male with episodes of palpitations, headache and perspiration. Laboratory investigations showed increased levels of urinary vanillylmandelic acid and plasma catecholamines. **A)** Anterior (left) and posterior (right) I-123 MIBG scintigrams demonstrate high uptake of tracer in the left adrenal area compatible with a phaeochromocytoma (arrow). (L = left, R = right). **B)** T1-weighted MR image (SE TR 300/TE 20) shows a smoothly marginated mass of the left adrenal gland with a low signal intensity (arrow). **C)** On the T2-weighted image (SE TR 2000/TE 100) the mass has high signal intensity (arrow).

On T1-weighted MR images phaeochromocytomas show a signal intensity lower or equivalent to liver, kidney or muscle, although they may have a higher signal intensity when they are complicated by haemorrhage. On T2-weighted images they are characterized by a high signal intensity (figure 4.1). After intravenous injection of gadopentetate dimeglumine (Magnevist<sup>®</sup>, Schering, Berlin, Germany), they mostly show a non-homogeneous enhancement (figure 4.2).

On T1-weighted MR images phaeochromocytomas show a signal intensity lower or equivalent to liver, kidney or muscle, although they may have a higher signal intensity when they are complicated by haemorrhage. On T2-weighted images they are characterized by a high signal intensity (figure 4.1). After intravenous injection of gadopentetate dimeglumine (Magnevist<sup>®</sup>, Schering, Berlin, Germany), they mostly show a non-homogeneous enhancement (figure 4.2).

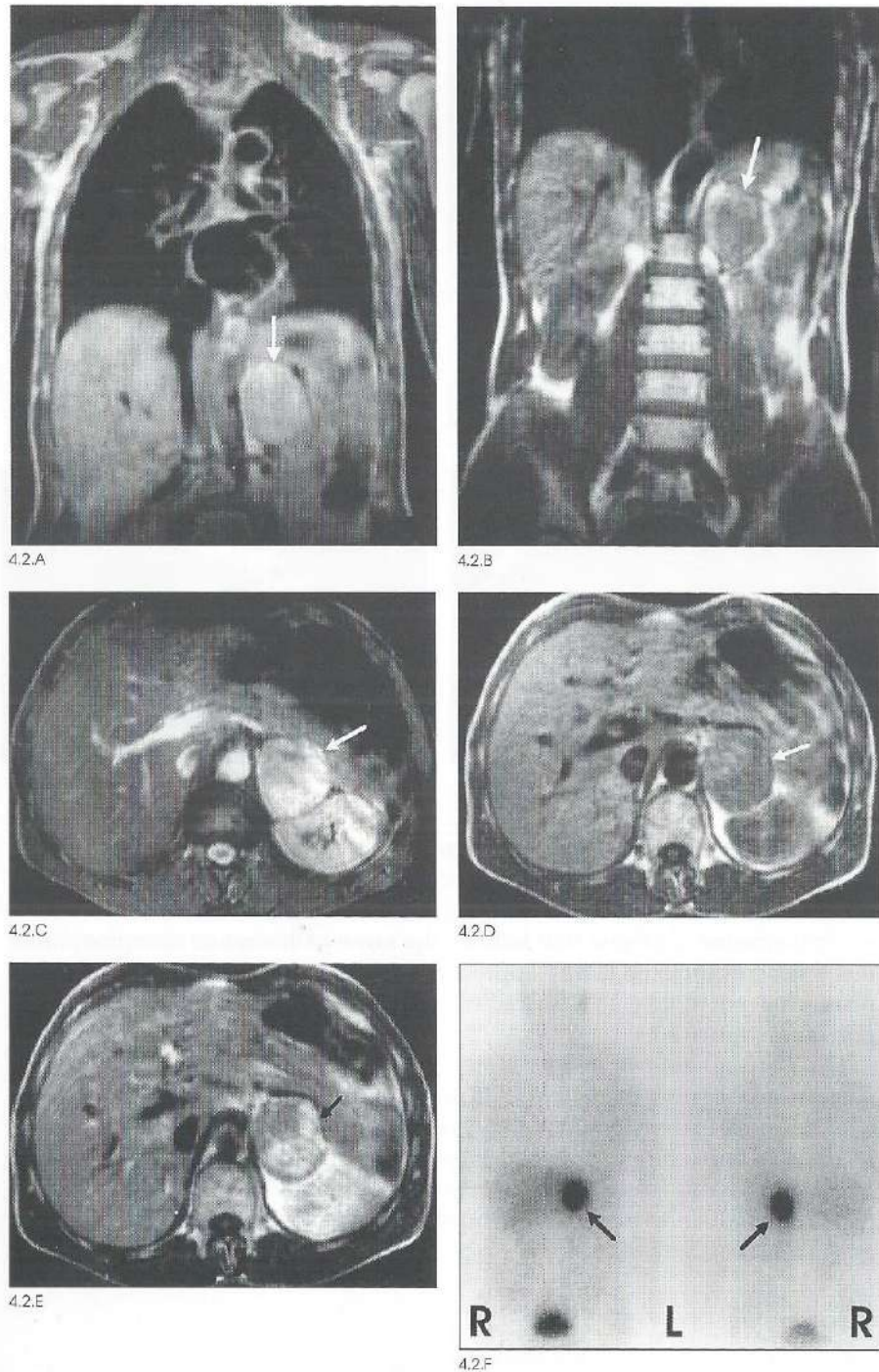


**Figure 4.2.** Phaeochromocytoma and contrast material-enhanced MR imaging. MR imaging was the initial localization technique in a patient with severe hypertension and elevated levels of urinary catecholamines. **A and B)** Coronal T1-weighted images (SE TR 650/TE 20 and SE TR 280/TE 20) of thorax and upper abdomen display a smoothly margined mass of the left adrenal gland with a signal intensity equal to that of the liver (arrow). **C)** T2-weighted gradient-echo image (TR 756/TE 28/30°) shows mass with increased intensity characteristic for a phaeochromocytoma (arrow). **D and E)** Transverse T1-weighted MR images obtained before and after intravenous injection of gadopentetate dimeglumine show inhomogeneous enhancement of the tumour (arrow). **F)** I-123 MIBG scintigrams reveal high uptake in the left adrenal area (arrow) confirming the presence of a phaeochromocytoma. (L = left, R = right).

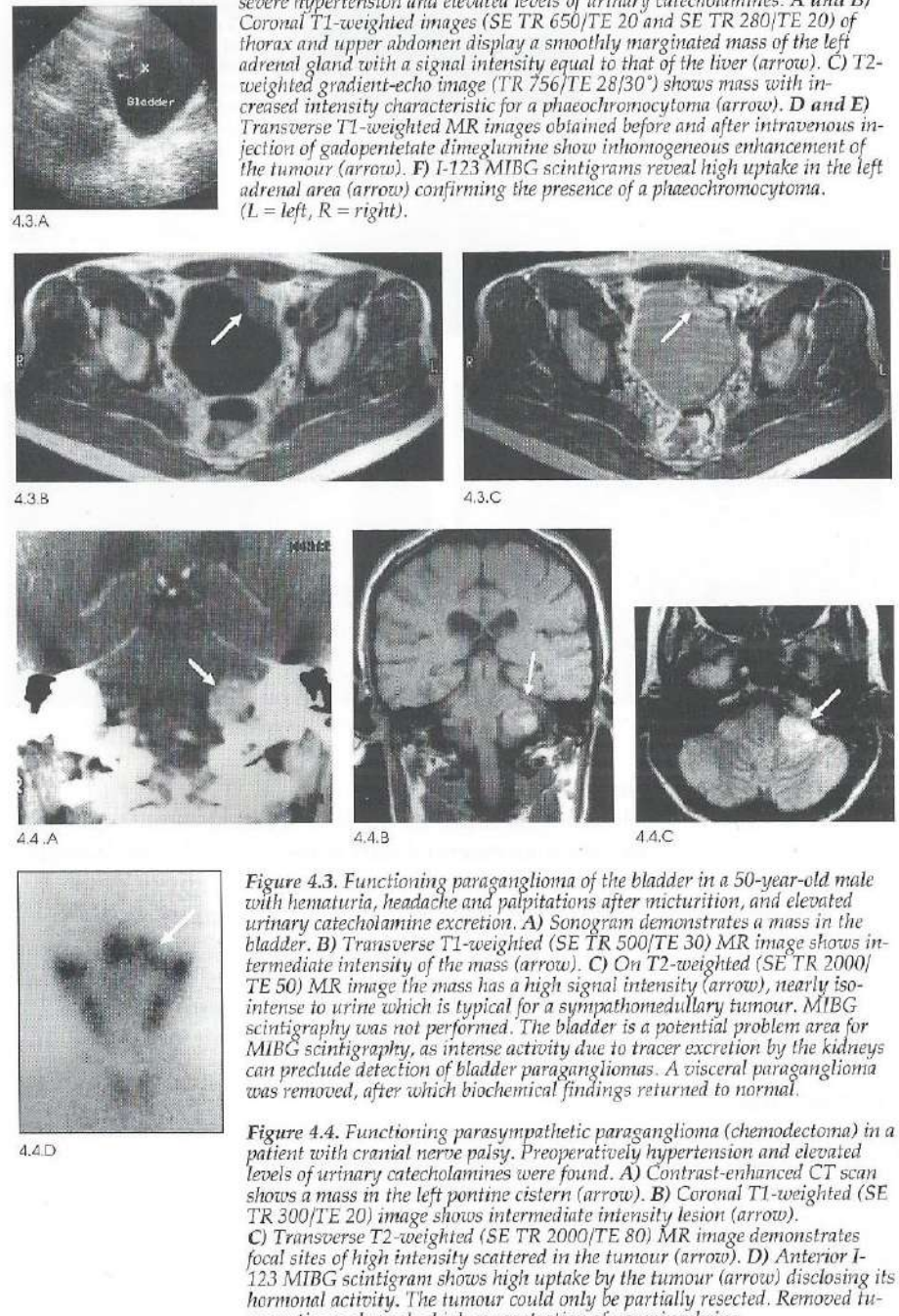
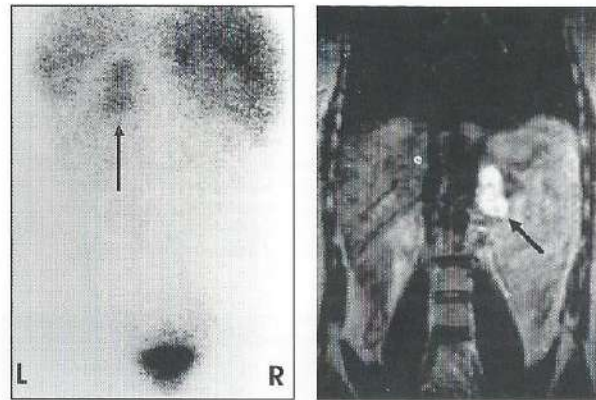
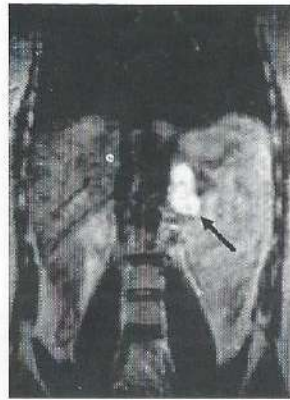


**Figure 4.3.** Functioning paraganglioma of the bladder in a 50-year-old male with hematuria, headache and palpitations after micturition, and elevated urinary catecholamine excretion. **A)** Sonogram demonstrates a mass in the bladder. **B)** Transverse T1-weighted (SE TR 500/TE 30) MR image shows intermediate intensity of the mass (arrow). **C)** On T2-weighted (SE TR 2000/TE 50) MR image the mass has a high signal intensity (arrow), nearly iso-intense to urine which is typical for a sympathomedullary tumour. MIBG scintigraphy was not performed. The bladder is a potential problem area for MIBG scintigraphy, as intense activity due to tracer excretion by the kidneys can preclude detection of bladder paragangliomas. A visceral paraganglioma was removed, after which biochemical findings returned to normal.

**Figure 4.4.** Functioning parasymphetic paraganglioma (chemodectoma) in a patient with cranial nerve palsy. Preoperatively hypertension and elevated levels of urinary catecholamines were found. **A)** Contrast-enhanced CT scan shows a mass in the left pontine cistern (arrow). **B)** Coronal T1-weighted (SE TR 300/TE 20) image shows intermediate intensity lesion (arrow). **C)** Transverse T2-weighted (SE TR 2000/TE 80) MR image demonstrates focal sites of high intensity scattered in the tumour (arrow). **D)** Anterior I-123 MIBG scintigram shows high uptake by the tumour (arrow) disclosing its hormonal activity. The tumour could only be partially resected. Removed tumour tissue showed a high concentration of norepinephrine.

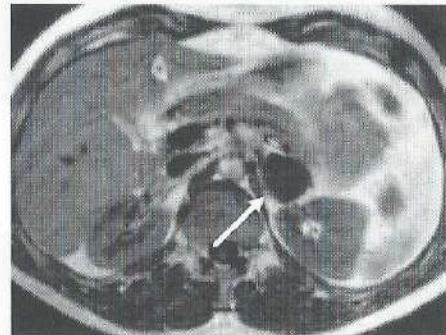


4.5.A

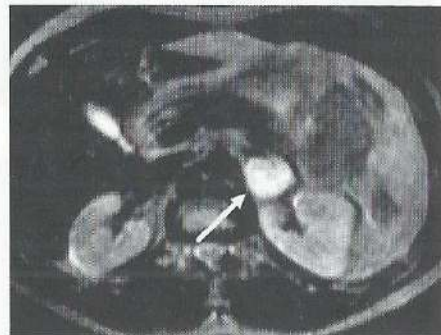


4.5.B

**Figure 4.5.** Combination of chemodectoma and pheochromocytoma. **A)** Posterior I-123 MIBG scintigram performed in patient with previously removed chemodectoma and elevated urinary catecholamine levels shows high uptake in left adrenal gland (arrow). L = left, R = right. **B)** Coronal T2-weighted (SE TR 2000/TE 100) MR image shows high intensity mass in the left adrenal gland (arrow) compatible with pheochromocytoma. **C and D)** Transverse T1-weighted (SE TR 300/TE 20) and T2-weighted image (SE TR 2000/TE 100) MR images of the tumour (arrow).



4.5.C



4.5.D

#### Solitary extra-adrenal functioning paragangliomas

The extra-adrenal localizations account for 10-20% of catecholamine producing paragangliomas and form an essential part in the evaluation of patients with excessive catecholamine secretion. Of the aorticosympathetic paragangliomas, up to 80% are located within the abdomen (figure 4.3). The radiological features of these tumours are similar to adrenal pheochromocytomas. The remaining 20% can be found in the thorax and head and neck area. In the latter region, extra-adrenal paragangliomas mainly consist of functioning chemodectomas that are of parasympathetic origin (figure 4.4).

#### Multiple tumours

In up to 20% of patients with paragangliomas, multiple tumours develop synchronously or metachronously [10]. A higher incidence of multiplicity has been noted in familial cases, particularly in the event of hereditary disorders such as the multiple endocrine neoplasia (MEN) syndromes. The disease is then usually present in both adrenals [1, 11].

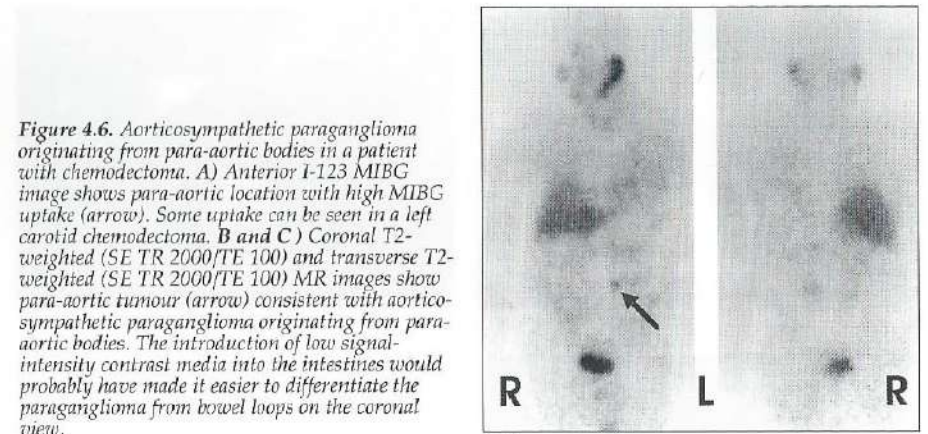
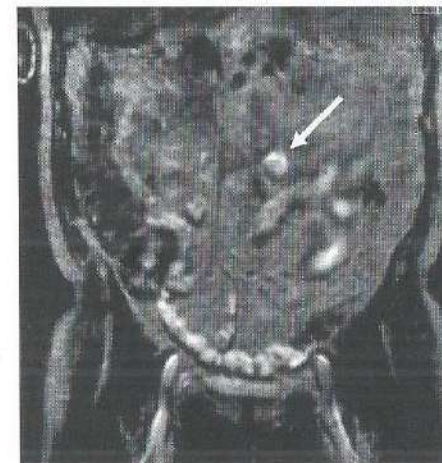
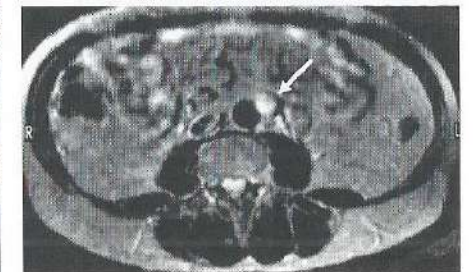


**Figure 4.6.** Aorticosympathetic paraganglioma originating from para-aortic bodies in a patient with chemodectoma. **A)** Anterior I-123 MIBG image shows para-aortic location with high MIBG uptake (arrow). Some uptake can be seen in a left carotid chemodectoma. **B and C)** Coronal T2-weighted (SE TR 2000/TE 100) and transverse T2-weighted (SE TR 2000/TE 100) MR images show para-aortic tumour (arrow) consistent with aorticosympathetic paraganglioma originating from para-aortic bodies. The introduction of low signal-intensity contrast media into the intestines would probably have made it easier to differentiate the paraganglioma from bowel loops on the coronal view.

4.6.A



4.6.B



4.6.C

The association of pheochromocytomas with extra-adrenal paragangliomas has been described in familial and non-familial cases, but it was thought to be rare [7]. However, our experience indicates a higher incidence of this association than has been reported in the literature [8]. In the past, many small tumours have probably escaped detection by conventional examinations, whereas metachronous tumours may not have been identified as such [12].

Beierwaltes found a high percentage of recurrences in 176 patients studied at the University of Michigan (46%), although his population showed an unambiguous selection bias [13]. It is often difficult to determine whether recurrences represent multiple paragangliomas (paragangliomatosis) or distant metastases of a single paraganglioma [14]. It is generally agreed that

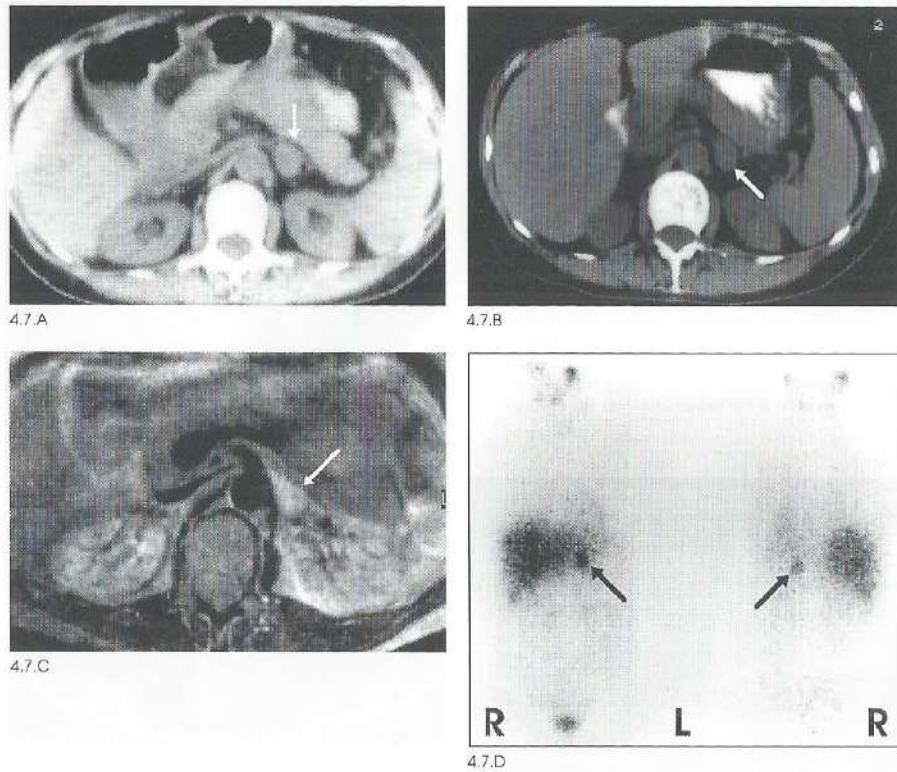
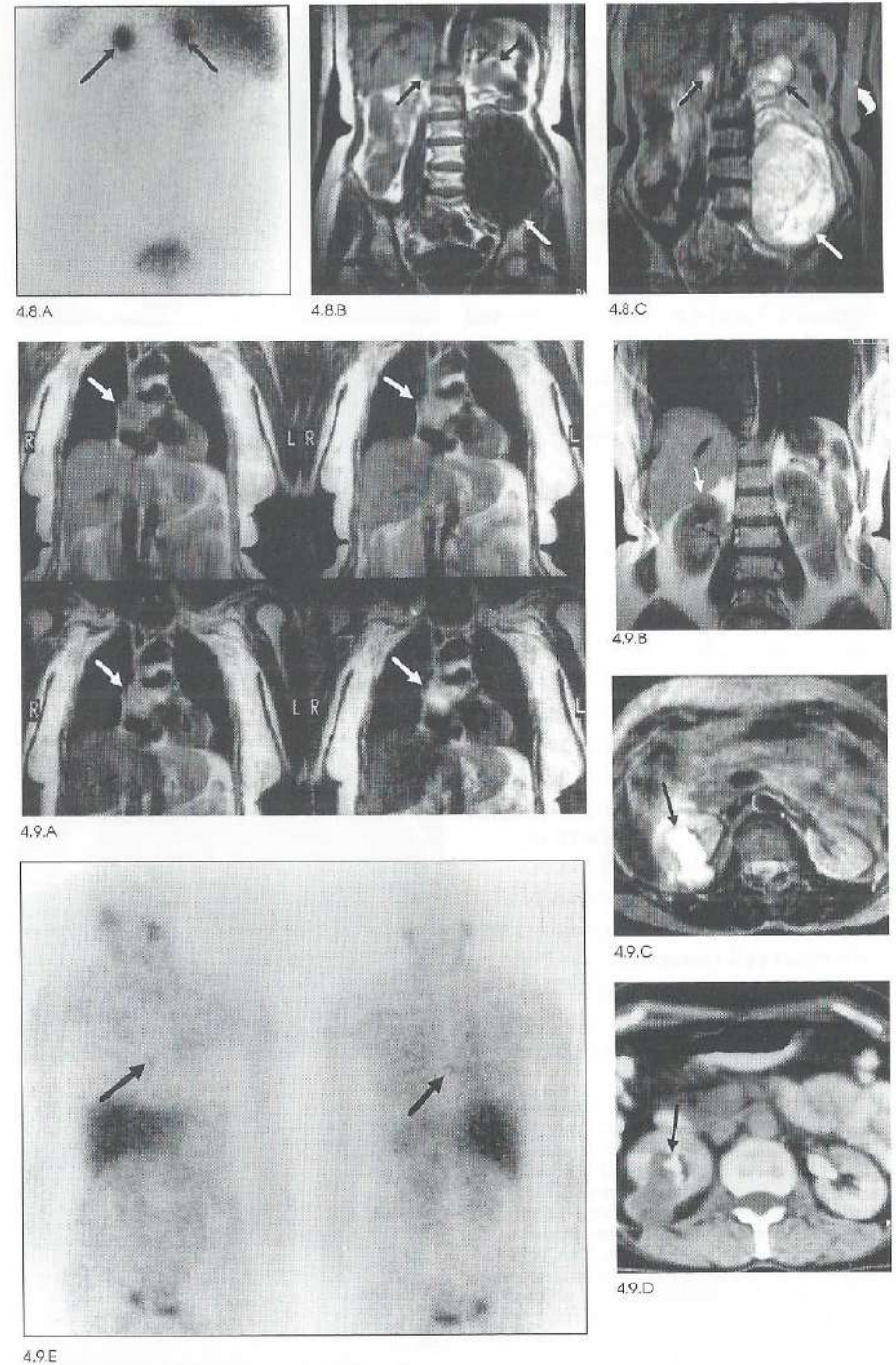


**Figure 4.7.** MEN II syndrome in a patient with normal urinary catecholamine levels. A) CT scan obtained in 1980 shows small mass in left adrenal gland (arrow). B) CT study six years later shows little enlargement of the mass (arrow). C) Transverse T2-weighted (SE TR 2000/TE 50) MR image and I-123 MIBG scintigram (D) demonstrate the left adrenal pheochromocytoma (arrow). This case emphasizes the auxiliary role of non-invasive imaging methods in screening of patients with familial disorders. (L = left, R = right).

**Figure 4.8.** Bilateral adrenal paragangliomas (pheochromocytomas) in a patient with neurofibromatosis. A) Posterior I-123 MIBG scintigram shows elevated uptake in both adrenal glands (arrows). (L = left, R = right). B) T1-weighted (SE TR 300/TE 20) coronal MR image shows bilateral adrenal tumours (black arrows) and a large neurofibroma in the pelvis (white arrow). C) T2-weighted (SE TR 2000/TE 100) coronal MR image better demonstrates the adrenal tumours (black arrows), with areas of necrosis in the left adrenal pheochromocytoma. Note small subcuta-

neous neurofibroma on the left (curved white arrow) and the high signal intensity of the pelvic neurofibroma (white arrow).

**Figure 4.9.** Combination of renal cell carcinoma and cardiac paraganglioma in a 60-year-old female with hypertension and excessive catecholamine excretion. A chemodectoma had been removed 20 years earlier. A) Coronal MR images obtained with increasing echo times (SE TR 400/TE 30-120) show high intensity mass above right atrium (arrow) and left ventricular hypertrophy. B) Coronal T1-weighted (SE TE 300/TE 20) MR image demonstrates a mass in the upper pole of the right kidney (arrow). C) Transverse T2-weighted (SE TR 2000/TE 100) MR image shows high intensity of the renal mass (arrow). D) On contrast-enhanced CT scan the renal lesion demonstrates little enhancement (arrow). E) I-123 MIBG scintigrams show faint uptake in the cardiac region (arrow). Venous sampling indicated a functioning tumour in the right atrium. At surgery a renal cell carcinoma was found. The cardiac tumour was not removed.



4.9.E

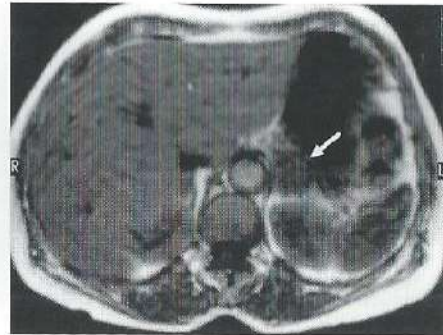
malignancy occurs in less than 10% of cases [15]. Some authors even think that malignancy is rare and involves no more than 2% of cases [14]. At any rate, the potential for multicentric origin of paragangliomas is clearly demonstrated and the fact that pheochromocytomas as well as the other types of paragangliomas can be part of a systemic disease is emphasized (figures 4.5 and 4.6). Because affected individuals directly benefit from early diagnosis of asymptomatic lesions, an active approach to diagnostic screening is certainly justified [12, 16].

#### Associated diseases

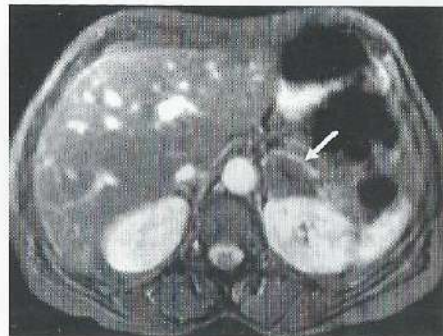
Adrenal paragangliomas constitute an essential part of the MEN II and III syndromes (figure 4.7). Further association has been demonstrated with neuro-ectodermal disorders such as tuberous sclerosis, von Hippel-Lindau disease and neurofibromatosis (figure 4.8) [1]. Gastric epithelioid leiomyosarcomas and pulmonary chondromas have occasionally been described in combination with paragangliomas [1]. The combination of paragangliomas with renal cell carcinoma has been reported in a few cases (figure 4.9) [17].

In contrast to sporadic pheochromocytomas, those associated

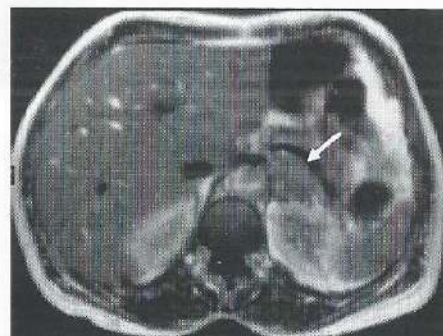
**Figure 4.10.** Non-hyperfunctioning adenoma in a 67 year old female with hypertension, headache, tremor, nausea and marginal elevated catecholamine excretion. **A)** T1-weighted (SE TE 500/TR 30) and **B)** T2-weighted gradient-echo (TR 650/TE 28/30°) images demonstrate a mass (arrow) in the left adrenal gland with low signal intensity, similar to the signal intensity of the liver, which is typical for a silent adenoma. **C)** MR image obtained after intravenous administration of gadopentate dimeglumine shows no enhancement of the mass (arrow). **D)** I-123 MIBG scintigrams appear normal. (L = left, R = right).



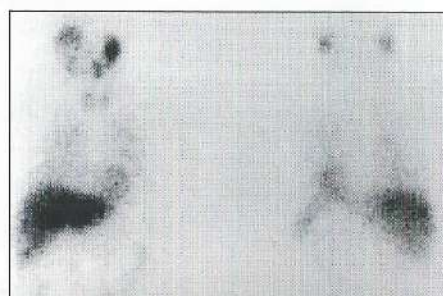
4.10.A



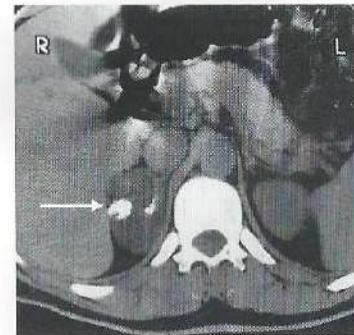
4.10.B



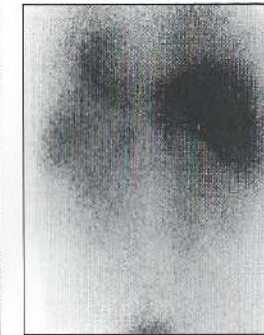
4.10.C



4.10.D



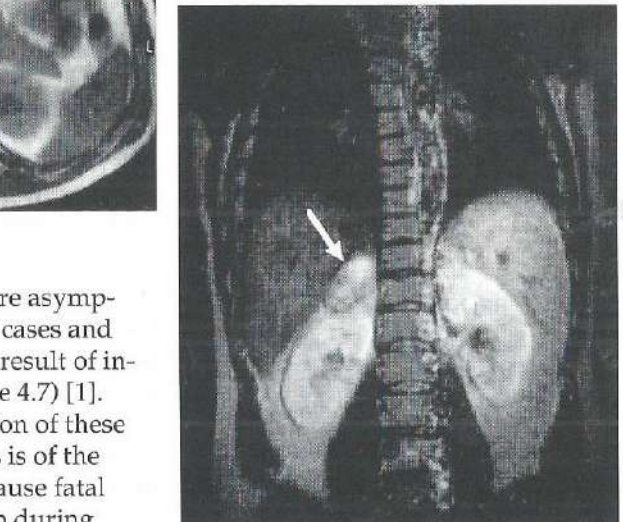
4.11.A



4.11.B



4.11.C



4.11.D

**Figure 4.11.** Adrenocortical carcinoma in a 34-year-old male with mild hypertension. **A)** Initially obtained CT scan shows mass with calcifications in right adrenal presumed to be a pheochromocytoma (arrow). **B)** Posterior I-123 MIBG scintigram shows normal bilateral uptake of the tracer in the adrenal glands. (L = left, R = right). **C)** Transverse T1-weighted (SE TR 400/TE 50) MR image reveals low intensity of the mass (arrow). **D)** Visual assessment of the intensity relative to the liver on coronal T2-weighted (SE TR 2000/TE 100) MR images suggested a pheochromocytoma (arrow). However, quantitative assessment revealed an intensity ratio of 2.3, which is unusually low for a pheochromocytoma and much too high for a silent adenoma. At surgery an adrenocortical carcinoma was found.

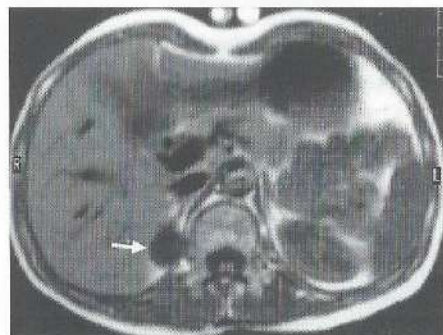
with MEN syndromes are asymptomatic in about 50% of cases and are only diagnosed as a result of increased suspicion (figure 4.7) [1]. Diagnosis and localization of these clinically silent tumours is of the utmost importance, because fatal paroxysms may develop during surgery for associated disorders. Pheochromocytomas are known to develop over a period of years in these patients, making long term follow-up essential.

#### Differential diagnosis of adrenal tumours

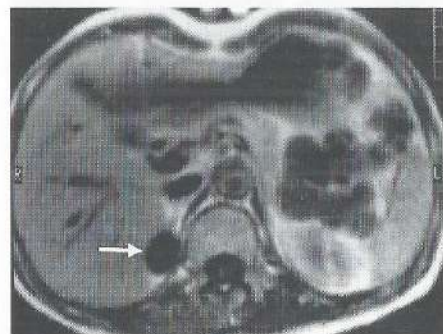
Most functioning paragangliomas are located in the adrenal glands. In patients suspected of having a pheochromocytoma but who do not have the disease, other lesions may simulate a pheochromocytoma on MR and CT images. Particularly, endocrine-silent adrenal masses may cause confusion when they coincide with clinical symptoms of catecholamine excess.



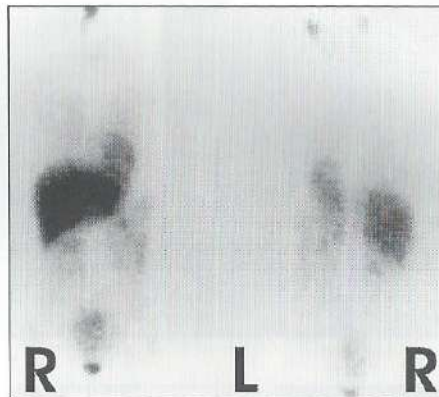
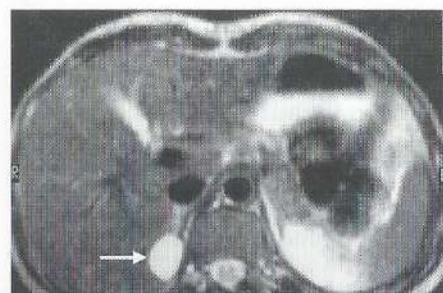
4.12.A



4.12.C



4.12.D



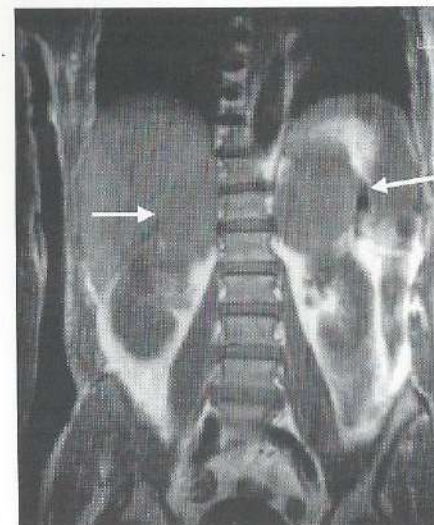
4.12.B

**Figure 4.12.** Adrenal cyst in a 21-year-old woman thought to have a functioning paraganglioma. *A*) Initially performed CT shows right adrenal mass (arrow). *B*) I-123 MIBG scintigraphy is normal. (L = left, R = right). *C*) T1-weighted (SE TR 300/TE 20) MR images obtained before and *D*) after administration of gadopentetate dimeglumine demonstrate no enhancement of the tumour (arrow). *E*) T2-weighted (SE TR 2000/TE 100) MR image shows homogeneous high-intensity mass without a rim in the right adrenal gland (arrow). Absence of enhancement and absence of a peripheral rim strongly favour the diagnosis of a simple cyst instead of a cystic pheochromocytoma.

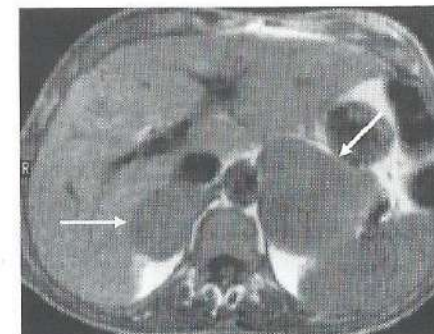
Especially in patients with hypertension silent adenomas are a frequent finding. Non-functioning adenomas visible to the naked eye are found at autopsy in 1-9% of adults [18]. Some examples of frequently and infrequently found adrenal masses are shown (figures 4.10-4.13). These cases also illustrate the fact that MIBG only visualizes adrenergic tumours.

### 4.3. MATERIAL AND METHODS

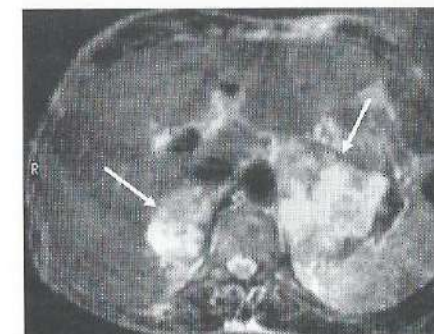
From 1985 through 1988 a total of 33 patients in whom a functioning paraganglioma was clinically suspected were referred to the Department of



4.13.A



4.13.B



4.13.C

**Figure 4.13.** Adrenal abscesses in a 43-year-old patient with generalized histoplasmosis and adrenal insufficiency. *A*) Coronal T1-weighted (SE TR 300/TE 20) MR image shows bilateral adrenal masses in patient with generalized histoplasmosis (arrows). *B*) Transverse T1-weighted MR image (SE TR 300/TE 20) (arrows). *C*) Transverse T2-weighted (SE TR 2000/TE 100) MR image shows areas of high intensity within the masses, simulating bilateral pheochromocytomas (arrows).

Diagnostic Radiology. All patients underwent both MR imaging and MIBG scintigraphic examinations. In 52% (17/33) of the patients MR imaging preceded MIBG scintigraphy.

Coronal and transverse MR images of the region of interest were acquired at 0.5 T (Gyrosan-S5®, Philips, Best, The Netherlands) using a body coil. Imaging sequences were obtained with a short TR/TE of 300/20 and a long TR/dual echo of 2000/50-100. In six patients intravenous administration of gadopentetate dimeglumine (0.1-0.2 mmol/kg body weight) was combined with T1-weighted imaging. Four patients underwent MR imaging at other hospitals with either a Technicare or Picker system and slightly different interpulse times.

MIBG scintigraphy was performed with a large field-of-view gamma camera (Toshiba GCA 90B®, Tokyo, Japan) equipped with a low-energy general purpose collimator and interfaced to a dedicated computer (Toshiba GMS-55®, Toshiba). In all cases anterior and posterior digitized images of the total body were obtained 24 hours and, in most patients, 48 hours after the injection. The scanning speed was 15 cm/min. In all cases detail images of the adrenal

area were taken. In selected cases, additional views were made of equivocal regions. Each patient was injected intravenously with 370 MBq I-123 MIBG ('Cygne' B.V., Eindhoven, The Netherlands). Thyroidal uptake was blocked by the administration of Lugol's solution, ten drops three times daily (50 mg of iodine) for five days, starting the day before the injection. In five patients 18.5 MBq I-131 MIBG was used instead of I-123 MIBG because of logistical or technical difficulties. In one case the positive repeat study with I-131 MIBG was used instead of the initial negative study with I-123 performed under labetalol medication.

Pathology findings, clinical and biochemical findings (from chromatography performed on 24-hour urine specimens for epinephrine, norepinephrine, dopamine and vanillylmandelic acid), and results of follow-up examinations were the standard for diagnosis. Both modalities were independently reviewed by two radiologists and two nuclear medicine physicians, respectively. The MR and MIBG examinations, including signal intensity and MIBG uptake were scored by visual appraisal before and after clinical information on the patients had been provided. From this data, sensitivity and specificity were calculated.

Table 4.1. Detection of lesions (no clinical information available).

Diagnosis	MIBG		MRI	
	Obs 1	Obs 2	Obs 3	Obs 4
Functioning paragangliomas*	17/22 <sup>†</sup>	18/22	20/22	20/22
Adrenocortical tumour	0/1	0/1	1/1	1/1
Neuroblastomas	1/2	1/2	2/2	2/2
Adenomas	0/2	0/2	2/2	2/2
Cyst	0/1	0/1	1/1	1/1
Renal cell carcinoma	0/1	0/1	0/1	1/1
Neurofibroma	0/1	0/1	1/1	1/1
Liver metastases of MCT	1/1	1/1	1/1	1/1
Total	19/31	20/31	28/31	29/31

\*In one case the positive repeat study with I-131 MIBG was used instead of the initial negative study with I-123 performed under labetalol medication.

<sup>†</sup>The ratio indicates the number of lesions detected by the observer compared to the total number of lesions present.

#### 4.4. RESULTS

Twenty-two functioning paragangliomas were present in 18 patients. Fourteen were located in the adrenal glands and eight were extra-adrenal. In addition, one renal cell carcinoma and one large neurofibroma had been found in these 18 patients. Seven did not have functioning paragangliomas, but surgery revealed adrenocortical carcinoma in one, neuroblastoma in two, adenoma in two, adrenal cyst in one and multiple liver metastases of a thyroid medullary carcinoma in one. Eight patients were considered to be free of disease on the basis of available data, including those from clinical follow-up over more than one year and from all radiographic investigations performed.

#### Lesion detection

The results of both modalities in tumour detection are summarized in table 4.1. In the eight patients considered to be free of disease, both methods obtained true-negative results. We found an overall sensitivity for localizing a paraganglioma of 91% for MR imaging and 80% for MIBG scintigraphy. On average 100% of the adrenal paragangliomas and 75% of the extra-adrenal paragangliomas were detected on MR imaging. The paragangliomas not detected by MR imaging were small (2-4 cm in diameter).

Table 4.2. Characterization of lesions as functioning paragangliomas from MIBG scintigraphic and MR imaging findings (with clinical information provided to observers).

Diagnosis	MIBG		MRI	
	Obs 1	Obs 2	Obs 3	Obs 4
Functioning paragangliomas	17/22 <sup>†</sup>	19/22	20/22	18/22
Adrenocortical tumor	0/1	0/1	1/1*	0/1
Neuroblastomas	0/2	0/2	0/2	0/2
Adenomas	0/2	0/2	0/2	0/2
Cyst	0/1	0/1	1/1*	1/1*
Renal cell carcinoma	0/1	0/1	0/1	0/1
Neurofibroma	0/1	0/1	1/1*	1/1*
Liver metastases of MCT	0/1	0/1	1/1*	0/1
Total	17/31	19/31	24/31	20/31

<sup>†</sup>The ratio indicates the number of lesions characterized as paraganglioma by the observer compared to the total number of lesions present.

\* Indicates false-positive characterization.

With MIBG scintigraphy 75% of the adrenal phaeochromocytomas and 88% of extra-adrenal paragangliomas were detected. The paragangliomas missed at MIBG scintigraphy measured from 1 to 4 cm in diameter. Of the false-negative scintiscans (i.e. failure of scintigraphy to demonstrate surgically proven paragangliomas) only one was caused by failure of the paraganglioma to take up MIBG. Sensitivity for MIBG scintigraphy was not decreased by the inclusion of I-131 MIBG studies, since both nuclear medicine physicians correctly identified the tumours in all five patients who underwent this alternative examination.

With respect to paraganglioma sites, all observers were in agreement in 77% of patients.

### Tumour characterization

The capacity to positively identify paragangliomas was assessed after revealing the clinical data to the observers. The results are summarized in table 4.2.

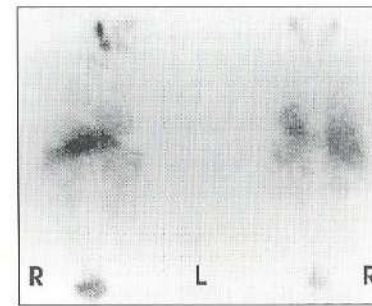
In the eight patients without disease all observers correctly scored the absence of a functioning paraganglioma (true-negative).

On the basis of these latter results overall sensitivity in the characterization of functioning paragangliomas is calculated as 82% for MIBG scintigraphy and 86% for MR imaging. Specificity in tumour characterization was 100% and 82% respectively.

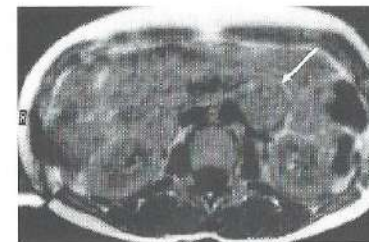
## 4.5. DISCUSSION

Thus far no study has provided a definite answer to the question as to what should be the first procedure to be performed for the detection and localization of functioning paragangliomas. In the past, comparison between I-131 MIBG scintigraphy, CT and MR imaging was made by Quint et al. [19] and Velchik et al. [20]. They found these modalities to be nearly equivalent in the detection of paragangliomas. We obtained similar results in the localization of functioning paragangliomas by MR imaging and I-123 MIBG scintigraphy. Because of its inherent limitations, the role of CT in the detection of functioning paragangliomas will certainly become less important and therefore it was not included in our study. As, until this moment, neither of the two other techniques has demonstrated absolute superiority, the choice of the first localization procedure to be performed should be based on the respective merits and demerits of these techniques.

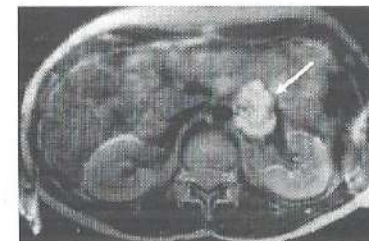
In our study, MR imaging demonstrated a high sensitivity in the detection of paragangliomas. This sensitivity could not be determined in the studies by Quint et al. [19] and Velchik et al. [20], which were performed on groups of patients with proved paragangliomas only. Our study included a substan-



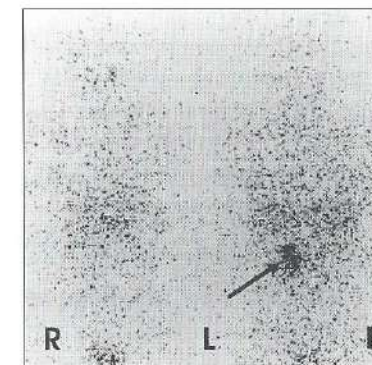
4.14.A



4.14.B



4.14.C

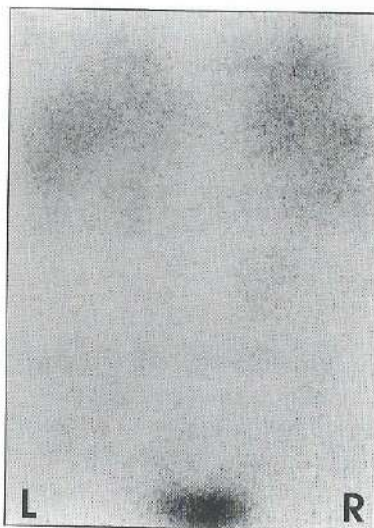


4.14.D

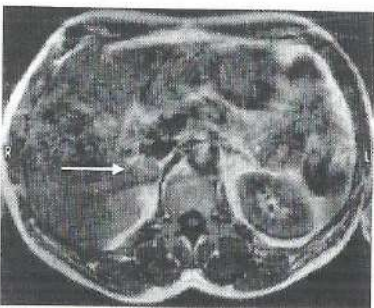
**Figure 4.14.** Functioning paraganglioma in a 25-year-old patient receiving labelalol medication for symptoms. A) Anterior (left) and posterior (right) I-123 MIBG scintigrams performed under labelalol medication show no abnormal uptake. B) Transverse T1-weighted (SE TR 300/TE 20) MR image and C) transverse T2-weighted (SE TR 2000/TE 100) MR image reveal left retroperitoneal extra-adrenal tumour displacing the left hilar renal vessels (arrow). The high signal intensity is compatible with a functioning paraganglioma. D) Anterior and posterior views of I-131 MIBG scintigrams obtained after cessation of labelalol medication demonstrate a functioning paraganglioma in left adrenal region (arrow). (L = left, R = right).

tial number of patients with other tumours mimicking functioning paragangliomas and a number of patients without a tumour. Even when strict criteria are applied for selection, the majority of patients imaged for possible functioning paragangliomas will not have the disease. In such patients other lesions may cause symptoms similar to those of functioning paragangliomas. As MIBG scintigraphy reflects tracer-uptake in adrenergic nervous tissue, tumours of the adrenal cortex producing hypertension are not visualized. Patients with sporadic or familial paragangliomas may have associated tumours such as renal tumours, islet cell tumours, neurofibromas and tumours associated with the MEN syndromes, that remain undetected with MIBG scintigraphy. Our study clearly demonstrated the superiority of MR imaging in the detection of associated tumours and adrenal tumours that mimic functioning paragangliomas. MR imaging is especially useful for differentiating adenomas from phaeochromocytomas on the basis of signal intensity characteristics. Differentiation from metastases and other adrenal tumours is possible to a certain degree, provided that quantitative data are used as well as other morphologic criteria [21, 22].

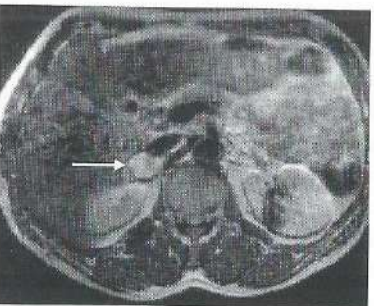
Metaiodobenzylguanidine scintigraphy has a high specificity in characterizing paragangliomas. However, early reports of



4.15.A



4.15.B



4.15.C

**Figure 4.15.** Pheochromocytoma in a 60-year-old man with symptoms typical of a functioning paraganglioma. He received no medication at the time. **A)** Posterior I-123 MIBG scintigram shows normal uptake. (L = left, R = right). **B)** Transverse T1-weighted (SE TR 250/TE 50) MR image shows small mass in right adrenal gland (arrow). **C)** Transverse T2-weighted (SE TR 1200/TE 50) MR image shows high-intensity mass, that proved to be a pheochromocytoma (arrow).

specificity approaching 100% must be amended, given the other neural crest-derived tumours reported to accumulate MIBG. These other types of tumours, capable of taking up MIBG (neuroblastoma, carcinoid, medullary carcinoma, choriocarcinoma, atypical schwannoma, Merkel skin cancer and oat-cell carcinoma) were virtually absent in our study. This has certainly contributed to the superior specificity of MIBG for tissue characterization in this study.

The effectiveness of MIBG scintigraphy can be adversely affected by concomitant use of medication. Metaiodobenzylguanidine uptake is inhibited by various agents, including insulin, imipramine, desmethyl imipramine, other tricyclic antidepressants, amphetamine like drugs, reserpine, cocaine, phenylpropanolamine, nifedipine and labetalol (figure 4.14) [23].

Some pheochromocytomas even have a deficient uptake or storage mechanism, which prohibits the portrayal of paragangliomas by MIBG altogether (figure 4.15). By contrast, the concomitant use of medication does not interfere with the localization of functioning paragangliomas by means of CT and MR imaging.

The possibility of MR imaging to screen multiple sites with optimal plane selection and outstanding contrast is an advantage over CT, by which screening of an extensive anatomical area is limited by the cumbersome 'salami technique'. Multiplanar

imaging with MR imaging allows large anatomic regions to be imaged with outstanding contrast and within a reasonable time by adjusting the scan plane. The imaging time taken to screen the mediastinum and abdomen using whole-body MR imaging is approximately 1.5 hours if no additional procedures are performed such as detailed imaging with surface coils or the intravenous injection of contrast media. The introduction and improvement of fast MR imaging methods should help reduce the examination time in the foreseeable future [24, 25].

Metaiodobenzylguanidine scintigraphy provides useful functional information and can be used for lesion detection. However, its images are limited by poor anatomical resolution which necessitates additional imaging studies (either CT or MR imaging) for more precise localization of lesions. The average imaging time with MIBG scintigraphy is about 20 minutes for each imaging day if no special procedures are performed such as SPECT or spot views of equivocal regions. Total procedure time with MR imaging is considerably less than scintigraphy which requires at least a day wait before definite results are available.

As a substantial number of patients not suffering from pheochromocytoma will inevitably be imaged it becomes questionable whether the risks of radiation hazard from whole-body CT or MIBG scintigraphy outweigh the disadvantages of whole-body MR imaging for the initial screening of the sympathetic chain. The absence of an ionizing radiation hazard with MR imaging is especially of interest when screening families at risk of developing functioning paragangliomas or in patients with a previous resection of a pheochromocytoma. Whole-body MR imaging might be found to be highly useful for the yearly follow-up to detect any recurrent tumour at an early stage without the potential danger of accumulating radiation dose.

Patients with pacemakers, artificial cardiac valves and vascular clips in the head can be evaluated with MIBG scintigraphy and CT without any risk, contrary to MR imaging. The relative disadvantages of claustrophobia and unco-operative patients can be reduced with proper medication prior to an examination with CT and MR imaging.

Adequate preoperative localization of sympathomedullary disease justifies posterior adrenalectomy without extensive surgical exploration in most patients, thus reducing the average hospitalization from two weeks to one week. To obtain accurate anatomic information MIBG scintigraphy has to be supplemented by either CT or MR imaging. In the screening of patients with sympathomedullary disorders, MR imaging is generally less expensive than the combined approach of MIBG scintigraphy (detection) followed by an anatomic imaging procedure (assessment). We have discussed the advantages and disadvantages of both techniques more extensively elsewhere [22]. Because of its important advantages, we suggest that MR imaging should be the modality of first choice in imaging patients with suspected paragangliomas. Metaiodobenzylguanidine scintigraphy should be performed

when MR imaging results are equivocal or when functional information is needed.

#### 4.6. PROPOSED PROTOCOL FOR MR IMAGING EXAMINATION

On the basis of our experience, we have developed the following proposal for whole-body MR screening of patients suspected of having functioning paragangliomas:

- 1) Patients are examined at 0.5 T using a body coil for initial screening of the abdomen (more than 95% of functioning paragangliomas is located in the abdomen). The imaging plane is coronal. A spin-echo technique is used to obtain T1-weighted (TR 300/TE 20) images. T2-weighted images are obtained with a gradient-echo technique (TR 650/TE 28/30°). The imaging technique includes multisection acquisition with a slice thickness of 1 cm, an intersection gap of approximately 1-2 mm, an acquisition matrix of 179 x 256 and a display matrix of 256 x 256. The introduction of low signal intensity contrast material into the bowel loops may facilitate differentiation between tumour masses and bowel loops on T2-weighted images.
- 2) Transverse T1- and T2-weighted images of the adrenal area are obtained using the same technique. The field of view is 300-400 mm.
- 3) Following investigation of the abdomen and adrenals the region of the diaphragm up to the base of the skull is imaged. Coronal images are obtained using a multislice spin-echo technique with ECG triggering. The repetition time is determined by the heartbeat interval. For T1-weighted images an echo time of 30 msec and a repetition time of one heartbeat interval is used, and for T2-weighted images echo times of 50 and 100 msec and a repetition time of two heartbeat intervals is used. For coronal images the field of view should be 500 mm. The number of measurements per data line is two for T2-weighted sequences and four for T1-weighted sequences.
- 4) The use of intravenous contrast agents such as gadopentetate dimeglumine is only recommended in selected cases, in order to differentiate between vascular adrenal masses such as malignant tumours and pheochromocytomas and hypovascular masses such as adenomas, cysts and haemorrhage. Because of the natural contrast between vascular structures and surrounding tissues in MR imaging, opacification of vessels with intravenous contrast agents as in CT is not necessary for delineation.

#### 4.7. CONCLUSIONS

MR imaging is at least as effective as MIBG scintigraphy in the detection of functioning paragangliomas. MR imaging allows a certain degree of tumour characterization that in conjunction with clinical and biochemical findings permits good differentiation of functioning paragangliomas from other tumours.

Because of absence of radiation hazard and superior anatomical resolution whole-body MR imaging should be the primary choice in imaging patients suspected of having functioning paragangliomas.

MR imaging is also well-suited for the screening and follow-up of patients with an increased risk of developing paragangliomas, eliminating the burden of accumulating ionizing radiation doses inherent to repeated CT and MIBG scintigraphic investigations.

As MIBG scintigraphy reflects concentration of adrenergic nervous tissue, incidental tumours of the adrenal cortex remain undetected. However, MIBG scintigraphy can provide functional information and is useful in cases where MR imaging findings are equivocal.

#### 4.8. REFERENCES

1. Sheps SG, Jiang NS, Klee GG. Diagnostic evaluation of pheochromocytoma. *Endocrin Metab Clin N Am* 1988;17:397-414
2. Shapiro B, Copp JE, Sisson JC, Eyre PL, Wallis J, Beierwaltes WH. Iodine-131 metaiodobenzylguanidine for the locating of suspected pheochromocytoma: experience in 400 cases. *J Nucl Med* 1985;26:576-585
3. Francis IR, Glazer GM, Shapiro B, Sisson JC, Gross BH. Complementary roles of CT and 131I-MIBG scintigraphy in diagnosing pheochromocytoma. *AJR* 1983;141:719-725
4. Falke THM, Strake L te, Shaff MI, et al. MR imaging of the adrenals: correlation with computed tomography. *J Comput Assist Tomogr* 1986;10:242-253
5. Schmedtje JF, Sax S, Pool JL, Goldfarb RA, Nelson EB. Localization of ectopic pheochromocytomas by magnetic resonance imaging. *Am J Med* 1987;83:770-772
6. Williams ED, Siebenmann RE, Sobin LH. Histological typing of endocrine tumors. In: WHO international histological classification of tumors. Geneva. World Health Organisation 1980;33-39
7. Dunn GD, Brown MJ, Sapsford RN, et al. Functioning middle mediastinal paraganglioma (phaeochromocytoma) associated with intercarotid paraganglioma. *Lancet* 1986;i:1061-1064
8. Gils APG van, Mey AGL van der, Hoogma RPJM, et al. I-123 Metaiodobenzylguanidine in the detection of chemodectomas in the head and neck region. *J Nucl Med* 1990;31:1147-1155
9. Mangner TJ, Tobes MC, Wieland DW, Sisson JC, Shapiro B. Metabolism of Iodine-131 Metaiodobenzylguanidine in patients with metastatic pheochromocytoma. *J Nucl Med* 1986;27:37-44

10. St John Sutton MG, Sheps SG, Lie JT. Prevalence of clinically unsuspected pheochromocytoma. Review of a 50-year autopsy series. *Mayo Clin Proc* 1981;56:354-360
11. McEwan AJ, Shapiro B, Sisson JC, Beierwaltes WH, Ackery DM. Radioiodobenzylguanidine for the scintigraphic location and therapy of adrenergic tumors. *Sem Nucl Med* 1985;15:132-153
12. Grimley PM. Multicentric paragangliomas and associated neuroendocrine tumors. In: Local invasion and spread of cancer. Brunson KW, ed. Dordrecht. Kluwer academic publishers 1989;49-61
13. Beierwaltes WH. Update on basic research and clinical experience with metaiodobenzylguanidine. *Med Pediatr Oncol* 1987;15:163-169
14. Symington T, Goodall AL. Studies in phaeochromocytoma: pathological aspects. *Glasgow Med J* 1953;34:75-96
15. Russell DS, Rubinstein LJ. Paragangliomas. In: Pathology of tumours of the nervous system. Russell DS, Rubinstein LJ, eds. London. Edward Arnold 1989:945-974
16. Gils APG van, Falke THM, Erkel AR van, Velde CJH van de, Pauwels EKJ. Non-invasive imaging of functioning paragangliomas (including phaeochromocytomas). *Front Eur Radiol* 1990;7:1-38
17. Horbach JMLM, Brenninkmeyer SJ, Velde CJH van de, Nieuwenhuyzen Kruseman AC. A forme fruste of von Hippel-Lindau disease: a combination of adrenal pheochromocytoma and ipsilateral renal cell carcinoma - a case report. *Surgery* 1989;105:436-441
18. Hedeland H, Ostberg G, Hokfelt B. On the prevalence of adrenocortical adenomas in autopsy material in relation to hypertension and diabetes. *Acta Med Scandinavica* 1968;184:211-214
19. Quint LE, Glazer GM, Francis IR, Shapiro B, Chenevert TL. Pheochromocytoma and paraganglioma: comparison of MR imaging with CT and I-131 MIBG scintigraphy. *Radiology* 1987;165:89-93
20. Velchik M, Alavi A, Kressel HY, Engelman K. Localization of pheochromocytoma: MIBG, CT, and MRI correlation. *J Nucl Med* 1989;30:328-336
21. Falke THM. Localization and identification of adrenocortical and sympathomedullary disorders with CT and MRI. Thesis. University of Leiden 1989
22. Falke THM, Gils APG van, Seters AP van, Sandler MP. Magnetic resonance imaging of functioning paragangliomas. *Magn Reson Q* 1990;6:35-64
23. Khafagi FA, Shapiro B, Fig LM, Mallette S, Sisson JC. Labetalol reduces Iodine-131 MIBG uptake by pheochromocytoma and normal tissues. *J Nucl Med* 1989;30:481-489
24. Mirowitz SA, Lee JKT, Brown JJ, Eilenberg SS, Heiken JP, Perman WH. Rapid acquisition spin-echo (RASE) MR imaging: a new technique for reduction of artifacts and acquisition time. *Radiology* 1990;175:131-135
25. Stehling MJ, Howseman AM, Ordidge RJ, et al. Whole-body echo-planar MR imaging at 0.5 T. *Radiology* 1989;170:257-263

## 5

MR IMAGING SCREENING  
OF KINDRED AT RISK  
OF DEVELOPING PARAGANGLIOMAS\*

## 5.1. INTRODUCTION

Paragangliomas of the head and neck region, also known as glomus tumours or chemodectomas, arise from paraganglionic tissue at the carotid bifurcation and in the jugular fossa, the middle ear and the superior mediastinum. Together with the aortic sympathetic, visceral autonomic and intravagal paragangliomas and adrenal phaeochromocytomas they form a class of tumours known as paragangliomas [1].

At least 30% of glomus tumours are familial in origin. Multiple tumours occur in approximately 25 to 35% of patients with familial disease, but in less than 5% of those with the non-familial type [2].

Several authors have found the hereditary pattern of familial glomus tumours to be autosomal dominant [2, 3]. Recently, however, during a retrospective analysis of medical records from 15 affected kindred groups, van der Mey et al. found that the clinical manifestation of the disease is determined by the sex of the transmitting parent [4]. Children of female gene carriers never showed tumour growth, while the prevalence in offspring of male gene carriers increased with age to the expected 50% for an autosomal dominant disorder. This finding can be explained by genomic imprinting, i.e. the maternally derived gene is inactivated during oögenesis and can only be reactivated during spermatogenesis. For several disorders including Huntington's disease and myotonic dystrophy, this new concept has been suggested as a possible explanation for differences in clinical presentation, age of onset and severity that seem to be related to the parental origin of the disease gene. Its suggested role in carcinogenesis is supported by the finding that deletions or losses of chromosome 11 that occur in sporadic cases of Wilms' tumour almost always involve the chromosome of maternal origin [5].

Paragangliomas are potentially capable of catecholamine production. The proportion of catecholamine-secreting paragangliomas is thought to be high for adrenal phaeochromocytomas, intermediate for aortic sympathetic and visceral-autonomic paragangliomas and low for paragangliomas of the head

\* MRI screening of kindred at risk of developing paragangliomas: support for genomic imprinting in hereditary glomus tumours. APG van Gils, AGL van der Mey, RPLM Hoogma, LA Sandkuijl, PD Maaswinkel-Mooy, THM Falke, EKJ Pauwels. *Br J Cancer* 1992;65:903-907

and neck region [6]. We previously reported that the prevalence of hormonally active glomus tumours and their association with other paragangliomas in non-familial cases might be well higher than has been previously suspected [7].

Initially, paragangliomas are often small and extremely slow-growing and hardly cause symptoms. As a result of this indolent growth pattern, the number of affected relatives and the percentage of hormonally active tumours may well have been underestimated in the past. It is, however, important to identify familial cases, as their offspring may also carry a 50% risk of developing tumours. Early identification of new cases and of new lesions in a known patient is relevant since glomus tumour growth may eventually lead to destruction of adjacent structures and to harmful hormonal activity.

Magnetic resonance (MR) imaging has been found very effective in the detection of paragangliomas. Its good anatomical resolution, the absence of radiation hazard, and the redundancy of contrast media containing iodine make MR imaging useful as a screening modality in patients suspected of having these tumours [8].

With these considerations and the above postulated new genetic theory in mind we screened a large, representative kindred group at risk of developing glomus tumours and other paragangliomas, using MR imaging as a primary screening tool. Free urinary catecholamines and vanillylmandelic acid (VMA) levels were measured to detect endocrine-active lesions. The purpose of our study was to acquire greater certainty as to the true number of affected family members and as to the number of lesions with endocrine activity by diagnosing all possible cases. Our extensive evaluation of this unique family also enabled us to test the hypothesis that tumour development only occurs in offspring of male gene carriers. Detection of subclinical lesions in children of female gene carriers would be inconsistent with the predictions according to the genomic imprinting theory.

## 5.2. PATIENTS AND METHODS

### Patients

Between January and December 1990 ninety (90) members of a large kindred group all aged above 18 years and at risk of developing paragangliomas were invited for screening. Two deceased and eight living members had been previously diagnosed as glomus tumour patients. Most relatives were resident in the neighbourhood of our hospital which facilitated screening. Seven relatives declined to participate for various reasons. All participants gave informed consent and the study was approved by the local ethics committee.

The screening programme included a medical history, physical and otolaryngological examination, whole-body MR imaging and determination of free urinary catecholamine excretion in all subjects. Blood was collected from participating family members for DNA linkage studies. For confirmation of glomus tumours, contrast-enhanced computed tomography (CT) or angiography was performed. Where a hormonally active lesion was suspected I-123 MIBG scintigraphy was used. Clinical information concerning deceased members of early generations of the kindred group was obtained from medical records or death certificates. All individuals found to have paragangliomas as well as their parents were classified as obligate gene carriers.

### Magnetic resonance imaging

Patients were examined at 1.5 T using a Gyroscan-S15® (Philips, Best, The Netherlands) scanner. In all cases a body coil was used. Imaging technique included multisectional acquisition of the head and neck area with 1 cm-thick transverse slices, intersection gaps of approximately 1 mm, an acquisition matrix of 179 x 256 and a display matrix of 256 x 256. The field of view was 240 mm. Patients were examined with a spin-echo sequence TR 2200/TE 30-80 and a spin-echo sequence TR 600/TE 20 before and after intravenous injection of 0.1 mmol/kg gadopentetate dimeglumine (Magnevist® Schering, Berlin, Germany). After imaging of the head and neck area, T1- and T2-weighted coronal images of the abdomen and mediastinum were taken in two series using a field of view of 500 mm. If this routine scan was equivocal, a more meticulous examination of the area of interest was carried out using transverse T1- and T2-weighted images. Total procedure time varied from 1.5 to 2 hours. All studies were reviewed independently by two investigators.

### Computer tomography

Patients who had one or more chemodectomas in the head and neck region on MR images were further investigated with contrast-enhanced CT using 6 mm thick adjacent coronal and 9 mm thick adjacent axial slices of the head and neck.

### Catecholamine measurements

The urinary excretion of norepinephrine, epinephrine, dopamine and vanillylmandelic acid was assessed in 24-hour urine samples collected on three consecutive days. Norepinephrine, epinephrine and dopamine levels were assayed by high-performance liquid chromatography (HPLC) and electro-

chemical detection (Coulchem 5100 A ESAR). Vanillylmandelic acid levels were measured by colorimetry after paper chromatography.

### Scintigraphy

Patients in whom elevated urinary catecholamine levels were found underwent I-123 MIBG scintigraphy. A list of all drugs recently used was obtained to rule out interference with I-123 MIBG uptake; special attention was paid to drugs such as reserpine, tricyclic anti-depressants, phenylpropanolamine and sympatholytic agents. Thyroidal uptake was blocked by the administration of Lugol's solution, ten drops three times daily (50 mg of iodine) for five days, starting the day before injection. Each patient was injected intravenously with 370 MBq I-123 MIBG while in the supine position.

Anterior and posterior digitized images of the total body and four images of the head and neck were obtained 24 hours and 48 hours after injection. Additional single photon emission computer tomography (SPECT) of the head and neck was performed 24 hours after the injection. From the SPECT study, 5.3 mm thick transaxial, sagittal and coronal slices were reconstructed.

### Statistical analysis

In all analyses an autosomal dominant mode of inheritance was assumed, with age-dependent penetrance as described elsewhere. Briefly, five age classes were defined (15-20 years, 20-30, 30-40, 40-50, and over 50 years of age) with penetrances of 10%, 35%, 65%, 90% and 95% respectively.

Likelihoods were calculated using version 5.03 of the Linkage package of computer programmes, with the frequency of the gene fixed at 0.0001 [9]. For the likelihood calculations under genomic imprinting the penetrance in children of female gene carriers was assumed to be 0.0, irrespective of age.

## 5.3. RESULTS

One member (V-25) underwent clinical examination but did not have an MR imaging examination because of claustrophobia. In this patient computed tomography of the head and neck was performed instead. Individual IV-15, who is an obligate carrier and may well have the disease subclinically, and three of his five children who are at high risk of being affected, refused MR imaging or CT screening despite several requests. All other participants completed the study.

### Glomus tumours

Table 5.1 lists the clinical, hormonal and MR imaging findings of the affected family members with one or more tumours. Examination of medical records revealed two deceased members (III-3, IV-18) in whom glomus tumours had been diagnosed by means of angiography and surgery. In the family member IV-4 who died from amyotrophic lateral sclerosis, no evidence of glomus tumours had been found on previously performed contrast-enhanced CT examinations. The past medical and familial history of relatives II-1, II-2, III-1, III-2 and IV-5 did not suggest the presence of paragangliomas.

Clinical examination of the eight previously diagnosed glomus tumour patients revealed no new tumours. Among their relatives one (IV-10) complained of unsteadiness which she attributed to old age, but no tumours were found on physical examination. In another relative (IV-20) who also suffered from neurofibromatosis, bilateral carotid masses were felt in the neck.

In the eight known patients, the MR imaging examinations of the head and neck demonstrated all previously diagnosed tumours and in addition, two hitherto unrecognized glomus tumours in two of the subjects (IV-17, V-13). In six undiagnosed relatives (IV-10, IV-13, IV-20, IV-22, V-64, V-66) ten chemodectomas were found on MR imaging. In total MR imaging demonstrated 20 glomus tumours comprising eight carotid body tumours, three vagal body tumours and nine jugulo-tympanic tumours. Of the 14 living patients seven had multicentric lesions (50%). Tumour diameter ranged from 5 mm to 70 mm. A small vagal body tumour and a carotid body tumour were not visible on CT, but were confirmed by angiography.

In the patient with neurofibromatosis on MR images subcutaneous neurofibromas and a large skull lesion were found. The latter proved to be a so-called 'lambdoid defect' on skull roentgenograms [10]. Furthermore, in one relative, MR imaging showed a small cerebellar vascular malformation that was considered to be a coincidental finding.

### Functioning paragangliomas

All participants underwent the urinary screening tests. Only one of the known patients (V-19) had a history that was indicative of a functioning paraganglioma, i.e. hypertension, episodic headaches, palpitations and heavy perspiration. This patient and two of the relatives (V-12, V-64) were found to have elevated urinary excretion of catecholamines. In two subjects (V-19, V-64) MR imaging and MIBG scintigraphy revealed an adrenal phaeochromocytoma. After removal of the phaeochromocytomas catecholamine production normalized in both patients. In the third person (V-12) there was a strong I-123 MIBG uptake by a small carotid body tumour. No other paragangliomas were present in this patient. On removal of the carotid body



Table 5.1. Demographic, clinical and imaging findings of paraganglioma patients.

<i>Pedigree identification</i>	<i>Age</i>	<i>Gender</i>	<i>Signs and symptoms</i>	<i>Endocrin. findings</i>	<i>MR imaging findings</i>	<i>Diagnosis</i>	<i>Special Remarks</i>
A (III-3)	49	M	puls. tinnitus, hearing loss	n.a.	n.a.	GJT Bilat.	Angiography and surgery findings only.
B (IV-10)*	70	F	vertigo, unsteadiness	hypertension	GJT	GJT	
C (IV-11)	53	F	hearing loss		GJT	GJT	
D (IV-13)*	64	M	none		GJT/GJT	GJT Bilat.	
E (IV-16)	48	M	hearing loss		GJT	GJT	
F (IV-17)	45	M	puls. tinnitus, cervical mass		GVT/GCT	GVT*/GCT	
G (IV-18)	19	F	n.a.	n.a.	n.a.	GJT	Died abroad from intracranial extension GJT.
H (IV-20)*	48	M	bilateral cervical mass		GCT/GCT Neurofibroma	GCT Bilat. Neurofibroma	Cutaneous neurofibromas and lambda skull defect on MR images.
I (IV-22)*	43	M	none	n.a.	GCT/GJT	GCT/GJT	
J (V-11)	29	M	vagal nerve lesion, middle ear mass		GJT	GJT	
K (V-12)	27	M	cervical mass	catechol	GCT	function. GCT	MIBG uptake by GCT.
L (V-13)	25	F	hearing loss		GJT/GVT	GJT/GVT*	GVT not visible on CT, confirmed by angiography.
M (V-19)	26	M	facial nerve lesion, middle ear mass	hypertension, catechol	GJT/Phaeo	GJT/Phaeo*	MIBG uptake by left adrenal.
N (V-64)*	31	M	none	hypertension, catechol	GVT/GCT/Phaeo	GVT/GCT/Phaeo	MIBG uptake by right adrenal. GCT only visible on angiogram.
O (V-66)*	27	M	none		GCT	GCT	
P (V-67)	18	F	cervical mass		GCT	GCT	

\* New patient or tumour diagnosis.

n.a. = not available.

patients with undetected tumours. A more accurate assessment of the proportion of isolated cases can only be obtained when the genetic defect has been characterized.

We dealt with a familial tumour syndrome. The common characteristics of the familial tumours are increased risk to the families of the patients, lower age of onset and multiplicity of tumours. The average age of tumour diagnosis in non-familial patients is 42.5 years, compared with a mean age at diagnosis of 38.8 years in our group [2]. In the fifth generation, in part due to

our screening efforts, tumours were even diagnosed at a much earlier age (table 5.1). The more advanced age for tumour diagnosis in non-familial patients is probably due to the lack of suspicion and the initial absence of symptoms. Even in our group with highly aware individuals, some affected members had reached an advanced age without any disturbing symptoms.

In the living patients, multiplicity (50%) and hormonal activity (21%) was diagnosed in a considerably higher frequency than has been reported in the past [2, 6]. This difference may entirely be accounted for by the high sensi-

vity of MR imaging and consistent testing for free urinary catecholamines with the highly accurate HPLC technique [11]. These procedures were not used until recently.

As a screening method for paragangliomas, MR imaging proves to be far superior to physical examination, during which small glomus tumours, in particular vagal and jugulo-tympanic tumours escape recognition altogether.

MR imaging offers several advantages compared with other diagnostic possibilities such as angiography, contrast-enhanced computed tomography and I-123 MIBG scintigraphy that we have discussed previously [8]. Moreover, MR imaging can detect chemodectomas smaller than 5 mm, while contrast-enhanced CT only allows detection of tumours greater than 8 mm [12]. In our group this higher sensitivity of MR imaging was nicely illustrated by two tumours which, because of their small size, could only be confirmed by angiography and not by contrast-enhanced CT.

Sequential MR imaging examinations can provide insight into the natural course of paragangliomas and provide essential information for genetic studies by exclusion of the disease in unaffected persons or by detection of tumours in a very early stage. A systematic search is currently under way to further elucidate the specific genetic defect in hereditary glomus tumours. Screening with MR imaging facilitates linkage analysis by increasing the number of affected members.

At present there are no guide-lines for screening at-risk relatives. Accurate risk assessment in family members depends on assumptions about the mode of inheritance and the role of genomic imprinting. Risk estimates for offspring of females will be very much different if one takes into account the possibility of genomic imprinting. When the gene responsible for familial chemodectomas has been mapped, further confirmation of the genomic imprinting theory will be possible and accurate risk calculations will indicate family members with a very high risk of being gene carriers. Regular screening including MR imaging can be offered to those high risk subjects. The absence of adverse side effects will be of major advantage as it is necessary to follow these individuals for several years given the metachronous tumour occurrence [13]. Considering the fact that tumours are already found in patients aged 18 to 25 and that morbidity and mortality are directly related to size and extent of the tumour, it would seem wise to initiate screening around the age of 20. Urine analysis for catecholamines should always be included as clinical symptoms suggestive for functioning tumours may be sparse [7]. This paucity of symptoms and the presence of only minimal biochemical abnormalities bears a striking resemblance to the behaviour of pheochromocytomas in MEN II patients [11].

In the case of multiple paragangliomas and elevated catecholamine levels, such as our cases V-19, and V-64, one is not certain which tumour is active. In these cases MIBG scintigraphy is invaluable to localize the functioning lesion that has to be removed first [7].

One patient showed cutaneous neurofibromas and a lambda defect in the skull together with two carotid body tumours. The association of neurofibromatosis with adrenal pheochromocytomas is well known but the combination of neurofibromatosis and multicentric extra-adrenal paragangliomas has only been reported once in English literature [14]. A third case was found in German literature [15]. Although rare this combination constitutes further evidence for Bolande's theory that both disorders are neurocristopathies [16].

In conclusion, by means of prospective screening with MR imaging, this study provides further evidence for the theory that inheritance of familial paragangliomas is subject to genomic imprinting. When a paraganglioma is detected an extensive search should be performed for additional tumours and familial occurrence should be considered. For this purpose, screening with MR imaging is the method of choice, not only because it has no adverse side-effects, but also because of its very high sensitivity. In keeping with our results in another non-familial patient group, hormonal activity was a not infrequent finding in this patient group. As symptoms and signs are usually minimal, periodic examination of individuals at risk will allow the detection of tumours and hormonal activity in a presymptomatic and still localized stage. This in turn allows therapeutic intervention at an early stage thus providing a basis for secondary prevention.

## 5.5. REFERENCES

1. Glenner GC, Grimley PM. Tumors of the extra-adrenal paraganglion system (including chemoreceptors). Atlas of tumor pathology: second series: fascicle 9. Washington DC. Armed Forces Institute of Pathology 1974
2. Grufferman S, Gillman MW, Pasternak LR, Peterson CL, Young WG. Familial carotid body tumors: case report and epidemiologic review. *Cancer* 1980;46:2116-2122
3. Parkin JL. Familial multiple glomus tumors and pheochromocytomas. *Ann Otol Rhinol Laryngol* 1981;90:60-63
4. Mey AGL van der, Maaswinkel-Mooy PD, Cornelisse CJ, Schmidt PJ, Kamp JJP van de. Genomic imprinting in hereditary paragangliomas: evidence for a new genetic theory. *Lancet* 1989;ii:1291-1294
5. Hall JG. Genomic imprinting: review and relevance to human disease. *Am J Hum Genet* 1990;46:857-874
6. Dunn GD, Brown MJ, Sapsford RN, et al. Functioning middle mediastinal paraganglioma (pheochromocytoma) associated with intercarotid paraganglioma. *Lancet* 1986;i:1061-1064
7. Gils APG van, Mey AGL van der, Hoogma RPJM, et al. I-123 Metaiodobenzylguanidine in the detection of chemodectomas in the head and neck region. *J Nucl Med* 1990;31:1147-1155
8. Gils APG van, Falke THM, Erkel AR van, et al. MRI and MIBG imaging of pheochromocytomas and extra-adrenal functioning paragangliomas. *Radiographics* 1991;11:37-57

9. Lathrop GM, Lalouel JM. Easy calculations of lod scores and genetic risks on small computers. *Am J Hum Genet* 1984;36:460-465
10. Resnick D. Bone and joint imaging. Philadelphia. WB Saunders 1989;1220-1221
11. Stein PP, Black HR. A simplified diagnostic approach to pheochromocytoma. A review of the literature and report of one institution's experience. *Medicine* 1991;70:46-66
12. Vogl T, Brüning R, Schedel H, et al. Paragangliomas of the jugular bulb and carotid body: MR imaging with short sequences and Gd-DTPA enhancement. *AJR* 1989;153:583-587
13. Grimley PM. Multicentric paragangliomas and associated neuroendocrine tumors. In: Local invasion and spread of cancer. Brunson KW, ed. Dordrecht. Kluwer academic publishers 1989;49-61
14. DeAngelis LM, Kelleher MB, Post KD, Fetell MR. Multiple paragangliomas in neurofibromatosis: a new neuroendocrine neoplasia. *Neurology* 1987;37(1):129-133
15. Löblich HJ, Baumann A. Die verschiedenen Kombinationen geschwulstartiger Hyperplasien des Nervensystems. Ein Beitrag zur Pathogenese der Systemhyperplasien am Beispiel eines Sektionsfalles. *Zentbl Allg Pathol* 1960;101:159-165
16. Bolande RP. The neurocristopathies: a unifying concept of disease arising in neural crest maldevelopment. *Hum Pathol* 1974;5:409-429

## 6

## QUANTITATIVE EVALUATION OF GADOPENTETATE DIMEGLUMINE PERFORMANCE IN MR IMAGING OF HEAD AND NECK PARAGANGLIOMAS INCLUDING AFROC ANALYSIS\*

### 6.1. INTRODUCTION

Paragangliomas of the head and neck are highly vascular lesions, that can be demonstrated by contrast-enhanced computed tomography (CECT) and angiography. They originate from paraganglionic tissue (glomera) located at the carotid bifurcation, along the nodose ganglia of the vagus nerve and in the jugular fossa and the tympanic cavity. These tumours frequently occur as an autosomal dominant hereditary disease with tumour expression determined by genomic imprinting [1]. Hereditary predisposition to develop paragangliomas can nowadays be assessed by genetic testing before symptoms arise [2]. In at least 30% of cases more than one tumour may be present simultaneously in the same patient at different locations [3].

In recent years magnetic resonance (MR) imaging has been applied to detecting and localizing these tumours. The absence of ionizing radiation and superb soft tissue contrast make MR imaging an ideal tool for screening and following subjects at risk of developing hereditary tumours including paragangliomas [4, 5].

Paragangliomas are isointense compared to surrounding structures on pre-contrast T1-weighted images and difficult to recognize when small. On T2-weighted images these tumours show an increased signal intensity. Multiple punctate and serpentine areas of signal void due to high-velocity flow in tumour vessels and a 'salt and pepper' heterogeneity were considered typical MR findings in a large majority of cases reported by Olsen et al. [6].

The administration of intravenous MR contrast media has been recommended for improved tumour detectability in paraganglioma patients [7]. Vogl et al. suggested the use of gadopentetate dimeglumine (Magnevist® Schering, Berlin, Germany) -enhanced T1-weighted imaging when no paragangliomas are seen on unenhanced T1-weighted images without performing T2-weighted series [8]. Although relatively safe, the intravenous administration of these contrast media still constitutes an invasive procedure, and a number of side effects including anaphylactoid reactions may occur [9-14].

\* Based on: MR diagnosis of paraganglioma of the head and neck: value of contrast enhancement. APG van Gils, R van den Berg, THM Falke, JL Bloem, HJ Prins, EH Dillon, AGL van der Mey, EKJ Pauwels. *AJR* (in press).

Furthermore, their use increases costs and may prolong examination time. For clinical MR examinations and in particular for studies performed to screen and follow-up persons at risk of developing paragangliomas, it is thus important to assess whether gadopentetate-enhanced imaging indeed gives a significantly better detectability than unenhanced T2-weighted imaging.

To date, comparative analysis of unenhanced MR imaging and contrast-enhanced MR imaging to assess the relative diagnostic efficacy of both methods in detecting head and neck paragangliomas has not, to our knowledge been carried out. The aim of this study was to compare the relative diagnostic value of unenhanced MR imaging with MR imaging after intravenous injection of 0.1 mmol/kg gadopentetate dimeglumine in the evaluation of head and neck paragangliomas, using quantitative measurements of diagnostic performance, free from observer bias. As the normal receiver-operating-characteristic (ROC) analysis does not take into account the location information or the presence of multiple lesions in one examination, we made use of a recently introduced method called alternative free-response receiver-operating-characteristic (AFROC) analysis that does not have these limitations [15].

## 6.2. MATERIAL AND METHODS

### Patient selection

A total of 60 subjects (aged 21-73) who were referred to the department of diagnostic radiology at our institution for MR imaging of the craniocervical area from July 1989 to February 1992 were studied. In 37 patients the presence of 71 paragangliomas in the head and neck region had been confirmed by CECT (n = 28 patients), angiography (n = 18 patients), sonography (n = 20 patients) and I-123 octreotide scintigraphy (n = 5 patients). Multicentricity occurred in 22 patients (59%). The highest number of tumours simultaneously present in one patient was five. There were 32 carotid body tumours, 17 glomus jugulare tumours, three tympanic tumours and 19 vagal body tumours. Ten of these tumours were postoperative tumour residues. Histology and surgical confirmation was available in 20 patients. Genetic confirmation of hereditary paragangliomatosis was available in 24 patients [2]. Twenty-three subjects who underwent the same investigation for various unrelated reasons and had been proved disease-free by genetic studies (n = 14) or normal findings on MR as well as on CT (n = 11) were used for comparison.

### MR imaging technique

Thirteen persons were examined with a 0.5-T Gyroscan-S5<sup>®</sup> scanner (Philips, Best, The Netherlands) and forty-seven persons with a 1.5-T Gyroscan-S15<sup>®</sup> scanner (Philips) using a head or body coil. To cover the entire region where head and neck paragangliomas may arise, imaging technique always included transverse multisectional acquisition of the head and neck area with 7 mm-thick slices, interslice gaps of approximately 1 mm, an acquisition matrix of 179 x 256 and a display matrix of 256 x 256. The field of view was 240 mm. Patients were examined at 0.5 T with unenhanced spin-echo sequences of TR 2500/TE 50-100 and TR 500/TE 30 and at 1.5 T with unenhanced spin-echo sequences of TR 2200/TE 30-80 and TR 600/TE 20. The T1-weighted sequence was repeated after intravenous injection of 0.1 mmol/kg gadopentetate dimeglumine. In all cases, the post-contrast sequence was performed in the same session as the unenhanced sequences. In most patients additional sequences were obtained with various other slice thicknesses and imaging planes and different imaging parameters.

### Image interpretation

The studies were organized and randomized by two radiologists who were not later involved in interpretation. The unenhanced T1-weighted series, the T2-weighted series (proton density-weighted and strong T2-weighted images combined) and the enhanced T1-weighted series were each placed in an individual folder. Each folder contained a complete view of the region of interest (C5 - falx cerebri). Where one or two anatomic sections were missing from any of the MR pulse sequence studies, corresponding sections were deleted from all sequences of that patient to be sure that the same region of interest was compared. To make comparison more fair, coronal and sagittal images as well as gradient-recalled-echo (GRE) sequences and sequences with thinner slices additionally obtained in a number of cases were left out of the study. All patient identifying information was obscured with tape on the original hard-copy, laser camera images. The three folders of all examinations were numbered sequentially.

Initially, two combinations: unenhanced T1-weighted and T1-weighted sequences after gadopentetate dimeglumine (combination A) and the unenhanced T1-weighted combined with the T2-weighted sequences (combination B) were presented in random order to four radiologists with extensive MR experience for independent interpretation and scoring. No clinical information was supplied. In the second phase of interpretation the three folders of each examination were aggregated and these combined sequences (combination C) were again randomized for scoring. The readings were spread over six months with at least a two-week interval between sessions.

The readers did not know the proportion of normal cases and were asked to separately describe the presence of paragangliomas larger than 5 mm and their location according to a four level scale of confidence: 4 = definitively positive, 3 = probably positive, 2 = possibly positive, 1 = probably negative. This scale corresponds with a five level ROC scale because a negative response is classified as 0. Time for reading was unlimited.

Furthermore, the readers were asked to comment on the following aspects: (1) the diagnostic quality of images; (2) the morphologic and signal characteristics of the unenhanced tumour, with special emphasis on the presence of flow-void phenomena in the tumour; (3) the degree of enhancement after gadopentetate dimeglumine administration, using a four grade scale: none, poor, moderate, and strong enhancement; (4) additional diagnostic information from post-contrast sequences; (5) the delineation of the tumour from surrounding structures, (6) the reader's subjective preference for a sequence. The results of the four readers for the image findings were averaged. Completed score sheets for each individual combination were then collected. The standard of reference was established by three study coordinators who did not take part in the interpretation sessions, and was based on all available genetic, imaging, clinical and surgical findings.

### Statistical analysis

The evaluation of the data consisted of two parts. First, the scoring results of the four readers for the subset of the 37 patients with disease were subjected to an AFROC analysis with assessment of the number of true-positive lesions and the number of false-positive images (FPI) for each confidence level [15]. From this data, the area under the AFROC curve (A1) was calculated for each reader and each combination using the ROCFIT programme developed by Metz [16]. The individual 'area under the curve' values were compared by generating a critical ratio  $z$  using the Kendall correlation coefficient to correct for the correlation between data sets, a method described by Hanley and McNeil [17]. The AFROC areas were averaged for each combination and tested for significance of differences in performance by applying a one-factor analysis of variance for repeated measurements at the 95% confidence level [18]. Paired comparisons between the combinations were performed with the Fisher protected least-significant-difference test [19]. Composite AFROC curves were obtained by applying the maximum-likelihood curve fitting algorithm to the data pooled from all observers. These composite curves were made for illustrative purposes only and were not used for statistical analysis [20].

Second, we also performed a matrix analysis of all cases. To this end, each study was divided into six regions i.e. bilateral carotid, vagal, and jugulo-tympanic regions. For practical purposes tumours arising in this latter

region were combined, as it was often not possible to determine the jugular or tympanic origin irrefutably [21]. The rating data were attributed to these six regions, taking '4', '3' and '2' as positive responses and '1' and the implicit '0' as negative responses.

Sensitivity and specificity were calculated for each individual reader. The sensitivity was defined as the ratio of true-positive diagnoses divided by the number of tumours actually present ( $n = 71$ ). The specificity was defined as the ratio of true-negative diagnoses divided by the number of negative regions ( $n = 289$ ). The McNemar test was used to compare sensitivity and specificity for the individual readers [22]. The results of the sensitivity and specificity comparisons were combined with the Fisher procedure [23]. Interobserver agreement with a correction for chance was assessed with the  $\kappa$  statistic [24]. The guide-lines suggested by Landis and Koch were used to interpret the degree of agreement: <0 poor, 0-0.20 slight, 0.21-0.40 fair, 0.41-0.60 moderate, 0.61-0.80 substantial and 0.81-1.00 indicating perfect agreement [25].

## 6.3. RESULTS

### Image findings

All examinations were considered adequate for interpretation by the four readers. Averaged over the interpreters, image quality was judged as excellent or good in 83% and as moderate or sufficient in 17%. Mean tumour diameter was 24 mm (range 5-90 mm) (figure 6.1). On T1-weighted images most tumours (74%) had a signal intensity comparable to muscle and lower than salivary gland tissue, whereas on T2-weighted images all tumours had a higher signal intensity than muscle. On T2-weighted images 60 percent

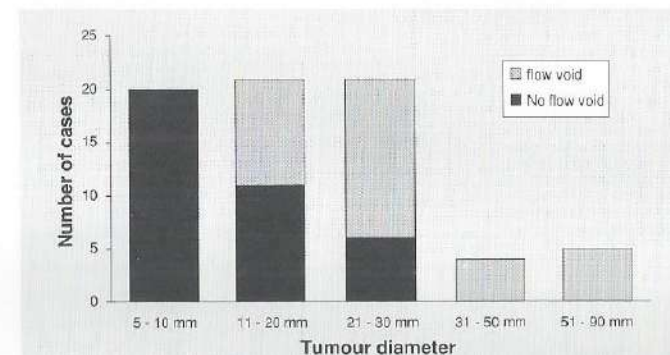


Figure 6.1. Graph shows distribution of sizes of paragangliomas and illustrates the relationship between size and flow-void phenomenon.

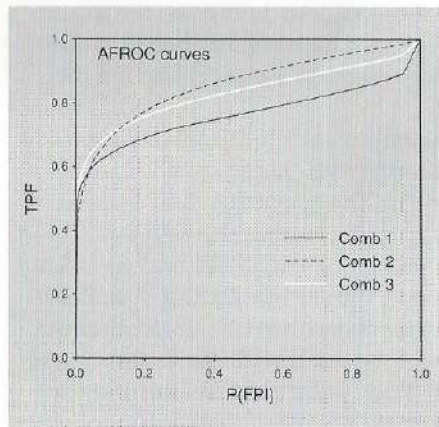


Figure 6.2. Composite AFROC curves of the three combinations. TPF = fraction of tumours detected and located correctly. P(FPI) = probability of image yielding a false-positive result.

had a signal intensity equal to salivary gland tissue and 40 percent a signal intensity higher than salivary gland tissue.

The flow-void phenomenon was more often noted on T2-weighted images than on T1-weighted images (40% versus 31%). Overall it was present in 34 tumours and occurred more frequently in tumours with a diameter of more than 20 mm (figure 6.1). Non-homogeneous appearance other than the flow voids caused by tumour vessels was present in 20% of the tumours.

All tumours showed enhancement. Enhancement was, on average, judged by the interpreters as mild in 1.4% of tumours, moderate in 35.2% of tumours, and strong in 63.4% of tumours. There was homogeneous enhancement in 77.4% of tumours and non-homogeneous enhancement in 22.6%. Substantial

Table 6.1. Areas under the AFROC curves.

Observer No.	Pre- and Post-Contrast T1-weighted MR imaging	T1-and T2-weighted MR imaging	All MR seq.
1	0.702	0.798*	0.775
2	0.786	0.847	0.835
3	0.796	0.924*	0.871*
4	0.753	0.867*	0.846
Mean (SD)	0.761 (.051)	0.856 <sup>†</sup> (.064)	0.827 <sup>†</sup> (.048)

\*Significant difference with pre- and post-contrast T1-weighted MR imaging at  $P < 0.05$  (Critical Ratio).

<sup>†</sup>Significant difference with pre- and post-contrast T1-weighted MR imaging at  $P < 0.05$  (Analysis of Variance).

Table 6.2. Totalled ratings of all observers for combinations A/B/C\*

Ratings	0 mm			5-10 mm			11-20 mm		
	A	B	C	A	B	C	A	B	C
0	1019	1054	1045	41	28	24	16	14	18
1	63	46	44	9	7	4	0	6	4
2	34	26	32	3	8	7	4	5	4
3	28	17	20	6	10	14	9	5	4
4	12	13	15	21	27	31	55	54	54

Ratings	21-30 mm			31-50 mm			51-90 mm		
	A	B	C	A	B	C	A	B	C
0	6	3	5	5	1	3	0	0	0
1	2	0	3	1	0	0	0	0	0
2	1	1	0	1	0	1	0	0	0
3	7	5	4	1	0	0	0	0	1
4	68	75	72	8	15	12	20	20	19

\*Combination A = unenhanced T1- and enhanced T1-weighted sequences combined.

Combination B = unenhanced T1- and T2-weighted sequences combined.

Combination C = all sequences combined.

Table 6.3. Overall Sensitivity/Specificity

Observer No.	Pre- and Post-Contrast T1-weighted	T1-and T2-weighted	All MR seq.
1	.69 / .91	.72 / .92	.73 / .93
2	.73 / .98	.80 / .96	.82 / .93
3	.76 / .96	.82 / .98	.80 / .96
4	.72 / .92	.82* / .94	.79 / .93
Mean	.73 / .94	.79 <sup>†</sup> / .95	.78 / .94

\*Significant difference with pre- and post-contrast T1-weighted MR imaging at  $P < 0.05$  (McNemar).

<sup>†</sup>Significant difference with pre- and post-contrast T1-weighted MR imaging at  $P < 0.05$  (Fisher procedure).

differences in enhancement rated to size were not observed. In all patients who underwent a second post-contrast sequence 6 to 12 minutes after injection, enhancement was found to be persistently high.

Tumour delineation was considered excellent or good in 77% and moderate or poor in 23% for proton density and T-2 weighted images versus 79% and 21% respectively for enhanced T1-weighted images. The readers preferred proton density-weighted images in 63% of cases, T1-enhanced images in 22%, T2-weighted images in 10% and T1-unenhanced images in 5%.

#### Comparison of MR imaging pulse sequences

AFROC curves for readers and combinations separately, show the areas under the AFROC curve for combinations B and C to be almost equal and both to be significantly larger than for combination A (table 6.1). The small difference between combinations B and C is largely due to the higher number of false-positives in the latter combination. As the method-related shifts in performance noted for the four readers were consistent, we pooled the data to make composite AFROC curves (figure 6.2). These curves were used for illustrative purposes only and not for statistical analysis.

After attributing and dichotomizing the test results we found an overall sensitivity for tumour detection of 73% (95% confidence interval: 65-91%) in combination A (unenhanced and enhanced T1-weighted sequences). In combination B (unenhanced T1- and T2-weighted sequences) the sensitivity was 79% (72-96%). In combination C (the combination of all sequences) sensitivity was 78% (68-94%). The overall specificity for the diagnosis of normality was 94% (85-98%), 95% (89-100%) and 94% (87-100%) respectively. The totaled responses of the four observers rated to tumour size are listed in table 6.2. There were no major inequalities between the three combinations in the distribution of interpretative ratings varied with size.

Interobserver agreement was substantial with  $\kappa$  values ranging from 0.56 to 0.77 and none of the combinations performing substantially better.

A statistically significant difference in individual sensitivity and specificity values when tested with the McNemar test was only found as regards the sensitivity of combinations A and B in the case of reader 4 (table 6.3). Combination of the McNemar results by means of the Fisher procedure yielded a significant difference in sensitivity between combinations A and B ( $p < 0.05$ ), whilst the difference between combinations A and C approached significance ( $p = 0.09$ ).

Analysis of tumours detected by combination C but not by combination B, showed 9 of the 25 instances (where the addition of gadopentetate dimeglumine influenced tumour detection positively) to be postoperative tumour residues (36%). The 50 false-positive interpretations made with method C but not

with method B were mostly due to strong enhancement of vessels or to errors involving enhancement of submandibular and parotid gland tissue.

#### 6.4. DISCUSSION

The results of this study demonstrate that for the detection of head and neck paragangliomas the performance of the combination of unenhanced and enhanced T1-weighted MR imaging is significantly poorer than that of the combination of unenhanced T1- and T2-weighted imaging and the combination of all sequences. There was little difference in performance between the latter two combinations, which both included T2-weighted series. In other words, the addition of a T2-weighted sequence to unenhanced and enhanced T1-weighted images increased the detection performance of MR imaging significantly. The addition of an enhanced T1-weighted sequence to unenhanced T1- and T2-weighted images on the other hand did not result in an increased overall detection rate. Indeed, although a procedure bias ought to have favoured the combination of all sequences, as this combination was studied separately after the first two combinations, its overall performance was marginally inferior. The slightly lower A1 values of all readers in the combination of all sequences as compared to the combination of unenhanced T1- and T2-weighted sequences are largely caused by a higher number of false-positives due to misleading enhancement of vessels or salivary gland tissue, but also, to a lesser extent, to lower sensitivity for two of the readers.

In addition, our results show that in selected cases there may be a complementary role for gadopentetate dimeglumine. Although not at a statistically significant level, the enhanced T1-weighted sequence assisted detection in some of the tumours smaller than 2 cm, in particular postoperative tumour residues.

The likelihood that a person will develop one or more paragangliomas in the head and neck can nowadays be predicted with very high accuracy by genetic testing [2]. This implies an additional screening role for MR imaging, subsequent to DNA analysis. Considering the absence of improved overall tumour detectability with gadopentetate dimeglumine, it would seem that the use of a contrast-enhanced sequence is not warranted under such circumstances. Only where there is clinical suspicion of a postoperative tumour residue, should the addition of a contrast-enhanced T1-weighted sequence be considered.

It can be argued that a higher dosage of gadopentetate dimeglumine (0.2 mmol/kg) will provide a higher contrast with surrounding tissue and increase the detectability of tumours. In the specific case of head and neck paragangliomas, however, benefit will probably be minimal as the majority of tumours already shows strong enhancement at a dose of 0.1 mmol/kg. In our study, the differences in enhancement between tumours probably reflect differ-

ences in vascularity. Variation in the time of starting the scan after injection could cause different degrees of enhancement, but in our study scanning was always started immediately after the injection. Moreover, although a highly increased signal intensity is present within 60 seconds [26] we found enhancement to be persistently high 6 to 12 minutes after injection. A dosage increase would therefore probably have had little effect on our results.

Our results may not quite equal those which might have been achieved in a clinical setting where more information is available. Our method of blinding the readers was, for purposes of investigation, intended to be as rigorous as practically possible and may partially be responsible for the moderate sensitivities found. Readers received no information as to hereditary history, clinical findings, previous surgery or results from other imaging studies and reading by consensus or with conference between readers was avoided. Moreover, a higher number of small tumours was included than would probably have been encountered in a clinical situation. This was due to the inclusion of a large number of familial patients who often show hypertrophic paraganglionic tissue at various sites. Pathologically, hypertrophic tissue is considered a tumour when weighing more than 30 mg [27]. MR imaging on the other hand is able to depict paragangliomas with a diameter as small as 5 mm [8]. We therefore considered 5 mm to be the maximum size for hypertrophic tissue. This choice explains the high number of small tumours in our study.

Consequently, we feel that our study results, although not completely representative of a clinical situation, certainly apply very well to a screening situation. On the other hand, this disproportionately high number of small tumours is outstandingly well suited to observer studies and provides excellent material with which to assess the efficacy of contrast media. Assessments of contrast media frequently rely on a visual grading with subjective assessment of diagnostic value. In our opinion such assessments would be of greater value if a more objective test was incorporated. In principle, ROC analysis is the most appropriate method, but it is subject to the above mentioned limitations. We therefore made use of AFROC analysis, a modified ROC technique. The implications of this technique as well as its advantages for dealing with an arbitrary number of lesions at multiple sites in one study instead of dealing with the presence or absence of one lesion per study have been clearly outlined by Chakraborty and Winter [15]. The area under the AFROC curve, just as that under the ROC curve, represents an index of performance and ranges from zero (chance accuracy) to one (perfect detection). It can easily be calculated by the widely available ROCFIT programme [15, 16].

Unlike the ROC curve, the AFROC plot does not indicate the false-positive fraction (FPF) of a modality on the x axis but rather the likelihood of obtaining a false-positive image, P(FPI). Although a FPI may contain an infinite number of false-positive responses at various sites in one image it is still counted as one false-positive decision. In theory this could favour one of the

combinations studied more than the others and cause a substantial difference with a binary test such as McNemar's. In our study, however, the false-positive responses were fairly equally distributed over all methods and examinations. The results of the additionally performed McNemar test thus largely concurred with those of the AFROC analysis. While not attempting to validate the AFROC technique we found this agreement of its results with those of the McNemar analysis to be striking.

Delineation was more often judged better on proton density images than on enhanced T1-weighted images, even though all tumours showed enhancement, most of them markedly. Our T2-weighted series consisted of a long TR and an uneven-echo technique with a short TE and a long TE. The proton-density images in particular, often have the highest signal-to-noise ratio available and provide excellent views of the overall anatomy, especially the vessels that are intimately related to the paraganglionic system. For the detection and delineation of paragangliomas the anatomic display of this sequence probably more than compensated for its lower soft-tissue contrast. In post operative cases the increased soft-tissue contrast with non-enhancing scar tissue, provided by gadopentetate dimeglumine, probably aided tumour detection where a distorted vascular anatomy and an already present asymmetry between left and right provided no clues as to the presence of a tumour.

Flow void was observed in a lesser percentage in our study than found by Olsen [6]. This finding can be explained by the inclusion in our study of a far greater number of small tumours that do not tend to show the flow-void phenomenon. Flow void was more often noted on the T2-weighted sequences than on the enhanced and unenhanced T1-weighted sequences, which can be explained by the sensitivity of the T2-weighted sequences for flow in vessels. A second explanation can be found in the masking effect of gadopentetate dimeglumine on the flow voids in the tumour vessels. These vessels then demonstrate a high signal intensity due to enhanced blood thus reducing contrast with the surrounding tumour tissue.

There is no doubt that the enhancing property of gadopentetate dimeglumine and its ability to make tumours stand out clearly are very valuable attributes in certain situations. Gadopentetate dimeglumine can also play an important role in characterization of various tumour types and lymph nodes. Contrast-enhanced MR imaging could potentially shorten the examination time if T2-weighted SE sequences are replaced by contrast-enhanced T1-weighted sequences. However, our study has shown that the combination of unenhanced and enhanced T1-weighted sequences as suggested by Vogl et al. [8] is insufficient for the detection of head and neck paragangliomas. This implies that in fact more time is required as the contrast enhancement can only be achieved during an additional sequence, after performing unenhanced T1- and T2-weighted series. Besides, time lost in dosing the patient with an intravenous infusion in the MR room also has to be taken into account. Furthermore, the advantages of MR imaging as a non-invasive investigation are for-

feited when a contrast agent is used. Although the risk of adverse reactions to gadopentetate dimeglumine is slight, it is certainly not negligible [28]. This fact applies under all circumstances but is particularly relevant in patients at risk of head and neck paragangliomas who require repeated examinations over a prolonged period. Considering also the added cost of the contrast medium itself, the administration of gadopentetate dimeglumine as a matter of routine does not seem justified.

As already stated, MR imaging for detection of paragangliomas will often be performed in persons at risk of developing these tumours or in patients already known to have such a tumour. Because this places more emphasis on tumour detection and tumour delineation than on tumour characterization we did not include other tumour types in this study and so the issue of efficacy of gadopentetate dimeglumine in differentiating paragangliomas from other tumour types was not addressed. Consequently, our findings cannot be directly transferred to the use of gadopentetate dimeglumine in other clinical situations. This, however, in no way detracts from the evident desirability of incorporating blinded observer studies to achieve objective assessment of the merits and deficits of contrast media for other tumour types.

In conclusion, our results indicate that the administration of gadopentetate dimeglumine does not improve detection of head and neck paragangliomas significantly. On the contrary, contrast enhancement in fact led to a slight decrease in specificity. The extra time, effort, cost and additional risks involved in obtaining contrast-enhanced images are generally not justified. In the authors' opinion the additional diagnostic yield of intravenous MR contrast media only outweighs the costs in patients with postoperative tumour residues. The results of this study have specific application only to the search for paragangliomas of the head and neck, but we believe that the evaluation of contrast media in other types of lesions should always include efficacy measurements by objective operator-independent tests. ROC or AFROC analysis could be valuable tools in this respect.

## 6.5. REFERENCES

1. Mey AGL van der, Maaswinkel-Mooy PD, Cornelisse CJ, Schmidt PJ, Kamp JJP van de. Genomic imprinting in hereditary paragangliomas: evidence for a new genetic theory. *Lancet* 1989; ii:1291-1294
2. Heutink P, Mey AGL van der, Sandkuijl LA, et al. A gene subject to genomic imprinting and responsible for hereditary paragangliomas maps to chromosome 11q23-qter. *Hum Mol Genet* 1992;1:7-10
3. Parkin JL. Familial multiple glomus tumors and pheochromocytomas. *Ann Otol Rhinol Laryngol* 1981;90:60-63

4. Gils APG van, Mey AGL van der, Hoogma RPLM, et al. MRI screening of kindred at risk of developing paragangliomas: support for genomic imprinting in hereditary glomus tumors. *Br J Cancer* 1992;65:903-907
5. Jackson CE, Tashjian AH. Limited progression of hereditary medullary thyroid cancer after conservative management (abstr). *Am J Hum Genet* 1992;51(P):235
6. Olsen WL, Dillon WP, Kelly WM, Norman D, Brant-Zawadzki M, Newton TH. MR imaging of paragangliomas. *AJR* 1987;148:201-204
7. Phelps PD, Cheeseman AD. Imaging jugulotympanic glomus tumors. *Arch Otolaryngol Head Neck Surg* 1990;116:940-945
8. Vogl T, Juergens M, Balzer J, et al. MR Imaging of the head and Neck. In: Lissner J, Baert AL, Pokieser H, van Waes PFGM, eds. *MR: State of the art*. Vienna. *Eur Congress Radiol* 1991;49-75
9. Tishler S, Hoffman JC Jr. Anaphylactoid reactions to i.v. gadopentetate dimeglumine. *AJNR* 1990;11(6):1167
10. Salonen OL. Case of anaphylaxis and four cases of allergic reaction following GD-DTPA administration. *J Comput Assist Tomogr* 1990;14(6):912-913
11. Weiss KL. Severe anaphylactoid reaction after iv Gd-DTPA. *Magn Reson Imaging* 1990;8:817-818
12. Goldstein HA, Kashanian FK, Blumetti RF, Holyoak WL, Hugo FP, Blumenfeld DM. Safety assessment of gadopentetate dimeglumine in United States clinical trials. *Radiology* 1990;174:17-23
13. Takebayashi S, Sugiyama M, Nagase M, Matsubara S. Severe adverse reaction to iv gadopentetate dimeglumine. *AJR* 1993;160:659
14. Tardy B, Guy C, Barral G, Page Y, Ollagnier M, Bertrand C. Anaphylactoid shock induced by intravenous gadopentetate dimeglumine. *Lancet* 1992;339:494
15. Chakraborty DP, Winter LHL. Free-response methodology: alternate analysis and a new observer-performance experiment. *Radiology* 1990;174:873-881
16. Metz CE, Kronman HB, Wang P-L, Shen J-H. ROCFIT: a modified maximum likelihood algorithm for estimating a binormal ROC curve from confidence-rating data. Chicago. University of Chicago 1985
17. Hanley JA, McNeil BJ. A method of comparing receiver operating characteristic curves derived from the same cases. *Radiology* 1983;148:839-843
18. Godfrey K. Comparing the means of several groups. *N Engl J Med* 1985;313:1450-1456
19. Armitage P, Berry G. *Statistical methods in medical research*. 2nd ed. Oxford. Blackwell 1987
20. Berbaum KS, Dorfman DD, Franken EA. Measuring observer performance by ROC analysis: indications and complications. *Invest Radiol* 1989;24:228-233
21. Mey AGL van der, Frijns JHM, Cornelisse CJ, et al. Does intervention improve the natural course of glomus tumors? *Ann Otol Rhinol Laryngol* 1992;101:635-642
22. Dwyer AJ. Matchmaking and McNemar in the comparison of diagnostic modalities. *Radiology* 1991;178:328-330
23. Rosenthal R. *Meta-analytic procedures for social research*. Beverly Hills. Sage publications 1984;93-110

24. Fleiss JL. Statistical methods for rates and proportions. 2nd ed. New York. Wiley 1981;212-236
25. Landis RJ, Koch GG. The measurement of observer agreement for categorical data. *Biometrics* 1977;33:159-174
26. Vogl T, Brüning R, Schedel H, et al. Paragangliomas of the jugular bulb and carotid body: MR imaging with short sequences and Gd-DTPA enhancement. *AJNR* 1989;10:823-827
27. Heath D. The human carotid body in health and disease. *J Pathol* 1991;164:1-8
28. Kieffer SA. Gadopentetate dimeglumine: reassessment of the clinical research process. *AJNR* 1990;11:1168-1169

# 7

## GENERAL DISCUSSION\*

### 7.1. INTRODUCTION

The prospective application of MR imaging and MIBG scintigraphy to relatively large groups of patients revealed two important but unknown aspects of these tumours. First, the clinical evidence for genomic imprinting in hereditary paragangliomas [1, chapter 5] and secondly, the occurrence of functional activity in glomus tumours and their association with other functioning paragangliomas. Remarkable is that these functioning paragangliomas caused relatively few symptoms of catecholamine excess [chapters 3 and 5].

In contrast to sporadic functioning paragangliomas, the functioning paragangliomas in MEN syndromes are asymptomatic in about 50% of cases, especially in the early course of development, and are only diagnosed as a result of increased suspicion [2, 3, 4]. This asymptomatic behaviour probably occurs likewise in hereditary paragangliomatosis and conceivably also in other syndromes associated with functioning paragangliomas such as von Hippel-Lindau disease and neurofibromatosis.

The importance of timely detection of functioning paragangliomas lies in the fact that hypertension caused by the systemic effects of catecholamines is surgically curable in the majority of patients but if unrecognized carries very high morbidity and mortality rates. An early diagnosis of functioning tumours in these syndromes may be suggested by abnormalities of norepinephrine or its metabolites in plasma or urine [5]. Diagnosis and localization of these clinically silent tumours is of the utmost importance, because these patients may develop fatal paroxysms during surgery for associated tumours.

In our studies by the combined use of biochemical methods and of the newer imaging techniques we detected a high number of catecholamine-secreting paragangliomas, causing little or no symptoms, in familial as well as non-familial patients [chapters 3 and 5]. Furthermore, despite fairly

\* Based on: Non-invasive imaging of functioning paragangliomas (including pheochromocytomas). APG van Gils, THM Falke, AR van Erkel, CJH van de Velde, EKJ Pauwels. *Front Eur Radiol* 1990;7:1-38, and on: MR imaging or MIBG scintigraphy for the demonstration of paragangliomas? Correlations and disparities. APG van Gils, AR van Erkel, THM Falke, EKJ Pauwels. *Eur J Nucl Med* (in press).

widespread acquaintance with the characteristics of catecholamine-secreting paragangliomas, there has been in the past a considerable discrepancy between the frequency of clinical detection of these tumours and their discovery at autopsy (1:4) [6, 7]. It is highly likely that the availability of the latest imaging techniques has reduced the extent of this discrepancy, although this has not as yet been established. These observations underscore the need for a regular follow-up of at-risk patients. Biochemical measurements alone are not completely sufficient, as the catecholamine secretion by paragangliomas is often intermittent [8]. The examination of these patients should therefore include whole-body imaging with a highly sensitive, non-invasive imaging modality.

The application of both new whole-body imaging methods in the course of several investigations in such a large group of patients has also provided us with the opportunity to compare the respective values of both methods. It is clear that, in the non-invasive imaging of paragangliomas, neither MR imaging nor MIBG scintigraphy can be described as demonstrating universal superiority. Several considerations play their individual and collective roles in the choice for one of the two methods or, when both are required, in the choice which one comes first.

## 7.2. MERITS AND DEMERITS IN PERSPECTIVE

There is general agreement that MIBG scintigraphy is not justified as a screening investigation for phaeochromocytomas in a general population of hypertensives. The patients referred for imaging should be under strong suspicion of having the disease as evidenced by a history of phaeochromocytomas, MEN syndromes or neuro-ectodermal disorders and by clinical and biochemical findings [9]. MIBG can depict functioning paragangliomas as focal collections of I-123 and I-131 radioactivity and may even allow early diagnosis of developing phaeochromocytomas in patients with MEN syndromes [10]. An important asset of MIBG scintigraphy is its inherent ability to portray the entire body within one examination. Observations regarding the localization of phaeochromocytomas with whole-body I-131 MIBG scintigraphy indicate an overall sensitivity varying between 77% and 96% when performed in the appropriate clinical setting [9, 11, chapter 4]. False-positive results are rare and are mostly caused by the radiopharmaceutical being accumulated in the liver, the heart and the urinary tract.

Another reason for false-positives is that MIBG uptake is not as specific for phaeochromocytomas as originally believed. Uptake has been noted in other neural crest-derived tumours, specifically carcinoid tumour, medullary carcinoma of the thyroid, and neuroblastoma [12, 13]. Sporadic cases of uptake by oat cell carcinoma, choriocarcinoma and Merkel cell carcinoma have also been described [12]. This possibility reduces specificity and may complicate

scintigraphic interpretation in some patients with MEN syndromes or associated neuro-ectodermal disorders.

The sensitivity of I-123 MIBG is at least equal to that of I-131 MIBG for the detection of functioning paragangliomas [14, chapter 4]. Its shorter half-life and higher costs, however, have greatly limited the extent to which I-123 MIBG has been used and studied. I-131 MIBG scintigraphy has been shown to be of particular value in the detection of extra-adrenal paragangliomas [15]. We found this to be also true for I-123 MIBG in case of aorticosympathetic paragangliomas, but sensitivity of I-123 MIBG scintigraphy for parasympathetic paragangliomas (chemodectomas) proved to be low, only about half of the chemodectomas showing low to moderate uptake [chapter 3]. There is no reason to believe that I-131 MIBG scintigraphy will perform better in this latter class of paragangliomas.

The sensitivity of whole-body MIBG scintigraphy in the detection of paraganglioma metastases has not been investigated separately, but Lynn et al. found a sensitivity of I-131 MIBG scintigraphy for the detection of bone metastases from malignant paragangliomas of 55%, compared to a sensitivity of bone scintigraphy of 74%. Furthermore, they found bone to be by far the most common site of metastasis (38 of 56 patients with metastases). In patients with malignant paragangliomas, therefore, MIBG scintigraphy should be accompanied by bone scintigraphy [16].

MIBG scintigraphy is not hampered by surgical clips or scarred fields, which is of benefit for the detection of residual tumour or recurrences in previously operated patients. Although surgical removal is the treatment of choice for paragangliomas, it is possible to treat most functioning and some non-functioning tumours by administration of large doses of I-131 MIBG, when they show high concentration of MIBG. It may even be the only appropriate therapy for metastases from malignant paragangliomas [17, 18].

Further restricting factors at present include poor anatomical resolution resulting in the need for augmentation with some other imaging method for surgical purposes, thus increasing the burden of ionizing radiation when supplemented by CT and <sup>99m</sup>Tc bone scintigraphy, susceptibility to interference from a wide range of drugs currently in use and cost, especially in the case of I-123 MIBG. As MIBG scintigraphy reflects concentration of adrenergic nervous tissue, incidental tumours of the adrenal cortex may be missed [chapter 4].

Sensitivity of MR imaging is at least equal to that of MIBG for adrenal and orthosympathetic paragangliomas and higher for chemodectomas [chapters 3, 4 and 6].

In addition, MR imaging at present allows a certain degree of tumour characterization, especially as regards phaeochromocytomas. In conjunction with clinical and biochemical findings, functioning paragangliomas can be perfectly differentiated from other tumours, as we have demonstrated [chapter 4]. MR imaging also offers the major advantages of permitting three-

dimensional portrayal and tumour siting which precludes the need to use other imaging methods preoperatively. MR imaging can be performed with equal effectivity without the administration of intravenous contrast agents [chapter 6]. Ionizing radiation presents no problem and there is no interference from concurrent medication. This makes MR imaging extremely well suited to the follow-up of patients known to have disorders carrying an increased risk for developing a paraganglioma, as it obviates the burden of accumulating ionizing radiation doses inherent to repeated CT and MIBG investigations. Pregnancy is another condition in which MR imaging is indicated for the same reason [19].

The combination of anatomical portrayal of the whole body with tissue characterization and the absence of ionizing radiation of MR imaging may well prove to be a decisive advantage for following at-risk patients, particularly so, as in genetically predisposed persons with a MEN syndrome, von Hippel-Lindau disease or neurofibromatosis, ionizing radiation may provide the final trigger for tumour development [20]. Moreover, in these patients functioning paragangliomas are supposed to be limited to the adrenal region [2, 7, 15]. In this region MR imaging has a higher sensitivity and definitely a higher spatial resolution than MIBG scintigraphy [chapter 4].

The time taken up by imaging the entire relevant area lasting at this moment about 1.5 hours is, although definitely longer than whole-body MIBG scintigraphy, reasonable. It may be reduced by the rapidly approaching prospect of high speed MR imaging.

Disadvantages of note are the contra-indication formed by pacemakers and certain prostheses and the fact that MR imaging in patients with claustrophobia requires sedation. The last but most important limitation is that MR imaging does not provide functional information.

### 7.3. FUTURE DIRECTIONS AND DEVELOPMENTS

There can be no doubt that MIBG has proved to be a very valuable non-invasive imaging technique. It is also very likely that further advances will be made in the detection of paragangliomas with the use of I-123 MIBG and SPECT, resulting in better functional imaging of these tumours. In our studies, I-123 MIBG uptake provided an important clue to the hormonal activity of seven of the eight functioning paragangliomas although the patients showed only minimal symptoms and marginally elevated catecholamine levels [chapters 3 and 5]. Even though, as already stated by von Moll et al. the ability of a tumour to take up MIBG can be independent of its ability to secrete catecholamines [chapter 3, 12] further study of the relationship between MIBG uptake and catecholamine excretion is warranted since this may provide important clues as to whether immediate surgical treatment is necessary or a 'wait and see' policy is more appropriate.

An improved understanding of the synthesis and kinetics of catecholamines may also provide information leading to more effective therapeutic intervention by means of MIBG administration in irresectable paragangliomas [chapter 3, 21].

The performance of MR imaging will certainly be further improved by recent technical innovations such as motion compensation software, faster imaging techniques and special coils. Fast spin-echo and ultra-fast gradient-echo sequences will reduce the time needed for whole-body imaging and the development of Magnetization Transfer Contrast methods may have a further impact on lesion conspicuity and lesion characterization. Undoubtedly MR imaging will play a leading role in monitoring tumour growth when in the future a 'wait and see' approach or 'workbench surgery' will be applied more often for paragangliomas [22, 23].

Lately octreotide scintigraphy has been applied with great success to visualize head and neck paragangliomas [24-26]. Octreotide scintigraphy seems less accurate in the detection of pheochromocytomas than of head and neck paragangliomas, although at this moment the number of adrenal paragangliomas imaged with octreotide scintigraphy is too small to draw general conclusions [25, 26]. The efficacy of octreotide scintigraphy has until now not been compared with that of MR imaging and MIBG scintigraphy. Again octreotide scintigraphy is a whole-body imaging method with certainly better results than MIBG scintigraphy for head and neck paragangliomas. It is however not specific to paragangliomas nor does it provide functional information as it reflects the presence of somatostatin receptors on the outside of tumour cells and has no relationship to tumoural somatostatin or catecholamine content [26, 27].

In conclusion, in view of the above mentioned factors it may be stated that MR imaging is the diagnostic tool of first choice for general localization of paragangliomas. It is unquestionably the best method for follow-up of at-risk persons and for monitoring known tumours that require a 'wait and see' approach rather than immediate surgical removal. When localization of a suspected functioning paraganglioma by MR imaging is unsuccessful or when functional information is required additional MIBG scintigraphy should be applied.

### 7.4. REFERENCES

1. Heutink P, Mey AG, van der Sandkuijl LA, et al. A gene subject to genomic imprinting and responsible for hereditary paragangliomas maps to chromosome 11q23-qter. *Hum Mol Genet* 1992;1:7-10
2. Raue F, Frank K, Meybier H, Ziegler R. Pheochromocytoma in multiple endocrine neoplasia. *Cardiology* 1985;72 (suppl.):147-149

3. Gagel RF, Tashjian AH Jr, Cummings T, et al. The clinical outcome of prospective screening for multiple endocrine neoplasia type 2a. *N Engl J Med* 1988;318:478-484
4. Telenius-Berg M, Berg B, Hamberger B, Tibblin S. Screening for early asymptomatic pheochromocytoma in MEN 2. *Henry Ford Hosp Med J*. 1987;35:110-114
5. Samaan NA, Hickey RC, Shutts PE. Diagnosis, localization and management of pheochromocytoma. *Cancer* 1988;62:2451-2460
6. St John Sutton MG, Sheps SG, Lie JT. Prevalence of clinically unsuspected pheochromocytoma. Review of a 50-year autopsy series. *Mayo Clin Proc* 1981;56:354-360
7. Sheps SG, Jiang NS, Klee GG. Diagnostic evaluation of pheochromocytoma. *Endocrin Metab Clin N Am* 1988;17:397-414
8. Plouin PF, Chatellier G, Delahousse M, et al. Recherche, diagnostic et localisation du pheochromocytome. *Presse Med* 1987;16:2211-2215
9. Shapiro B, Copp JE, Sisson JC, Eyre PL, Wallis J, Beierwaltes WH. Iodine-131 Metaiodobenzylguanidine for the locating of suspected pheochromocytoma: experience in 400 cases. *J Nucl Med* 1985;26:576-585
10. Valk TW, Frager MS, Gross MD, et al. Spectrum of pheochromocytoma in multiple endocrine neoplasia. A scintigraphic portrayal using I-131 metaiodobenzylguanidine. *Ann Intern Med* 1981;94:762-767
11. Swensen SJ, Brown ML, Sheps SG. Use of <sup>131</sup>I-MIBG scintigraphy in the evaluation of suspected pheochromocytoma. *Mayo Clin Proc* 1985;60:299-304
12. Moll L von, McEwan AJ, Shapiro B, et al. Iodine-131 MIBG scintigraphy of neuroendocrine tumors other than pheochromocytoma and neuroblastoma. *J Nucl Med* 1987;28:979-988
13. Hoefnagel CA, Voûte PA, Kraker J de, Marcuse HR. Radionuclide diagnosis and therapy of neural crest tumors using Iodine-131 Metaiodobenzylguanidine. *J Nucl Med* 1987;28:308-314
14. Lynn MD, Shapiro B, Sisson JC, et al. Portrayal of phaeochromocytoma and the normal adrenal medulla: improved visualization with I-123 MIBG scintigraphy. *Radiology* 1985;155:789-792
15. McEwan AJ, Shapiro B, Sisson JC, Beierwaltes WH, Ackery DM. Radio-iodobenzylguanidine for the scintigraphic location and therapy of adrenergic tumors. *Sem Nucl Med* 1985;15:132-153
16. Lynn MD, Braunstein EM, Wahl RL, Shapiro B, Gross MD, Rabbani R. Bone metastases in pheochromocytoma: comparative studies of efficacy of imaging. *Radiology* 1986;160:701-706
17. Sisson JC, Shapiro B, Beierwaltes WH, et al. Radiopharmaceutical treatment of malignant pheochromocytoma. *J Nucl Med* 1984;25:197-206
18. Baulieu JL, Guilloteau D, Baulieu F, et al. Therapeutic effectiveness of Iodine-131 MIBG metastases of a nonsecreting paraganglioma. *J Nucl Med* 1988;29:2008-2013
19. Greenberg M, Moawad AH, Wieties BM, et al. Extraadrenal pheochromocytoma: detection during pregnancy using MR imaging. *Radiology* 1986;161:475-476
20. Jackson CE, Tashjian AH. Limited progression of hereditary medullary thyroid cancer after conservative management (abstr). *Am J Hum Genet* 1992;51(P):235

21. Sandler MP. The expanding role of MIBG in clinical medicine. *J Nucl Med* 1988;29:1457-1458
22. Mey AGL van der, Frijns JHM, Cornelisse CJ, et al. Does intervention improve the natural course of glomus tumors? *Ann Otol Rhinol Laryngol* 1992;101:635-642
23. Loughlin KR, Gittes RF. Urological management of patients with von Hippel-Lindau's disease. *J Urol* 1986;136:789-791
24. Lamberts SWJ, Bakker WH, Reubi JC, Krenning EP. Somatostatin-receptor imaging in the localization of endocrine tumors. *N Engl J Med* 1990;323:1246-1249
25. Kwekkeboom DJ, Urk H van, Pauw BKH, et al. Octreotide scintigraphy for the detection of paragangliomas. *JNM* 1993;34:873-878
26. Reubi JC, Waser B, Khosla S, et al. In vitro and in vivo detection of somatostatin receptors in pheochromocytomas and paragangliomas. *J Clin Endocrinol Metab* 1992;74:1082-1089
27. Kwekkeboom DJ, Krenning EP, Bakker WH, Yoe Oei H, Kooy PPM, Lamberts SWJ. Somatostatin analogue scintigraphy in carcinoid tumours. *Eur J Nucl Med* 1993;20:283-292

Paragangliomas are tumours arising from paraganglionic tissue dispersed from the base of the skull to the pelvic diaphragm. Anatomically they are divided into extra-adrenal and adrenal paragangliomas (phaeochromocytomas). These tumours produce symptoms by secreting catecholamines (functioning tumours) or by local tumour expansion. Paragangliomas can be part of several hereditary disorders.

The introduction of both magnetic resonance (MR) imaging and meta-iodobenzylguanidine (MIBG) scintigraphy has added new dimensions to the study of paragangliomas and has resulted in significant improvements in the diagnosis of paragangliomas over the past years. In this thesis the use of these two recently introduced non-invasive imaging methods in the examination of paragangliomas is described.

Paragangliomas are rare tumours with a low incidence. Literature on these tumours largely consists of case reports or retrospective studies. This study was undertaken in a large group of patients to explore and evaluate MR imaging and MIBG scintigraphy as procedures for detecting functioning as well as non-functioning paragangliomas and screening at-risk individuals.

In CHAPTER 1 the goal and the outline of the study presented in this thesis are discussed.

CHAPTER 2 presents an introduction to the anatomic-pathological and clinical features of paragangliomas and sketches the principles of MIBG scintigraphy and MR imaging of these tumours. The necessity of a highly sensitive, non-invasive imaging method for displaying these tumours is explained.

In CHAPTER 3 the application of I-123 MIBG scintigraphy for paragangliomas of the head and neck is described. I-123 MIBG uptake by one or more tumours was noticed in only 50% of patients. I-123 MIBG scintigraphy is therefore not suitable as a primary screening method for paragangliomas of the head and neck. Coincidentally, endocrine activity was detected in five patients. In three of these patients a norepinephrine-secreting abdominal paraganglioma was subsequently removed. One patient had a norepinephrine-secreting glomus tumour and one had a dopamine-secreting glomus tumour.

This endocrine activity was suspected in only one of them before the investigation started. Considering also the large number of case reports, it is likely

that the prevalence of catecholamine-secreting tumours in patients with paragangliomas of the head and neck is higher than 1% as is assumed in literature.

CHAPTER 4 compares the potential of MR imaging and MIBG in localizing and characterizing functioning paragangliomas. The results of both modalities in 33 patients suspected of having these tumours were analyzed. Overall sensitivity as regards detection was 91% for MR Imaging and 80% for MIBG scintigraphy. MR imaging detected 100% of the adrenal paragangliomas and 75% of the extra-adrenal paragangliomas, whereas MIBG scintigraphy detected 75% and 88% respectively. MIBG was more specific in the characterization of functioning paragangliomas than MR imaging (100% versus 82%). MR imaging demonstrated nine other lesions not visualized by MIBG scintigraphy. This ability, together with the superior anatomical resolution and the absence of ionizing radiation, makes MR imaging the preferred initial technique for localization when a functioning paraganglioma is suspected and for screening persons at risk of developing paragangliomas.

CHAPTER 5 describes a screening exercise performed on 83 members of a large family at risk of developing hereditary paragangliomas in order to detect the presence of subclinical paragangliomas. For that purpose we used whole-body MR imaging and urinary catecholamine testing. In eight previously diagnosed members, eight known glomus tumours of which one functioning, and two unknown glomus tumours as well as one unknown pheochromocytoma were present. Six unsuspected members showed ten glomus tumours and one pheochromocytoma. A substantial number of paragangliomas, functioning as well as non-functioning, may thus be present without symptoms.

There were no tumours in the descendants of female gene carriers. This finding provides clinical evidence for genomic imprinting, i.e. the manifestation of hereditary glomus tumours is determined by the sex of the transmitting parent. Comparing the likelihood of inheritance with genomic imprinting versus inheritance without genomic imprinting we found an odds ratio of 23,375 : 1 in favour of genomic imprinting.

The question in CHAPTER 6 is whether the use of gadopentetate dimeglumine is necessary to detect paragangliomas of the head and neck. This was investigated in an observer study in which unenhanced MR imaging examinations performed in 23 normal subjects and 37 patients having 71 tumours were compared with the examinations after administration of gadopentetate dimeglumine. Computed tomography (CT), scintigraphy, angiography and surgico-pathological findings were used as the standard of reference. Four blinded readers reviewed these studies in a random order using a four-point scale of certainty. Results were subjected to alternative free-response receiver-operating-characteristic (AFROC) scoring and statistical analysis. The addition of contrast-enhanced imaging did not increase the sensitivity or specificity compared to imaging without enhancement. We conclude that, in general, the use of gadopentetate dimeglumine is not necessary for the detection

of head and neck paragangliomas. Only when searching for small postoperative tumour residues is the addition of gadopentetate dimeglumine warranted.

In CHAPTER 7, the relative advantages and disadvantages of MR imaging and MIBG scintigraphy are discussed. MR imaging is superior to MIBG scintigraphy in the detection of paragangliomas, functioning and non-functioning, without the hazard of ionizing radiation. This combined with several, ancillary considerations makes MR imaging an ideal method for screening persons at risk of developing paragangliomas, in particular MEN II patients and patients with hereditary paragangliomas of the head and neck. It would be of interest to investigate whether this also applies to patients with other hereditary disorders at risk of developing paragangliomas, such as von Hippel-Lindau disease and neurofibromatosis.

In conclusion, the advent of the new non-invasive imaging techniques MR imaging and MIBG scintigraphy has provided new insights on paragangliomas and has tremendously changed the topographic diagnosis of these tumours. Our results with MR imaging and MIBG scintigraphy of paragangliomas and theoretical considerations on the respective merits and demerits of these techniques strongly suggest that MR imaging should be the imaging modality of first choice. There is a need for gadopentetate dimeglumine in selected cases only. Otherwise MIBG scintigraphy continues to be a reliable method for non-invasive detection of functioning paragangliomas. MIBG scintigraphy should be reserved for cases where a strong suspicion of the presence of a functioning paraganglioma persists, despite normal MR imaging findings and for cases where doubt exists about functional activity of one or more multicentric tumours.

Paragangliomen zijn tumoren die ontstaan uit paraganglion weefsel. Dit weefsel is aanwezig in het gebied tussen de schedelbasis en de bekkenbodem. Paragangliomen kunnen zowel afzonderlijk als ook in het kader van verschillende erfelijke aandoeningen voorkomen. Anatomisch gezien worden paragangliomen onderverdeeld in extra-adrenale en adrenale paragangliomen. Deze laatste groep paragangliomen is beter bekend onder de naam pheochromocytomen. Paragangliomen die ontstaan in het hoofd-hals gebied, worden ook wel glomus tumoren genoemd. Paragangliomen geven klachten door productie en excretie van catecholamines (hormonaal actieve tumoren) of door locale tumor uitbreiding.

De introductie van zowel kernspintomografie (MRI) als metaiodobenzylguanidine (MIBG) scintigrafie heeft in de afgelopen jaren geresulteerd in een verbeterde diagnostiek van paragangliomen en nieuwe mogelijkheden gecreëerd voor de bestudering van deze tumoren.

In dit proefschrift wordt de toepassing van deze beide, niet-invasieve afbeeldingstechnieken bij paragangliomen beschreven, vergeleken en kritisch beschouwd.

In HOOFDSTUK 1 worden doel en opzet van dit proefschrift uiteengezet. Doel was MRI en MIBG scintigrafie te evalueren als middel om zowel hormonaal actieve als hormonaal niet-actieve paragangliomen op te sporen en om personen met een erfelijke aanleg te screenen. Daarvoor is onderzoek verricht bij relatief grote groepen patiënten met paragangliomen en personen met een verhoogd risico op het ontstaan van deze tumoren.

HOOFDSTUK 2 geeft een inleiding op de pathologie en de symptomatologie van paragangliomen en schetst de basis beginselen van de gebruikte afbeeldingstechnieken, MIBG scintigrafie en MRI. Het belang van een sensitieve, niet-invasieve afbeeldingstechniek voor het localiseren van deze tumoren wordt uiteengezet.

In HOOFDSTUK 3 wordt de toepassing van I-123 MIBG scintigrafie bij paragangliomen van het hoofd-hals gebied beschreven. Opname van I-123 MIBG in één of meerdere tumoren werd slechts bij zeven van de veertien onderzochte patiënten waargenomen. I-123 MIBG scintigrafie is derhalve niet

geschikt als primaire screeningsmethode voor paragangliomen van het hoofd-hals gebied. Opvallend was echter, dat bij vijf patiënten (36%) overmatige productie van catecholamines kon worden vastgesteld. Bij drie van deze vijf patiënten bleek dit te berusten op noradrenaline producerende abdominaal gelocaliseerde paragangliomen. Eén patiënt had een noradrenaline producerende glomus tumor en de vijfde had een dopamine producerende glomus tumor. Deze endocriene activiteit werd slechts in één van deze vijf patiënten vermoed op grond van klinische symptomen. Deze symptomen waren echter nooit als zodanig onderkend voor de aanvang van deze studie. Gezien onze bevindingen mag worden aangenomen, dat de prevalentie van catecholamine producerende tumoren bij patiënten met paragangliomen van het hoofd-hals gebied hoger is dan 1%, zoals tot nu toe verondersteld werd in de literatuur.

HOOFDSTUK 4 vergelijkt de waarde van MRI en MIBG scintigrafie bij het localiseren en diagnostiseren van hormonaal actieve paragangliomen. De onderzoeksresultaten van beide technieken bij 33 patiënten, van wie vermoed werd dat ze één of meer hormonaal actieve paragangliomen hadden, werden geanalyseerd. De sensitiviteit van MRI was 91% en die van MIBG scintigrafie 80%. MRI detecteerde 100% van de in de bijnier gelegen paragangliomen (pheochromocytomen) en 75% van de buiten de bijnier gelegen paragangliomen, terwijl MIBG scintigrafie respectievelijk 75% en 88% detecteerde. MIBG scintigrafie bleek specifiekere dan MRI in het karakteriseren van hormonaal actieve paragangliomen (100% en 82% respectievelijk). MRI liet negen andere laesies zien, die niet werden afgebeeld met MIBG scintigrafie. Dit voordeel, in combinatie met de hogere anatomische resolutie en het ontbreken van ioniserende straling, maakt dat MRI de voorkeur heeft zowel voor het localiseren van paragangliomen als voor het screenen van personen met een verhoogde kans op het ontstaan van deze tumoren.

Paragangliomen kunnen familiair voorkomen en erven dan op een autosomaal dominante wijze over. HOOFDSTUK 5 beschrijft een screeningsonderzoek bij een familie met erfelijk voorkomende paragangliomen in het hoofd-hals gebied. Drie en tachtig leden van deze familie werden onderzocht middels MRI en middels catecholamine bepalingen in de urine, met als doel asymptomatische tumoren op te sporen. Bij acht reeds bekende patiënten uit de familie, werden naast de negen al eerder vastgestelde glomus tumoren, waarvan er één hormonaal actief was, twee nog niet eerder ontdekte glomus tumoren en één pheochromocytoom ontdekt. Bij zes nog niet als patiënt bekende familieleden waren negen glomus tumoren en één pheochromocytoom aanwezig. Een groot percentage paragangliomen, zowel hormonaal actief als hormonaal niet-actief, kan dus blijkbaar aanwezig zijn zonder symptomen te veroorzaken.

Bij de afstammelingen van vrouwelijke gen dragers werden geen tumoren gevonden. Deze bevinding geeft klinische steun aan de "genomic imprinting" theorie. Deze theorie houdt in dat het ontstaan van erfelijke glomus

tumoren bij familieleden met het gen, wordt bepaald door het geslacht van de het gen overdragende ouder. Bij het vergelijken van de waarschijnlijkheid van overerving met "genomic imprinting" en overerving zonder "genomic imprinting" vonden wij een waarschijnlijkheidsratio van 23.375 : 1 ten gunste van "genomic imprinting".

In HOOFDSTUK 6 wordt in gegaan op de vraag of het gebruik van gadopentetate dimeglumine noodzakelijk is om paragangliomen van het hoofd-hals gebied te detecteren. In een "observer" studie werden de MRI onderzoeken, vervaardigd zonder toediening van gadopentetate dimeglumine bij 23 controle personen en bij 37 patiënten met 71 paragangliomen in het hoofd-hals gebied, vergeleken met de MRI onderzoeken vervaardigd bij dezelfde personen na intraveneuze toediening van gadopentetate dimeglumine. Computer tomografie (CT), scintigrafie, angiografie, en chirurgische en pathologisch-anatomische bevindingen werden gebruikt als standaard. Vier radiodiagnosen beoordeelden deze onderzoeken in willekeurige volgorde, zonder gebruik te maken van klinische gegevens. De mate van zekerheid over de aanwezigheid en de plaats van een tumor, werd aangegeven op een schaal van vier graden. De resultaten werden onderworpen aan een "alternative free-response receiver-operating-characteristic" (AFROC) analyse en een statistische analyse. Het gebruik van gadopentetate dimeglumine bleek geen duidelijke voordelen te bieden voor het detecteren van paragangliomen in het hoofd-hals gebied. Alleen in post-operatieve gevallen kan dit contrastmiddel soms een aanvullende rol spelen.

De nieuwe niet-invasieve afbeeldingstechnieken MRI en MIBG scintigrafie hebben nieuwe inzichten verschaft over paragangliomen en hebben, in vergelijking met de tot voor kort gebruikelijke technieken, het localiseren van paragangliomen aanzienlijk vergemakkelijkt. In HOOFDSTUK 7 worden de voor- en nadelen van MRI en MIBG scintigrafie besproken. Onze bevindingen met MRI en MIBG scintigrafie bij paragangliomen alsmede theoretische overwegingen ten aanzien van de voor- en nadelen van beide technieken wijzen erop dat MRI de afbeeldingstechniek van eerste keuze is voor deze tumoren. MRI blijkt sensitiever dan MIBG scintigrafie bij de detectie van zowel hormonaal actieve als niet hormonaal actieve paragangliomen. Alleen in uitzonderingsgevallen is hierbij het gebruik van een contrastmiddel als gadopentetate dimeglumine noodzakelijk. Bij MRI wordt bovendien geen gebruik gemaakt van ioniserende straling. Deze voordelen maken MRI ook tot de methode bij uitstek om personen met een verhoogd risico op het ontstaan van paragangliomen, zoals patiënten met het "multiple endocrine neoplasia" syndroom type II en patiënten met erfelijke paragangliomen van het hoofd-hals gebied, te screenen en te vervolgen.

MIBG scintigrafie blijft echter een betrouwbare methode voor de niet-invasieve diagnostiek van hormonaal actieve paragangliomen. MIBG scintigrafie kan gebruikt worden wanneer er een sterke verdenking blijft bestaan op de aanwezigheid van een hormonaal actief paraganglioom, ondanks

normale MRI bevindingen. Bovendien kan MIBG scintigrafie, in het geval van meerdere tegelijk voorkomende paragangliomen, een indicatie geven welke tumoren hormonaal actief zijn.

## LIST OF OWN PUBLICATIONS USED IN THIS THESIS

Parts of this thesis are reported in the following publications:

- Gils APG van, Mey AGL van der, Hoogma RPJM, Falke THM, Moolenaar AJ, Pauwels EKJ, Kroonenburgh MJPG van. I-123 Meta-iodobenzylguanidine in the detection of chemodectomas in the head and neck region. *J Nucl Med* 1990;31:1147-1155
- Falke THM, Gils APG van, Seters AP van, Sandler MP. Magnetic resonance imaging of functioning paragangliomas. *Magn Reson Q* 1990;6:35-64
- Gils APG van, Falke THM, Erkel AR van, Velde CJH van de, Pauwels EKJ. Non invasive imaging of functioning paragangliomas (Including pheochromocytomas). *Frontiers Eur Radiol* 1990;7:1-38
- Gils APG van, Falke THM, Erkel AR van, Arndt J-W, Sandler MP, Mey AGL van der, Hoogma RPLM. MR imaging and MIBG scintigraphy of pheochromocytomas and extra-adrenal functioning paragangliomas. *Radiographics* 1991;11:37-57
- Gils APG van, Falke THM, Kroonenburgh MJPG van, Sandler MP. MR imaging and MIBG scintigraphy of pheochromocytomas and extra-adrenal functioning paragangliomas. *Radiology* 1989;173(P):507 (certificate of merit RSNA, Chicago 1989)
- Gils APG van, Falke THM, Arndt JW, Sandler MP. MRI and MIBG imaging of pheochromocytomas and extra-adrenal paragangliomas. *AJR* 1990;155:645 (certificate of merit American Roentgen Ray Society, Washington 1990) (P)
- Kroonenburgh MJPG van, Gils APG van, Mey AGL van der, Hoogma RPLM, Falke THM, Moolenaar AJ, Pauwels EKJ. Iodine-123 MIBG uptake by chemodectomas. *J Nucl Med*. 1989;30:769 (P)
- Gils APG van, Mey AGL van der, Hoogma RPLM, Falke THM, Moolenaar AJ, Pauwels EKJ, Kroonenburgh MJPG van. High incidence of catecholamine-secreting tumors among patients with chemodectomas in the head and neck region. *Eur J Nucl Med* 1989;15(C):10 (P)
- Gils APG van, Falke THM, Sandler MP, Pauwels EKJ, Erkel AR van. Comparison of MRI and I-123 MIBG in the detection of functioning paragangliomas. *J Nucl Med* 1990;31:935 (P)

Gils APG van, Mey AGL van der, Hoogma RPLM, Sandkuijl LA, Maaswinkel-Mooy PD, Falke THM, Pauwels EKJ. MRI screening of kindred at risk of developing paragangliomas: support for genomic imprinting in hereditary glomus tumours. *Br J Cancer* 1992;65:903-907

Heutink P, Mey AGL van der, Sandkuijl LA, Gils APG van, Bardoel A, Breedveld GJ, Vliet M van, Ommen G-JB van, Cornelisse CJ, Oostra BA, Weber JL, Devilee P. A gene subject to genomic imprinting and responsible for hereditary paragangliomas maps to chromosome 11q23-qter. *Hum Mol Genet* 1992;1:7-10

Gils APG van, Berg R van den, Falke THM, Bloem JL, Prins HJ, Dillon EH, Mey AGL van der, Pauwels EKJ. MR diagnosis of paraganglioma of the head and neck: value of contrast enhancement. *AJR* 1994 (in press)

Gils APG van, Erkel AR van, Falke THM, Pauwels EKJ. MR imaging or MIBG scintigraphy for the demonstration of paragangliomas? Correlations and disparities. *Eur J Nucl Med* 1994 (in press)

## A CKNOWLEDGEMENTS

The studies presented in this thesis have been performed in the Department of Diagnostic Radiology and Nuclear Medicine of the Leiden University Hospital (Head: Prof. Dr. A.E. van Voorthuisen). The help of the co-authors and the following people is gratefully acknowledged:

J. Beentjes, I. Boot, J. Doornbos, R. Byrne, J. Camps, E. Coerkamp, T. Hagendoorn, C. Hoefnagel, P. Kop, G. Kracht, C. Kruitwagen, H. Lemmers, N. Matheijssen, P. Roes, A. de Roos, Y. Soons, R. Valkema, J. Wondergem, and the technicians of the Department of Diagnostic Radiology and Nuclear Medicine of the Leiden University Hospital.

I would also like to thank my colleagues from the radiological departments of the Leiden University Hospital, the Utrecht University Hospital, and the Central Military Hospital for their encouragements and support during the preparation of this thesis.

Permission to publish figures was obtained from Magnetic Resonance Quarterly, the American Journal of Roentgenology, British Journal of Cancer, the Journal of Nuclear Medicine, and Radiographics.

# CURRICULUM VITAE

De auteur van dit proefschrift werd op 3 juni 1955 geboren te Diessen. In 1973 behaalde hij het diploma gymnasium- $\beta$  aan het St. Odulphus Lyceum te Tilburg. In hetzelfde jaar begon hij met de studie Geneeskunde aan de Katholieke Universiteit Nijmegen. In 1980 werd het artsexamen afgelegd. Aansluitend trad hij in dienst van het Ministerie van Defensie als beroepsmilitair arts bij de Koninklijke Landmacht. In de periode 1980-1982 was hij bataljonsarts bij 103 Verkenningsbataljon te Seedorf (BRD). Van november 1982 tot november 1983 volgde hij de huisartsenopleiding aan de Rijksuniversiteit Utrecht (opleider: R. Vergroesen, gezondheidscentrum Woensel, Eindhoven). In de periode van 1983 tot 1986 was hij Commandant Geneeskundige Verzorgingsgroep te Grave. In februari 1986 werd begonnen met de opleiding radiodiagnostiek in het Academisch Ziekenhuis Leiden (opleider: Prof. dr. A.E. van Voorthuisen). Vanaf zijn inschrijving in het Specialisten Register op 1 februari 1991 is hij werkzaam als radiodiagnost in het Academisch Ziekenhuis Utrecht en het Centraal Militair Hospitaal te Utrecht in de rang van kolonel.

## Sellingen

1. Een CT onderzoek zonder intraveneus contrast is de beste niet-invasieve methode om adenomen te differentiëren van andere tumoren in de bijnier.
2. Scintigrafisch onderzoek met I-123 metaiodobenzylguanidine is in principe niet geschikt voor het detecteren van tumoren uitgaande van de bijnierschors.
3. Voorafgaand aan de chirurgische verwijdering van paragangliomen van het hoofd-halsgebied moet altijd hormonale activiteit worden uitgesloten.
4. Beoordeling van de effectiviteit van contrastmiddelen dient te geschieden aan de hand van objectieve en hanteerbare criteria, bijvoorbeeld door middel van ROC analyse en AFROC analyse.
5. Met de komst van 'ultrafast MRI' zal het mogelijk worden de doorgankelijkheid van de eileiders te onderzoeken, zonder gebruik te maken van ioniserende straling.
6. Scintigrafie met behulp van In-111 DTPA-octreotide vraagt om anatomische referentiepunten.
7. Een onderzoek naar het ontstaan van cervicale discopathie door het dragen van een helm is wenselijk.
8. Voor interventies in het kader van de Verenigde Naties geldt: inzet zonder inzicht leidt tot uitzending zonder uitzicht.
9. Televisie programma's over medische onderwerpen hebben soms meer het karakter van sluikreclame dan van patiëntenvoorlichting.
10. De waarneming dat veel artsen tweelingen hebben, verdient nader onderzoek.
11. Verstand op nul en blik op oneindig is vaak niet alleen een goede houding voor militairen, maar ook voor promovendi.
12. Dat slechts een gering percentage militaire artsen gepromoveerd is, valt te verklaren uit het feit dat enkelen er de voorkeur aan geven onder te duiken, anderen zich ingraven en sommigen liever laagvliegen.